EUMETSAT

esa

→ MONITORING VOLCANIC ASH FROM SPACE

ESA–EUMETSAT workshop on the 14 April to 23 May 2010 eruption at the Eyjafjöll volcano, South Iceland (ESA/ESRIN, 26–27 May 2010)

C. ZEHNER (Editor)
ESA/ESRIN

STM-280
January 2012

→ MONITORING VOLCANIC ASH FROM SPACE

ESA–EUMETSAT workshop on the 14 April to 23 May 2010 eruption at the Eyjafjöll volcano, South Iceland (ESA/ESRIN, 26–27 May 2010)

C. ZEHNER (Editor)
ESA/ESRIN

How to cite this document:

"C. Zehner, Ed. (2012). Monitoring Volcanic Ash from Space. ESA–EUMETSAT workshop on the 14 April to 23 May 2010 eruption at the Eyjafjöll volcano, South Iceland (ESA/ESRIN, 26–27 May 2010)
ESA Publication STM-280. doi:10.5270/atmch-10-01"

An ESA Communications Production

Publication *Monitoring Volcanic Ash from Space* (ESA STM-280 January 2012)

Production editor K Fletcher

Coordinator J Oakley, Serco

Layout ESA EO Graphics Bureau

Publisher ESA Communications
ESTEC, PO Box 299, 2200 AG Noordwijk, the Netherlands
Tel: +31 71 565 3408 Fax: +31 71 565 5433 www.esa.int

ISBN 978-92-9221-901-7

ISSN 0379-4067

Contents

Preface

This report presents the technical results, including lessons learned and recommendations, of the ESA–EUMETSAT workshop on Volcanic Ash Monitoring, which took place on 26–27 May 2010 at ESA/ESRIN in Frascati (Italy). 53 invited scientists participated, from universities, meteorological offices, research laboratories, and national and international agencies (e.g. DLR, EC, ECMWF, NASA, USGS) from Europe and the United States.

The purpose of the 2-day workshop was to bring together experts to take stock of Europe's remote-sensing capabilities to address the impact of the Eyjafjöll eruption (14 April–23 May 2010).

The first day was dedicated to oral presentations addressing the specifics of the Eyjafjöll eruption, the modelling of its ash plume movement during the event, and remote sensing measurements of the ash plume as performed by *in situ* research aircraft and satellite instruments.

All oral presentations can be found at:
http://earth.eo.esa.int/workshops/Volcano/index.php?page=26&type=s

The second day was organised into three splinter meetings, with three working groups addressing the following questions in parallel:

- Are we making best use of existing observing systems to address the problems created by the Eyjafjöll eruption (airborne, ground-based, satellite)? This meeting was chaired by D. Schneider.

- How can the R&D community best contribute to improving the Volcanic Ash Advisory Centres' (VAACs) analysis, and to prediction of the volcanic ash plume in European airspace (dispersion models, validation of models, inclusion of remote sensing measurements into models, accuracy, confidence levels)? This meeting was chaired by H. Elbern.

- What are the observations VAACs need and what are the implications for future satellite observing systems (e.g. MetOp, MTG, post-EPS, ADM, EarthCARE, Sentinels)? This meeting was chaired by A. J. Prata.

Oral presentations contributing to the discussions can be found at:
http://earth.eo.esa.int/workshops/Volcano/index.php?page=30&type=s

The responses to each question and the recommendations of each working group are summarised in separate chapters of this report.

The organisers wish to acknowledge the enthusiastic support and cooperation of all workshop participants in making the workshop successful and stimulating, and in providing contributions to the writing of this report.

The workshop was sponsored by ESA on behalf of the ESA Earth Observation Programme.

Executive summary

The purpose of this workshop, held at Frascati, Italy, in May 2010 was to examine the information available about the Eyjafjöll eruption (14 April–23 May 2010) and to try to assess whether the eruption and subsequent associated actions were adequately addressed by current European remote sensing capabilities.

The Eyjafjöll eruption caused major disruptions of air traffic over Europe during April and May 2010.

The ash plume of the Eyjafjöll eruption was observed at many places in Europe from satellites, from aircraft, and from ground-based instruments. The study of such an event on this scale requires expertise from many different disciplines, e.g. volcanology, chemistry, geology, engineering, meteorology, modelling, and physics.

The monitoring of the movement of the ash cloud over Europe was performed by using various remote sensing techniques and instrumentation. Ash plume model forecasts were evaluated against actual remote sensing measurements.

The eruption itself, the eruption source measurements/information and their impact on operational and R&D ash dispersion modelling were addressed. The impact of the new guidelines for aviation that were introduced in Europe during this event (changing from zero tolerance to new ash threshold values), and the consequences on ash plume modelling and remote sensing measurements and retrieval techniques were discussed.

Furthermore, implications for already-planned future satellite missions and possible new missions were examined as a component of an end-to-end system (including *in situ*, research aircraft and modelling capabilities), necessary to be able to address such an event better in the near future.

The major findings and recommendations of the workshop are given on the next pages.

Lessons learned so far from the Eyjafjöll eruption

— As a consequence of the phreatomagmatic phase of the eruption, the distal ash cloud contained a large amount of very fine grained ash that was dispersed rapidly throughout the troposphere from 2–10 km. The interaction of glacial water and hot magma contributed to the production of small particles and contributed to a high ice content in the early phase. This made initial identification of the plume difficult.

— The collection of remote sensing data, acquired over the period of the eruption of Eyjafjöll, presents a remarkably rich source of information for studying this event.

— Operational Near Real Time (NRT) datastreams typically contain quantitative information about height or concentration of hazardous species but only started to be explored after the beginning of this event.

— The tolerance to ash of commercial aircraft engines was critical. The decision-making process towards putting in a new safety limit was not based on extensive scientific consultation.

— The data used in the response is stored at many different locations.

— Collaboration between groups who specialise in different sensors was remarkable and considered to have been the best effort possible in view of the available resources and lack of coordination.

— Knowledge transfer between the research and operational communities could be improved.

— One of the largest uncertainties was information on the eruption source parameters for model initialisation. This leads to discrepancies in model outputs.

— A second big uncertainty was obtaining information on ash cloud concentrations. Aircraft measurements, primarily from research facilities with appropriate instrumentation (Annex 1c), were a key tool but these were unable to fly through thick ash due to engine manufacturer constraints. In addition to aircraft, Unmanned Aircraft Systems (UAS) provided more flexibility in terms of safety and readiness, as well as formal requirements.

— It proved difficult to make definitive statements about the ash cloud extent from any single observational source. There is a need to integrate all observing sources in NRT (if possible) to have a best estimate of geographical coverage, height, depth, and concentration. No single source or even multiple observation sources can provide all this information at present.

— Exchange of information and sharing of best practices are vital.

— The London VAAC did an excellent job on the monitoring and forecasting of the movement of the volcanic ash during the Eyjafjöll eruption.

Summary recommendations

The following list summarises the recommendations which were the outcome of the workshop. Detailed recommendations are specified in chapter 4.

1. Access to all data sources of volcanic plume observations in Europe should be accelerated, improved and open.

2. Existing observing capabilities within Europe should be further consolidated and enhanced by combining satellite, airborne and ground-based systems for detecting and characterising volcanic ash clouds.

3. There is a need for better observations at volcanoes. Actions should be taken to ensure that accurate and timely data are available from volcano observatories or monitoring stations situated near volcanoes.

4. Concerted developments should be undertaken to integrate existing advanced retrieval methods into operational systems.

5. Techniques for assimilation and inversion of satellite data in dispersion models should be further developed and applied to provide quantified ash cloud advisory information.

6. Relevant satellite observation systems and data products should be formally validated with observations from other sources and should, where appropriate, be certified with respect to quantitative requirements for volcanic plume monitoring.

7. Actions should be taken to ensure that planned future European satellites will provide more efficient guaranteed support for ash cloud related crises: both operational systems (MTG, Sentinels) and research missions.

8. Studies should be made of potential new satellites and instruments dedicated to monitoring volcanic ash plumes and eruptions.

9. Intensive basic research should be conducted on the physical, chemical and radiometric properties of volcanic ash, from crater to aged clouds.

10. European recommendations and actions should be coordinated with International Civil Aviation Organization (ICAO), as the global presiding aviation regulatory authority, and with World Meteorological Organization (WMO), as coordinator of the global system of VAACs.

11. A follow-up workshop should be organised to review progress on these recommendations after one year.

Workshop participants

Dr Donny Aminou	ESA
Dr Federico Angelini	Institute of Atmospheric Sciences and Climate – National Research Council
Dr Jean-Louis Brenguier	European Facility For Airborne Research
Dr Dominik Brunner	Eidgenössische Materialprüfungs- und Forschungsanstalt
Dr Maria Fabrizia Buongiorno	Istituto Nazionale Geofisica e Vulcanologia
Dr Elisa Carboni	University of Oxford
Eng. Giovanni Carlesimo	University of L'Aquila
Dr Lieven Clarisse	Université Libre de Bruxelles
Dr Cathy Clerbaux	Centre National de la Recherche Scientifique
Dr Stefano Corradini	Istituto Nazionale Geofisica e Vulcanologia
Dr Alain Dabas	Météo-France CNRM/GMEI/LISA
Prof Dr Gerrit de Leeuw	Finnish Meteorological Institute
Dr Yevgeny Derimian	University of Lille
Dr Mark Doherty	ESA
Dr Sabine Eckhardt	Norwegian Institute for Air Research
Dr Hendrik Elbern	University of Cologne
Dr Richard Engelen	European Centre for Medium-Range Weather Forecasts
Dr Thorsten Fehr	ESA
Prof Fabrizio Ferrucci	Institut de Physique du Globe de Paris
Mr Pierre Fritzsche	German Meteorological Service
Dr Gian Paolo Gobbi	Institute of Atmospheric Sciences and Climate – National Research Council
Dr Kenneth Holmlund	European Organisation for the Exploitation of Meteorological Satellites
Dr Michael Höpfner	Karlsruher Institut für Technologie
Mr Philippe Husson	Météo-France - Toulouse VAAC
Dr Marco Iarlori	Centre of Excellence for the forecast of Severe Weather
Dr Ralph Kahn	NASA
Ms Marianne Koenig	European Organisation for the Exploitation of Meteorological Satellites
Dr Jean-Paul Malingreau	European Commission
Dr Hermann Mannstein	Deutsches Zentrum für Luft– und Raumfahrt
Dr Giovanni Martucci	National University of Ireland Galway
Prof Frank Silvio Marzano	Sapienza University of Rome
Dr Ina Mattis	Leibniz Institute for Tropospheric Research
Dr Luca Merucci	Istituto Nazionale Geofisica e Vulcanologia
Dr Rosemary Munro	European Organisation for the Exploitation of Meteorological Satellites
Dr Nicole Papineau	Institut Pierre-Simon Laplace
Dr Gelsomina Pappalardo	Centre National de la Recherche Scientifique
Dr Nicola Pergola	Institute of Methodologies for Environmental Analysis
Dr Simon Pinnock	ESA
Dr Fred Prata	Norwegian Institute for Air Research
Prof John Remedios	University of Leicester
Dr Andreas Richter	University of Bremen
Ms Meike Rix	Deutsches Zentrum fur Luft –und Raumfahrt
Prof Dr Bill Rose	Michigan Technological University
Dr David Schneider	US Geological Survey
Dr Simona Scollo	Istituto Nazionale Geofisica e Vulcanologia
Dr Petra Seibert	University of Natural Resources (Vienna)
Dr Claudia Spinetti	Istituto Nazionale di Geofisica e Vulcanologia
Dr Piet Stammes	The Royal Netherlands Meteorological Institute
Dr Steve Tait	French Volcanologic and Seismologic Observatories
Dr Werner Thomas	German Meteorological Service
Dr Nicolas Theys	Belgian Institute for Space Aeronomy
Dr Thor Thordarson	University of Edinburgh
Dr Hrobjartur Thorsteinsson	Icelandic Met. Office
Dr Michel Van Roozendael	Belgian Institute for Space Aeronomy

Dr Saji Varghese	National University of Ireland
Dr Matthew Watson	University of Bristol
Dr Claus Zehner	ESA

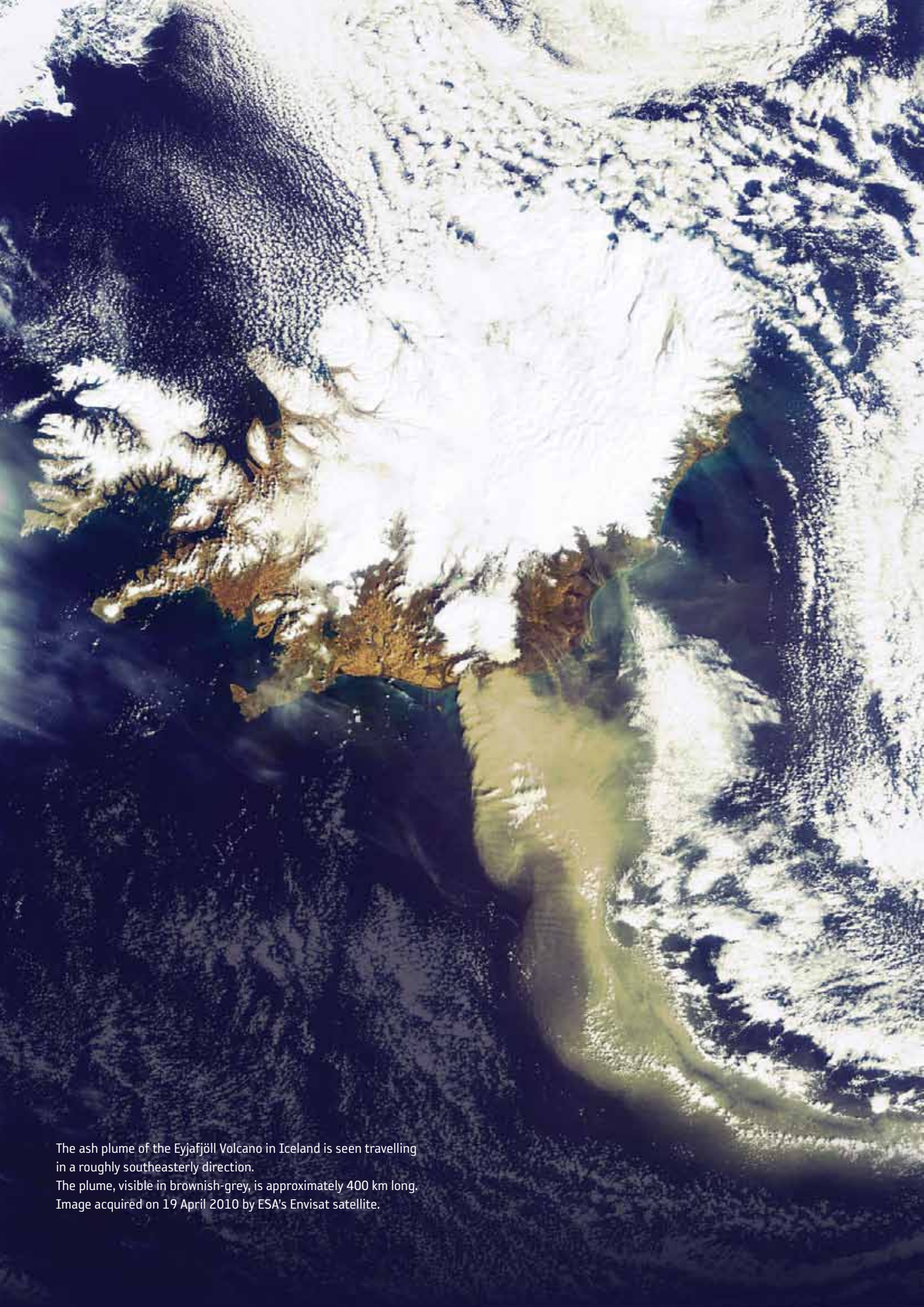

The ash plume of the Eyjafjöll Volcano in Iceland is seen travelling in a roughly southeasterly direction.
The plume, visible in brownish-grey, is approximately 400 km long.
Image acquired on 19 April 2010 by ESA's Envisat satellite.

Question 1:

Are we making the best use of existing observing systems to address the problems created by the Eyjafjöll eruption (airborne, ground-based, satellite)?

Watson, I.M. , Prata A.J., Rose W. I., Saunders R., Schneider D., Thomas H. E., Thordason T., and Zehner C.

1.1 The Eyjafjöll eruption

The 14 April to 23 May 2010 explosive eruption at the 1666 m-high, ice-capped Eyjafjöll volcano, South Iceland, rather unexpectedly caused widespread and unprecedented disruption to aviation and everyday life in large parts of Europe, resulting in economic difficulties that were felt across the globe. Three key factors contributed to producing this widespread problem:

(a) unrelenting explosive activity at the Eyjafjöll volcano,
(b) the high proportion of ash generated by the eruption, and
(c) an atmospheric circulation that directed the ash plume towards Europe.

Prior to this event the Eyjafjöll volcano has not been particularly productive, only producing three small eruptions since ~900 AD, compared with >70 explosive eruptions at the Grímsvötn volcano, the most active volcano in Iceland. The last eruption at Eyjafjöll took place in 1821 and featured intermittent explosive events that deposited a thin tephra layer on the flanks of the volcano over a period of ~18 months.

Over the last 20 years the Eyjafjöll volcano has showed signs of unrest, featuring distinct seismic swarms in 1994, 1996, 1999 and 2009–10. The 1994 and 1999 episodes were associated with significant crustal deformation and interpreted to be a consequence of shallow (4–6 km deep) intrusions. The 2009–10 episode was of similar magnitude to its predecessors, but differed in that it culminated in a small, effusive, alkali-basalt eruption on the eastern flank of Eyjafjöll on 20 March 2010. This event lasted until 12 April 2010, and produced two scoria/spatter cones and a small lava flow with a combined

Fig 1. Steam-rich Eyjafjöll eruption plume at 14:27 on 14 April (first day of the eruption); view is to the North. (Á. Höskuldsson)

Fig 2. Very weak and ash-poor magmatic Eyjafjöll eruption column and plume at 14:43 on 23 April; view is to the West. (Á. Höskuldsson)

volume of ~0.02 km^3. Two days later, following an intense seismic swarm, an eruption began from the summit of the Eyjafjöll volcano at 01:15 UTC on 14 April 2010. Initially the activity was subglacial, but at around 06:00 UTC a white (steam-rich) eruption plume rose from the summit (Fig. 1). This sighting was followed by large-scale discharge of melt water reaching the sandur (i.e. glacial river outwash) plains to north of the volcano at ~06:50 UTC. At the same time a smaller flood event came down the southern flanks of the volcano. Explosive activity picked up later in the day, and shortly after 19:00 UTC a black ash-rich plume rose above the active vents. A sustained phreatomagmatic eruption followed, with an estimated average magma discharge of several hundred tonnes per second, producing large quantities of very fine to fine ash of trachyandesite composition. This phase of the eruption maintained a 5–9 km-high eruption column and lasted until midnight on April 17. Prevailing winds carried the ash-rich eruption plume towards the southeast and south and thereafter over Europe.

Towards the evening of 18 April there was a marked change in style and intensity of the eruption although the composition of the erupted magma was unchanged. The eruption style changed from phreatomagmatic to magmatic, implying that external water no longer had ready access to the vents. This change coincided with a change in the eruption intensity, which dropped by an order of magnitude, and a comparable reduction in ash production. This state of activity continued through 4 May. At this time, the magma discharge ranged from a few tonnes per second to a few tens of tonnes per second and the height of the eruption column fluctuated between 2 km and 5 km above sea level. Lava emerged from the vents on 19 April and advanced to the north at a steady rate over a period of ~30 days, slowly melting its way through the ice of the Gígjökull outlet glacier. Following an episode of renewed seismic activity between 3 May and 5 May, the intensity of explosive activity increased, featuring 5–9 km-high eruption columns and increased production of ash. This resurgence in activity led to further disruption to air traffic in Europe.

The Eyjafjöll eruption of 2010 was the largest explosive eruption in Iceland since that of Hekla in 1947. In the last forty years, eight eruptions have occurred in Iceland with explosive phases resulting in tephra fallout in parts of Iceland. Four of these events were magmatic (i.e. Hekla 1971, 1980, 1991, and 2000) and three were phreatomagmatic (i.e. Gjálp 1996, Grímsvötn 1998 and 2004). The 2010 Eyjafjöll eruption featured both styles, the initial phase being phreatomagmatic and the remaining phases magmatic. In six of these events (i.e. Hekla 1971, 1980, 1991, and 2000, Gjálp 1996, Grímsvötn 2004) the eruption plumes were dispersed to the north and northeast over the Arctic region and therefore the impact on air traffic was minimal. However, it is worth noting that phreatomagmatic eruptions, including possible future eruptions at the subglacial Katla volcano, have the potential to cause considerable disruption to air traffic, because they are pronounced ash-producing events that typically

last for days or weeks. However, it was the very small grain size of the ash from the 2010 Eyjafjöll eruption that particularly facilitated the long-range dispersal and the widespread effects.

1.2 Operational observation capacity

1.2.1 Volcanic ash cloud observations close to the volcano

The Iceland-based eruption monitoring and observation activities were carried out by the IMO (Icelandic Meteorological Office) in close collaboration with the IES (Institute of Earth Sciences at the University of Iceland). These included:

- Continuous GPS-based ground deformation measurements (these are an important monitoring tool prior to and during an eruption).

- Eruption-related seismicity. This was twofold:

  - Recording of volcano-tectonic earthquakes, which are generated by rupture of solid (brittle) rock; and
  - Recording of volcanic tremor, which is a sustained harmonic or spasmodic seismic signal observed during active stages. The seismic signal results from the interaction between magmatic (or hydrothermal) fluids and the surrounding rocks.

- IMO weather radar estimates of the height of the eruption column.

- Surveillance flights, i.e. visual observations of the nature/style of the activity, conditions around the eruption site, and estimates of eruption column heights. These were coordinated by the IES and largely carried out by IES staff.

- On-site observations and measurements, including characterisation of the tephra (ash) fallout at various times and changes therein.

  This activity was primarily carried out by IES staff, who were also responsible for grain-size analyses of the ash samples collected from the fallout in Iceland. This information contributed significantly to changes of the NAME model input parameters during the eruption.

- A FALCON (DLR research aircraft) measurement campaign of the eruption plume in Icelandic airspace.

The near-source methods provided the following information:

- GPS-measurements:
  Realtime ground deformation recorded at several GPS stations located around the Eyjafjöll volcano.

- Seismicity:
  Volcano-tectonic earthquakes can be caused by renewed intrusion of magma into the roots of the volcano, i.e. inflation and establishment of new subsurface magma pathways, or by deflation/subsidence of the volcano. In no way do they provide information on the eruption intensity. Volcanic tremor sometimes appears to show positive correlation with eruption intensity, but a number of times during the Eyjafjöll eruption it exhibited inverse relation with the intensity of the eruption.

- Documentation of the principal dispersal direction and broad-scale visual character of the eruption plume by near-source satellite (coordinated and

carried out by Ingibjörg Jónsdóttir at the IES), and INSAR-type measurements (carried out and researched by the Deformation Team at IES).

— Satellite-based estimates of the height of the eruption plume, ash concentration within it and effective grain size (carried out by institutions outside Iceland, and generally not coordinated with the observations undertaken in the near-source field).

— Estimates of the magma discharge from the erupting vents. These were primarily based on an empirical relationship established between observed eruption column heights and magma discharge for 'Plinian eruptions'. Estimates of concentration of solid material (i.e. ash) in the eruption plume/cloud were primarily based on theoretical assumptions.

Notes:

— No lidar-based observations were carried out in Iceland.

— Near-source observations did not include estimates of the ash concentration in the eruption plume.

— Theoretical assumptions were later supported by satellite-based observations of the mid- to far-field ash plume/cloud.

1.2.2 VAAC volcanic ash observation and monitoring capability

Satellite images of volcanic eruptions are at present used in three main ways by VAACs (Volcanic Ash Advisory Centres):

— When possible (which is rarely), providing data on the thermal output of an eruption as well as estimates of the height of the eruption column at time of observation plus some information on the behaviour of the column top and/or collapsing eruption columns.

  This capability of satellite observations was underused in terms of near-realtime monitoring of the 2010 Eyjafjöll eruptions. This capability is restricted to the high spatial resolution sensors (e.g. ASTER) that have very long repeat times (days) and narrow swath widths, severely restricting the chances of making such measurements.

— Observing the movement and extent of the ash cloud (in terms of height, thickness/depth, location, and mass loadings).

— Informing and validating numerical model predictions of ash cloud extent. The largest uncertainty in the ability of numerical models to predict the spread of volcanic ash, and hence to advise aviation regulators, is in observations of the eruption itself. Specifically, more accurate information on how high the ash is being emplaced at source, the mass eruption rate and near source plume dynamics, leads to better constraints on downstream ash locations.

Current and planned UK VAAC remote sensing measurement usage is detailed in Annex 1a.

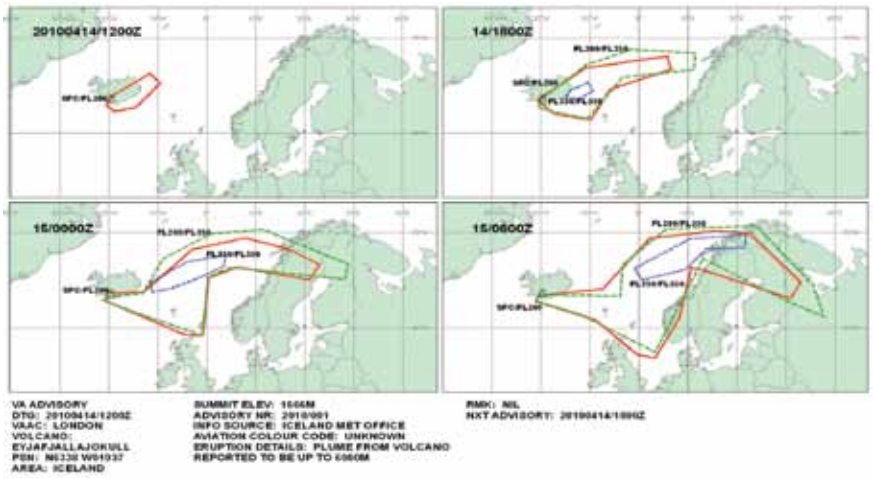

Fig 3. Ash Advisory issued by the London VAAC on April 14 including forecasts for April 15. (UK Met Office)

1.3 UK VAAC volcanic ash cloud modelling, its official role, and Met Office response to regulators

The UK Met Office's role throughout the eruption has been defined by its internationally-designated remit as a VAAC. The Met Office provides this service in accordance with the requirements of the International Civil Aviation Organization (ICAO).

The Met Office's capability to predict the transport and spread of pollution is delivered by the NAME (Numerical Atmospheric-dispersion Modelling Environment) computer model. Development of the model began following the Chernobyl nuclear accident in 1986, and since that time it has been used to model a wide range of atmospheric dispersion events, including previous volcanic eruptions and the Buncefield explosion in 2005. In addition to its role as an emergency response guidance tool, the model is used for routine air-quality forecasting and meteorological research activities. NAME provides a flexible modelling environment, able to predict dispersion over distances ranging from a few kilometres to the whole globe, and for time periods from minutes upwards.

The Met Office London VAAC products are based on six-hour averages and on averages over three flight layers: 0 to 20 000 feet (FL 000 to FL 200), 20 000 to 35 000 feet (FL 200 to 350), and 35 000 to 55 000 feet (FL 350 to FL 550).

For forecasts which have been initialised consistently there has been a remarkably good agreement between VAAC predictions (London, Toulouse and Montreal) and those from other models that are applicable to the eruption (NILU-FLEXPART and GMES MACC EURAD products).

There needs to be proper interpretation of products from different models, as there are not direct one-to-one comparisons. For instance, certain models provide total-column SO_2: a single, vertically-integrated product which gives the boundaries of an aerosol closely related to volcanic ash. The VAACs provide thresholds of ash concentration at a number of different layers in the atmosphere. Furthermore the open question has to be addressed how these models account for removal of ash from the atmosphere during transport!

1.3.1 Supplementary products: red, grey and black areas

At the request of the CAA in the UK, the Met Office has added new, supplementary products to the official VAAC advisories that can be found at the Met Office website:
www.metoffice.gov.uk/corporate/pressoffice/2010/volcano/forecasts.html

The outer edges of the **red zones** on these charts represent the standard threshold (200 µg of ash per cubic metre). The **grey areas** represent

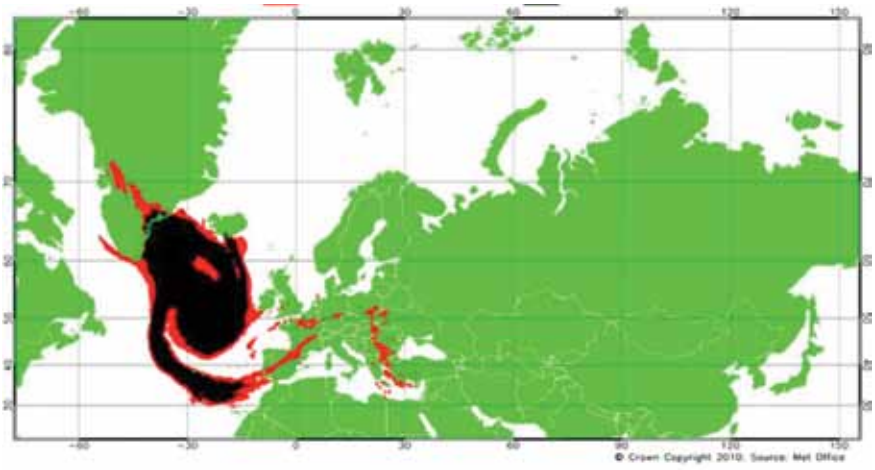

Fig 4. London VAAC modelled Eyjafjöll ash plume extension and concentration over Europe for 5 May 2010. Black areas indicate airspace where the ash concentration exceeds threshold values (no-fly zone) and red areas indicate airspace where ash might be encountered by aeroplanes. (UK Met Office)

ash concentrations that are 10 to 20 times the standard (red) threshold, representing an ash concentration of 2000 to 4000 µg m^{-3}. To operate in this new zone, airlines need to present the CAA with a safety case that includes the agreement of their aircraft and engine manufacturers. The **black areas** represent ash concentrations that are 20 times the standard (red) threshold and twice the grey threshold (concentrations greater than 4000 µg m^{-3}). These are areas within which engine manufacturer tolerances are exceeded.

Note: Each model forecast of the extent of the ash cloud assumes that the volcano will continue to erupt at the same intensity for the duration of the forecast period. During the course of the Eyjafjöll eruption, the volcano's activity did not remaine constant for more than a couple of days.

1.4 Impact on European airspace in the period 14 April – 23 May 2010

The eruption of the Eyjafjöll volcano on 14 April 2010 affected economic, political and cultural activities in Europe and across the world. In response to concerns that ash ejected by the volcano would damage aircraft engines, the warning system put in place under the International Civil Aviation Organization (ICAO) has been successful in preventing aircraft from flying through potentially-dangerous ash. The controlled airspace of many countries was closed, resulting in the largest air traffic shutdown since World War II. The closures caused millions of passengers to be stranded, not only in Europe but across the world. With large parts of European airspace closed to air traffic, many more countries were affected as flights to and from Europe were cancelled.

After an initial uninterrupted shutdown over much of northern Europe from 15 April to 21 April, the restrictions were lifted over Europe through the introduction of new guidelines on volcanic ash density. Although the ICAO's 'any ash, no fly' policy may work over airspaces in vast countries such as the US, where flights can easily re-route or find alternative flight paths, it triggered unexpected levels of disruption in Europe, where a single ash cloud covered and closed down most major European airports, bringing air commerce to a standstill.

After 21 April, airspace was closed intermittently in different parts of Europe, as the path of the ash cloud did not intersect the major part of continental Europe. The ash cloud caused further disruptions to air travel operations in Ireland, Northern Ireland and Scotland on 4 and 5 May, and in Spain, Portugal, northern Italy, Austria and southern Germany on 9 May. Irish and UK airspace closed again on 16 May and reopened on 17 May.

The International Air Transport Association (IATA) estimated that the airline industry worldwide lost about €148 million per day during the disruption (about €2.5 billion in total). There was also a wider impact on the economies of several countries. Some sectors that depend on air-freighted imports and exports (e.g. Kenya) were badly affected by the flight disruptions. Shortages of imported flowers, fruits and electronic hardware were reported in the days immediately after the disruption.

1.5 Change from zero tolerance to an ash threshold value (from CAA report)

This section summarises the position reached by the UK Civil Aviation Authority (CAA) and provides an evidence-based case for a change to the current volcanic ash zoning arrangements following a review, conducted in conjunction with aircraft and engine manufacturers, airlines, NATS and the UK Met Office, of the latest service experience and flight test data. The aim of the CAA is to reduce the level of disruption to flights resulting from volcanic activity in the region whilst ensuring the safety of the travelling public.

The current volcanic ash zones are based on the following definitions:

— No Fly Zone (NFZ): Any area where volcanic ash concentrations are predicted to be higher than 2×10^{-3} g m^{-3}.

— Enhanced Procedures Zone (EPZ): Any area where volcanic ash concentrations are predicted to be between 2×10^{-4} g m^{-3} and 2×10^{-3} g m^{-3}.

These definitions were based on agreed tolerance levels as determined by the aircraft and engine manufacturers. In response to the exceptional operational circumstances being experienced in the UK due to volcanic ash, the airframe and engine manufacturers continued to review service experience and flight test data, and to hold discussions with regulators, airlines, research centres, air traffic control service providers and meteorological agencies, with a view to further refining the airworthiness safeguards put in place to manage operations in UK airspace.

Please take note that the international ICAO rules are still at zero tolerance (no threshold value) at the time of writing.

1.5.1 The risk to be addressed

The key risk to be addressed remains one of airworthiness: the ability of an aircraft to continue to function safely when exposed to volcanic ash. The most likely reason that flight continued safely is that the ash was avoided and hence there was no severe engine damage. There is evidence also that there are lower concentrations of ash which will not prejudice continued safe flight but will cause damage resulting in accelerated engine wear and a need for increased engineering interventions. However, if addressed by appropriate inspection and maintenance procedures, such damage will not put at risk the continued safe flight of the aircraft. At yet lower levels, no adverse impact is discernible.

1.5.2 Airworthiness limits

Data on the effects of volcanic ash ingestion are not sufficient to determine the specific level of ash contamination which would preclude continued safe flight and landing, particularly as the effects can be expected to vary across different types of engine. However, the level of ash which analysis has judged to have resulted in two multiple engine shutdown events is understood to be approximately 2 g m^{-3}. At this level of ash density, engine shutdown occurred

after a matter of minutes of exposure. The current maximum tolerable level for continuous operation, as determined by manufacturers based on engineering judgment and other data, is 2 x 10^{-3} g m^{-3}: this is three orders of magnitude lower than the level thought to cause engine shutdown.

The boundary has not been determined between the level of ash contamination that causes damage sufficient to prevent continued safe fight and landing, and the level that causes damage that would cause accelerated engine wear and increased engineering interventions. The manufacturers have specified their requirements for such intervention and, for the vast majority of products, little intervention has been found to be necessary in practice for continuous operations in the EPZ, i.e. concentrations up to 2 x 10^{-3} g m^{-3}. For some older engine types from certain manufacturers, however, borescope inspection has been required increasingly often. No Mandatory Occurrence Report (MOR) received by the CAA to date has indicated damage from flying in the EPZ, supporting the judgment of the manufacturers. The results from pathfinder flights conducted in the early stages of the crisis were also positive.

The aircraft and engine manufacturers have now had the opportunity to review further the information available to them from instrumented flight tests and encounters with volcanic ash around the world. Certain manufacturers have determined that, for specified airframe and engine combinations, transient (i.e. time-limited) operations in areas of volcanic ash with densities predicted by the UK Met Office of up to 4x10^{-3} g m^{-3} are acceptable. It is possible that this limit may be raised even further as more information becomes available from flight test data and service experience. Such operations may be time-limited. In addition, precautionary maintenance practices may be specified to airlines by the aircraft manufacturers in conjunction with their engine suppliers. To facilitate this new limit a 'Time Limited Zone' has been introduced which is defined as:

> *"The volumes of airspace as marked on the Met Office London VAAC NWP Volcanic Ash Concentration Charts where ash concentrations are predicted to exist within which flight for a limited time duration may be permitted before engine manufacturer tolerance levels are exceeded."*

In summary:

- Volumes of airspace of volcanic ash with densities predicted by the Volcanic Ash Advisory Centre (VAAC) to be in excess of 2 x 10^{-3} g m^{-3} remain No Fly Zones;

- Operations in volumes of airspace declared as Time Limited Zones are acceptable provided that:

  - the VAAC predicted volcanic ash density is less than 2 x 10^{-3} g m^{-3}
  - the operator has a safety case, supported by data from their aircraft and engine manufacturers, that supports operation in this zone

1.5.3 Conclusions

The risk to be addressed is the likelihood of an encounter with ash that results in the aircraft being unable to continue safe flight. To address this risk the CAA needs to be satisfied that the airworthiness limits are well understood and the likelihood of an ash encounter at concentrations that would result in the aircraft being unable to continue safe flight is acceptably low. With regard to airworthiness limits, the lowest ash concentration that would result in an aircraft not being able to continue safe flight is not known, however the current tolerance level agreed by the manufacturers is three orders of magnitude lower than the concentration thought to have caused multiple engine shutdown.

Confidence in the ongoing safety of operations in the presence of ash contamination has grown significantly through the experience gained in this volcanic event and has also helped determine how the aviation community might improve the way it uses the VAAC forecasts. The boundary of 2 x 10^{-3} g m^{-3} provided by the VAAC forecast process is a probability of a mean value and is not a fixed line in space. There can, therefore, never be complete certainty of the position of the ash. However, the model is considered to have a satisfactory level of accuracy and to include a good level of conservatism. There are additional levels of conservatism in the system that further mitigate any residual risk.

1.6 Non-operational (research) observational capacity

There exist an extensive range of satellite-borne sensors on various platforms, in both geostationary and low earth orbit (LEO), which span a range of wavelengths, repeat times, footprints and sensitivities (Table 1). The most heavily used during the eruption were SEVIRI, AVHRR, MODIS and OMI. Some general observations can be made about the retrieval of volcanogenic components:

— No one sensor provides a magic bullet for detection of volcanogenic material in the atmosphere. The collection of sensors used is better termed 'magic buckshot': in conjunction, the sensors used together form a powerful observational tool.

— Shortwave (UV and visible) sensors can only measure during daylight and are hampered by clouds and generally cannot discriminate ash; IR sensors are also hampered by clouds.

— Many sensors have limited temporal coverage.

— Imaging sensors tend to have a smaller footprint than high resolution spectrometers (UV or IR instruments).

— Most observations measure volcanic ash and/or SO_2. These measurements are typically presented in units of column integrated burden[1] (DU, g m^{-2}), brightness temperature differences or some form of a qualitative index.

— SO_2 is easier to quantify than volcanic ash, due to the fact that background values are generally very low and there is good sensitivity to absorption in the UV and IR.

— Vertically-resolved quantitative information (e.g. concentration) is not typically available in NRT.

— Infrared imagers can provide retrieval of IR optical depth, effective radius, column integrated mass and cloud top altitude.

— Satellite lidars can measure at night as well as during daytime and are less hampered by clouds than passive sensors, but observe only along a fixed line of sight. Ash can be identified using polarisation and two-wavelength backscatter profiles, although there are currently no automated algorithms. Mass concentration profiles can be estimated from lidar profiles, given an estimate of particle size and density.

[1] Dobson Unit (DU) = molecules per square metre or g m^{-2}

Table 1. (Adapted from Thomas and Watson, 2009)

	Instrument	Platform	Altitude (km)	Equator crossing time (local)	Operational since	Spatial resolution (nadir)	Spectral range	Species	Examples in the literature
Infrared	GOES	GOES 10-13	35 790	Geostationary	10/1975	1 – 4 km	5 channels: 0.52 – 12.5 μm	Ash	Hilliger & Clark, 2002 Yu et al., 2002
	AVHRR	NOAA 14 & K,L,M,N	833 ± 19	Variable	10/1978	1.1 km	5 channels: 0.5 – 12.5 μm	Ash Aerosol	Webley et al., 2008 Pergola et al., 2004 Prata, 1989
	TOVS (HIRS)	NOAA 14 & K,L,M,N	833 ± 19	Variable	10/1978	~ 17 km	19 Channels: 3 – 15 μm & one at 0.7 m	SO_2	McCarthy et al., 2008 Prata et al., 2003
	ASTER	Terra	705	10:30 (desc.)	12/1999	15 m (VNIR) 30 m (SWIR) 90 m (TIR)	14 Channels: 0.5 – 11.6 μm	Ash SO_2	Urai, 2004
	MODIS	Terra, Aqua	705	10:30 (desc.) 13:30 (asc.)	12/1999 06/2002	250 m (1 – 2) 500 m (3 – 7) 1 km (8 – 36)	36 Channels: 645 nm – 14.2 μm	Ash Aerosol SO_2	Novak et al., 2008 Watson et al., 2004 Corradini et al., 2008 Pavolonis et al., 2006
	AATSR	Envisat	800	10:00 (desc.)	03/2002	Ocean: 1 x 1 km Land: 1 x 1 km	VIS – NIR: 0.55, 0.659, 0.865 μm SWIR: 1.6 μm MWIR: 3.7 μm TIR: 10.85, 12 μm	Ash Aerosol	Spinetti et al., 2008
	MIPAS	Envisat	800	10:00 (desc.)	03/2002	Vert: 3 km Vert. scan: 5 – 150 km Horiz: 3 x 30 km	MWIR – TIR: 4.15 – 14.6 μm	Cloud top alt. SO_2	Burgess et al., 2004
	TES	Aura	705	13:45 (asc.)	05/2002	0.5 x 5 km	3.2 – 15.4 μm in 200 – 300 cm^{-1} bands	SO_2	Clerbaux et al. 2008
	AIRS	Aqua	680	13:30 (asc.)	06/2002	14 km	2378 channels: 3.6 – 15.4 μm	Ash SO_2	Prata & Bernardo, 2007 Carn et al., 2005 Gangale et al., 2010
	SEVIRI	MSG	35 800	Geostationary	08/2002	1 km (visible) 3 km (all others)	12 channels: 0.4 – 13.4 μm	Ash Aerosol SO_2	Prata & Kerkmann, 2007 Corradini et al., 2009
	MTSAT	MTSAT-1R	35 800	Geostationary	02/2005	1 – 4 km	5 channels: 0.55 – 4.0 μm	Ash	Tokuno, 2000
	IASI	MetOp	817	09:30 (desc.)	10/2006	12 km	8461 channels: 3.7 – 15.5 μm	Ash SO_2 Aerosol	Clarisse et al., 2008

(asc.) = ascending, (desc.) = descending

Table 1. Adapted from Thomas and Watson, 2009. (Continued)

	Instrument	Platform	Altitude (km)	Equator crossing time (local)	Operational since	Spatial resolution (nadir)	Spectral range	Species	Examples in the literature
Ultraviolet	SBUV/2	NOAA 9–16, M	833 ± 19	Variable	12/1984	200 x 200 km	12 Channels: 160 – 400 nm	SO_2	McPeters (1971–1974)
	GOME GOME-2	ERS-2 MetOp	795 817	10:30 (desc.) 09:30 (desc.)	04/1995 10/2006	320 x 40 km 80 x 40 km	240 – 793 nm	SO_2 Aerosol index	Khokhar et al, 2005 Eisinger & Burrows, 1998 De Graaf et al., 2005 Thomas et al., 2003 Rix et al, 2009
	SCIAMACHY	Envisat	800	10:00 (desc.)	03/2002	60 x 30 km	240 – 2380 nm	SO_2 Aerosol index	Afe et al., 2004 Bramstedt et al., 2004 Tilstra et al., 2007
	OMI	Aura	705	13:45 (asc.)	07/2004	13 x 24 km	270 – 500 nm	Ash SO_2 Aerosol Aerosol index	Yang et al., 2007 Krotkov et al., 2006 Torres et al., 2002
Visible	MERIS	Envisat	800	10:00(desc.)	03/2002	Ocean: 1040 x 1200 m Land: 260 x 300 m	15 Channels: 390 – 1040 nm	Ash Aerosol	Spinetti et al., 2008
	CALIOP	CALIPSO	705	13:31 (asc.)	04/2006	Vert: 30 – 300 m Horiz: 0.3 – 5 km	2 lasers at 531 & 1064 nm	Aerosol plume altitude	Winkler et al., 2007
	MISR	Terra	705	10:30 (desc.)	12/1999	From 275 x 275 m up to 1.1 x 1.1 km	9 cameras with 4 wavelengths: 443 nm, 555 nm, 670 nm, 865 nm	Aerosol plume altitude	Kahn et al., 2007 Urai et al., 2004
µwave	MLS	AURA	604 705	13:45 (asc.)	05/2002	Vert: 2–3 km Horiz: 160 km	3 channels: 63 – 203 GHz 7 Channels: 118 – 2250 GHz	SO_2 HCl	Prata et al., 2003 Waters et al, 2006

(asc.) = ascending, (desc.) = descending

Although the radius of the bulk of the solid material (i.e. tephra) produced by the eruption on 14–15 April was > 10 µm, on-site observations along with grain size analysis of samples from the ash fallout in Iceland indicate that more than 50% of the solids ejected at this time were less than 50 µm in diameter and ≤20% was smaller than 10 µm. This is in line with the on-site observations that magma fragmentation was enhanced by explosive interaction between the magma and external water provided by melting of the glacier that caps the volcano. The observations, primarily from OMI, AIRS and IASI, of the amount of SO_2 produced during the magmatic phase increased in line with petrological estimates. The AIRS concavity index accurately observed the transition from basaltic to magmatic glass dominating the fine ash. This was, again, corroborated by laboratory studies of the ash undertaken by the IMO. Ground-based, airborne and satellite-based lidars provided critical information on height and layering of volcanic ash.

Of the 'operational' satellites, SEVIRI (having the ability to map SO_2 in two IR channels and ash in the split window) provided the most regular insight into the cloud's evolution. These data were augmented by regular observations from AVHRR and MODIS (ash), OMI, AIRS, IASI and GOME-2 (SO_2 and Aerosol Index) and supported by the full range of products providing height, from instruments such as MISR, CALIOP and ASTER. These products were used to corroborate the output from the NAME model, and, for the most part agreement in horizontal extent was very good. There are a few examples (as Fig 5 below) where some of the observed plume lay outside the boundaries suggested by the dispersion model.

1.7 IUGG Statement "Volcanological and Meteorological Support for Volcanic Ash Monitoring"

A statement was adopted by the IUGG Bureau on 28 May 2010 and follows the IUGG Statement of 20 April 2010 on Volcanic Ash Clouds.

"*The eruptions of the Eyjafjöll volcano, Iceland, during early 2010, have highlighted the importance of a close understanding of the eruptive state of each of the world's active volcanoes, for the safety and health of local residents as well as for air traffic and other purposes. It has become increasingly evident during the eruption that accurate specification of the ash column height and the ash characteristics from the eruption are necessary for safe and efficient routing of air traffic. To be able to forecast ash clouds for the aviation hazards, the clouds' concentration, particle size and total mass is required in real time. The work of the volcanologists and meteorologists of Iceland, bringing together earth and atmospheric sciences, in support of the operations of the London Volcanic Ash Advisory Centre, has been critically important in this regard.*

"*In improving the global response to volcanic clouds as aviation hazards, it must be understood that the great majority of the Earth's active volcanoes are located in less industrialised countries or in remote locations, and are*

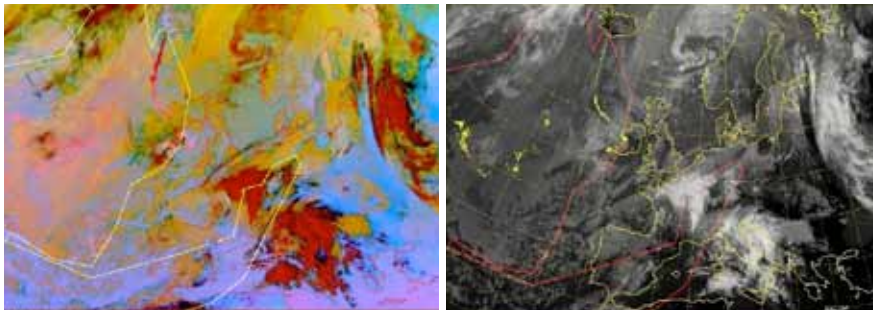

Fig 5. MSG SEVIRI 'dust image' (left) and threshold of –1.3K on T108-T120 (right). Also shown is the polygon contour of the observation for FL000–FL200 from VAAC advisory of 11 May 2010, 06:00 UTC. The contour of the forecast for 12:00 UTC captured most, but not all parts of the ash cloud moving southeastward over Ireland. (DLR/EUMETSAT)

not monitored to the standards of Iceland. Only about 50% of the world's volcanoes that currently threaten air operations have any sort of ground based monitoring. Also, less than 50 of the 1300 volcanoes with Holocene age eruptions (approximately the last 12 000 years) worldwide are considered to be well monitored.

"In this regard, the IUGG emphasises:

- *"The capability to understand, forecast and promptly report eruptions, based on thorough study and instrumentation of active volcanoes, remains vital for aviation safety, for residents exposed to local volcanic hazards, and also for assessing the magnitude and effects of volcanic emissions on our atmosphere and climate;*

- *"An improvement in support for local volcano observatories would improve the timing, scope, and accuracy of information on volcanic activity;*

- *"In meeting requirements from the International Civil Aviation Organization (ICAO) for States to provide volcanological information to aviation, the long term sustainability of such support for volcano observatories is an important consideration. ICAO, advised by the International Union of Geodesy and Geophysics and other organisations including the World Meteorological Organization (WMO), has prepared arrangements where a State may choose to recover reasonable costs for the provision of information to aviation from the aviation industry. A State could, alternatively, choose to support observatories directly without such arrangements. Guidelines on these issues are now available as referenced below;*

- *"Any volcanic crisis places high pressure on the responsible agency: support for aviation functions is typically only one of many aspects of a volcanic crisis that volcanologists must consider. International science protocols, prepared by IUGG constituent association, the International Association of Volcanology and Chemistry of the Earth's Interior (IAVCEI), already exist to assist in scientific cooperation during a crisis, and may be useful in the context of an aviation-focused volcanic crisis;*

- *"Where observations exist (such as satellite data, pilot reports and meteorological radar coverage over a volcanic area), arrangements for multidisciplinary observation sharing between all those concerned with the hazard assessment from the volcanic activity should be specified and followed to ensure the best possible use of observations.*

"In summary, increased support for the volcano observatories of the world, as part of the international science effort to improve volcanic cloud monitoring, is a necessary measure for improving volcanic impact management and aviation safety as well as for aiding natural hazard mitigation on the ground."

References

Afe, O. T., Richter, A., Sierk, B., Wittrock, F. and Burrows, J. P. (2004). BrO emission from volcanoes: A survey using GOME and SCIAMACHY measurements. Geophysical Research Letters 31(24)

Bramstedt, K., Richter, A., van Roozendael, M. and de Smedt, I. (2004). Comparisons of SCIAMACHY Sulfur Dioxide Observations. Proceedings of the Second Workshop on the Atmospheric Chemistry Validation of Envisat (ACVE-1)

Burgess, A.B., Grainger, R.G., Dudhia, A. (2004). Progress in the retrieval of sulphur species from MIPAS. ESA Envisat Symposium, ESA SP-572.

Carn, S. A., Strow, L. L., de Souza-Machado, S., Edmonds, Y. and Hannon, S. (2005). Quantifying tropospheric volcanic emissions with AIRS: The 2002 eruption of Mt. Etna (Italy). Geophysical Research Letters 32(2).

Clarisse, L., Coheur, P. F., Prata, A. J., Hurtmans, D., Razavi, A., Phulpin, T., Hadji-Lazaro, J. and Clerbaux, C. (2008). Tracking and quantifying volcanic SO_2 with IASI, the September 2007 eruption at Jebel at Tair. Atmospheric Chemistry and Physics Discussions 8: 16917–16949.

Clerbaux, C., Coheur, P. F., Clarisse, L., Hadji-Lazaro, J., Hurtmans, D., Turquety, S., Bowman, K., Worden, H. and Carn, S. A. (2008). Measurements of SO_2 profiles in volcanic plumes from the NASA Tropospheric Emission Spectrometer (TES). Geophysical Research Letters 35(22).

Corradini S., Merucci L., and Prata A. J., Retrieval of SO_2 from Thermal Infrared Satellite Measurements: Correction Procedures for the Effects of Volcanic Ash, Atmos. Meas. Tech., 2, 177–191, 2009.

De Graaf, M., P. Stammes, O. Torres, and R.B.A. Koelemeijer, Absorbing Aerosol Index: Sensitivity analysis, application to GOME and comparison with TOMS, J. Geophys. Res. 110, D010201, doi:10.1029/2004JD005178, 2005.

Eisinger, M. and Burrows, J. P. (1998). Tropospheric Sulfur Dioxide observed by the ERS-2 GOME Instrument. Geophysical Research Letters 25(22): 4177–4180.

Gangale, G., Prata, A.J., Clarisse, L., The infrared spectral signature of volcanic ash determined from high-spectral resolution satellite measurements, Remote Sensing of Environment 114 (2), pp. 414–425 (2010).

Gudmundsson MT et al., 2010 Eruptions of Eyjafjallajökull Volcano, Iceland. Eos 91, 21, 25 May, 2010.

Hilliger, D. W. and Clark, J. D. (2002). Principal Component Image Analysis of MODIS for Volcanic Ash. Part I: Most Important Bands and Implications for Future GOES Imagers. Journal of Applied Meteorology 41.

Kahn, R. A., W.-H. Li, C. Moroney, D. J. Diner, J. V. Martonchik, and E. Fishbein, 2007. Aerosol source plume physical characteristics from space-based multiangle imaging, J. Geophys. Res., 112, D11205, doi: 10.1029/2006JD007647

Khokhar, M. F., Frankenberg, C., Van Roozendael, M., Beirle, S., Kühl, S., Richter, A., Platt, U. and Wagner, T. (2005). Satellite observations of atmospheric SO_2 from volcanic eruptions during the time-period of 1996–2002. Advances in Space Research 36: 879–887.

Krotkov, N. A., Carn, S. A., Krueger, A. J., Bhartia, P. K. and Yang, K. (2006). Band residual difference algorithm for retrieval of SO_2 from the aura Ozone Monitoring Instrument (OMI). IEEE Transactions on Geoscience and Remote Sensing 44(5): 1259–1266.

Larsen, (1999). The Eyjafjoll eruption in 1821–23 AD. Short summary of course of events and impact as depicted in contemporary accounts. Scientific Report RH-28–99, Science Institute, University of Iceland; 14 pp. [in Icelandic]

McCarthy, E. B., Bluth, G. J. S., Watson, I. M. and Tupper, A. (2008). Detection and analysis of the volcanic clouds associated with the 18 and 28 August 2000 eruptions of Miyakejima volcano, Japan. International Journal of Remote Sensing 29(22): 6597–6620.

McPeters RD (1971–1974) The atmospheric SO_2 budget for Pinatubo derived from NOAA-11 SBUV/2 spectral data. Geophys Res Lett 20(18)

Novak, M. A. M., Watson, I. M., Delgado-Granados, H., Rose, W. I., Cardenas-Gonzalez, L. and Realmuto, V. J. (2008). Volcanic emissions from Popocatepetl volcano, Mexico, quantified using Moderate Resolution Imaging Spectroradiometer (MODIS) infrared data: A case study of the December 2000–January 2001 emissions. Journal of Volcanology and Geothermal Research 170(1–2): 76–85.

Pavolonis, M.J., Wayne, F.F., Heidinger, A.K., Gallina, G.M., (2006). A daytime complement to the reverse absorption technique for improved automated detection of volcanic ash. Journal Of Atmospheric And Oceanic Technology 23, 1422–1444.

Pedersen R. and Sigmundsson F., (2006). Temporal development of the 1999 intrusive episode in the Eyjafjallajökull volcano, Iceland, derived from InSAR images. Bull Volcanol (2006) 68: 377–393 DOI 10.1007/s00445-005-0020-y

Pergola, N., Lacava, T., Marchese, F., Scaffidi, I., & Tramutoli, V. (2004). Improving volcanic ash cloud detection by a robust satellite technique. Remote Sensing of Environment, 90, 1–22.

Prata, A. J. (1989a) Infrared radiative transfer calculations for volcanic ash clouds Geophys. Res. Lett.,

Prata, A. J. (1989b). Observations of volcanic ash clouds in the 10–12 μm window using AVHRR/2 data. International Journal of Remote Sensing, 10, 751–761.

Prata, A.J. and Grant, I. F. (2001) Retrieval of microphysical and morphological properties of volcanic ash plumes from satellite data: Application to Mt. Ruapehu, New Zealand., Quarterly journal of the Royal Meteorological Society, 127 (576B), 2153–2179.

Prata, A. J., Rose, W. I., Self, S. and O'Brien, D. M. (2003). Global, Long-Term Sulphur Dioxide Measurements from the TOVS Data: A New Tool for Studying Explosive Volcanism and Climate. Geophysical Monograph 139: 75–92.

Prata, A. J. and Bernardo, C. (2007). Retrieval of volcanic SO_2 column abundance from atmospheric infrared sounder data. Journal of Geophysical Research-Atmospheres 112.

Prata, A. J. and Kerkmann, J. (2007). Simultaneous retrieval of volcanic ash and SO_2 using MSG-SEVIRI measurements. Geophysical Research Letters 34(L05813).

Rix M., Valks P., Hao N., van Geffen J., Clerbaux C., Clarisse L., Coheur P.-F., Loyola D., Erbertseder T., Zimmer W. and Emmadi S. (2009). Satellite Monitoring of Volcanic Sulfur Dioxide Emissions for Early Warning of Volcanic Hazards, IEEE Journal of Selected Topics in Applied Earth Observations and Remote Sensing, vol. 2, no. 3, pp. 196–206.

Spinetti, C., Corradini, S., Carboni, E., Thomas, G., Grainger, R., Buongiorno, M.F. (2008). Mt. Etna Volcanic Aerosol and Ash Retrievals using MERIS and AATSR Data. ESA Proc.2nd MERIS/(A)ATSR Workshop, ESA SP-666.

Thomas, H.E. and Watson, I.M., Observations of volcanic emissions from space: current and future perspectives. Natural Hazards, 10.1007/s11069-009-9471-3

Thomas, W., Erbertseder, T., Ruppert, T., van Roozendael, M., Verdebout, J., Balis, D., Meleti, C. and Zerefos, C. (2005) On the Retrieval of Volcanic Sulfur Dioxide Emissions from GOME Backscatter Measurements, J. Atm. Chem. 50, 295–320.

Thordarson, T. and Höskuldsson, Á. 2008. Postglacial volcanism in Iceland. Jökull, 58: 197–228.

Tilstra, L.G., M. de Graaf, I. Aben, and P. Stammes (2007). Analysis of 5 years of SCIAMACHY Absorbing Aerosol Index data, Proceedings of the 2007 Envisat Symposium, ESA SP-636.

Tokuno, M. (2000) MTSAT Window Channels (IR1 and IR2) "Potential for Distinguishing Volcanic Ash Clouds. Meteorological Satellite Center Technical Note, L1032A, 38: 1–11.

Torres, O., Decae, R., Veefkind, J.P., and de Leeuw, G. (2002): OMI Aerosol Retrieval Algorithm, in OMI Algorithm Theoretical Basis Document: Clouds, Aerosols, and Surface UV Irradiance, Vol. 3, version 2, (OMI-ATBD-03, P. Stammes, Ed.), *http://eospso.gsfc.nasa.gov/eos_homepage/for_scientists/atbd/docs/OMI/ATBD-OMI-03.pdf*.

Urai, M. (2004). Sulfur dioxide flux estimation from volcanoes using Advanced Spaceborne Thermal Emission and Reflection Radiometer – a case study of Miyakejima volcano, Japan. Journal of Volcanology and Geothermal Research 134(1–2): 1–13.

Waters J.W., Froidevaux L., Harwood R.S. et al (2006). The earth observing system microwave limb sounder (EOS MLS) on the Aura satellite. IEEE T Geosci Remote 44(5): 1075–1092

Watson, I.M., Realmuto, V.J., Rose, W.I., Prata, A.J., Bluth, G.J.S., Gu, Y., Bader, C.E. and Yu, T. (2004). Thermal infrared remote sensing of volcanic emissions using the moderate resolution imaging spectroradiometer. Journal of Volcanology and Geothermal Research 135(1–2): 75–89.

Webley, P.W., Wooster, M.J., Strauch, W., Saballos, J.A., Dill, K., Stephenson, P., Stephenson, J., Escobar Wolf, R. and Matias, O. (2008). Experiences from Real-time Satellite-Based Volcano Monitoring in Central America: Case Studies at Fuego, Guatemala. International Journal of Remote Sensing 29(22): 6618–6644.

Winker, D. M., Hunt, W. H. and McGill, M. J. (2007). Initial performance assessment of CALIOP. Geophysical Research Letters 34(L19803).

Yang, K., Krotkov, N.A., Krueger, A.J., Carn, S.A., Bhartia, P.K. and Levelt, P.F. (2007). Retrieval of large volcanic SO_2 columns from the Aura Ozone Monitoring Instrument: Comparison and limitations. Journal of Geophysical Research-Atmospheres 112(D24).

Yu T.X., Rose W.I., Prata A.J. (2002). Atmospheric correction for satellite-based volcanic ash mapping and retrievals using "split window" IR data from GOES and AVHRR. Journal of Geophysical Research-Atmospheres, Volume: 107, Issue: D16, Article Number: 4311.

The Eyjafjöll volcanic ash plume as observed from the DLR Falcon research aircraft on 1 May about 70 km south-east of the volcano. (B. Weinzierl, DLR)

Question 2:

How can the R&D community best contribute to improving VAAC analysis and prediction of volcanic ash plumes?

Elbern, H., Broad A., Engelen R., Husson P., Scollo S., Seibert P., Stohl A., Tait S., Thordarsen T., and Varghese S.

2.1 Introduction

During the first days of the Eyjafjöll eruption, the London VAAC's NAME model simulations were used for flight-ban decisions, on a zero tolerance basis. Models from other VAACs and various R&D models across Europe were set up to provide further simulations. However, the experience from the last few months demonstrates that there is insufficient combination of sophisticated transport models with the wealth of new Earth observation data for improved eruption plume predictions. The present chapter seeks to identify weaknesses and proposes actions to achieve substantial progress from combining existing developments to achieve a better volcanic ash cloud forecasting infrastructure.

2.2 Ash plume models

A wide range of numerical models exist that can be used to predict the transport of gases and aerosols emitted during volcanic eruptions. The models used range from simple trajectory models to complex chemistry transport models that can include detailed treatment of aerosol microphysics. Some of these models are even run online with the meteorological forecast model. It is beyond the scope of this document to describe all of these models, but the most widely used (including the VAAC models) are briefly explained in "Annex 2a: Description of some European ash transport models".

The models used for volcanic ash plume prediction have been validated extensively – however, mostly not in the context of simulation of volcanic ash clouds. For instance, a number of long-range tracer experiments have been conducted in Europe and North America with the specific purpose of validating numerical transport and dispersion models. The most recent one was the European tracer experiment ETEX. Practically all currently-used models for long-range transport from point releases were tested in this experiment, and the first results were published in a special issue of Atmospheric Environment (Volume 32, Issue 24, December 1998).

A follow-up activity is the JRC ENSEMBLE project which has conducted a large number of model inter-comparisons for (mostly nuclear) emergency response models. A further inter-comparison is planned for the Eyjafjöll eruption. A limitation of both ETEX and ENSEMBLE with respect to volcanic ash applications is their limitation to ground-level releases of more or less inert gaseous tracers. Many of the models have also been validated by comparing their predictions of specific long-range transport episodes such as transport of Saharan dust or North American or even Asian pollution plumes to Europe with available ground-based, aircraft or remote sensing observations.

The models' ability to predict volcanic ash transport has not been tested as extensively. Mostly, individual models were compared against satellite observations of SO_2 or volcanic ash. The last inter-comparison of VAAC dispersion models was conducted after the Grimsvötn Icelandic eruption

of 2004 (Witham et al., 2007), but there seems to be a need to redo these comparisons with a larger ensemble of models and using quantitative skill measures (coordinated with other modelling activities, e.g. WMO). The Grimsvötn inter-comparison showed that the models generally simulated very similar dispersion patterns. However, the model forecasts were highly dependent on the amount of eruption information assumed to be available at the time of the model runs. This already highlights one main difficulty of volcanic ash dispersion calculations, namely to constrain the source term well enough. This problem becomes even more pronounced now that quantitative predictions are required to include certain ash concentration thresholds.

Currently-used transport models already include many of the relevant processes, such as dry and wet deposition. Nevertheless, for future applications, more sophisticated modules for aerosol modelling are required, to simulate all relevant aerosol processes. These include simple sedimentation, but also interaction like coagulation and aggregation of aerosols of different sizes and formation of water-soluble aerosols from emitted gas phase precursors. The interaction between ice particles and aerosols is also a relevant process, especially considering that eruptions often include water vapour and that ash particles may act as ice nuclei. Prioritisation is required of which processes are important to volcanic eruptions.

2.3 How can we make better use of remote sensing to improve model forecasts?

2.3.1 Eruption source and ash cloud extent information

Eruption source information is essential to initialise volcanic ash dispersion models, improve their skills, and reduce the hazard from volcanic ash forecast failures to aviation. In the case of single, discrete plume or short time eruptions, qualitative emission information was probably sufficient to predict the regions affected by volcanic ash. For instance, approximate plume top heights as a function of time (as they were available from local observers, webcams, or radar during the Eyjafjöll eruption) are commonly used in conjunction with numerical volcanic eruption column models to predict the magma discharge from the source vents, which in turn is used as a proxy for the mass loading

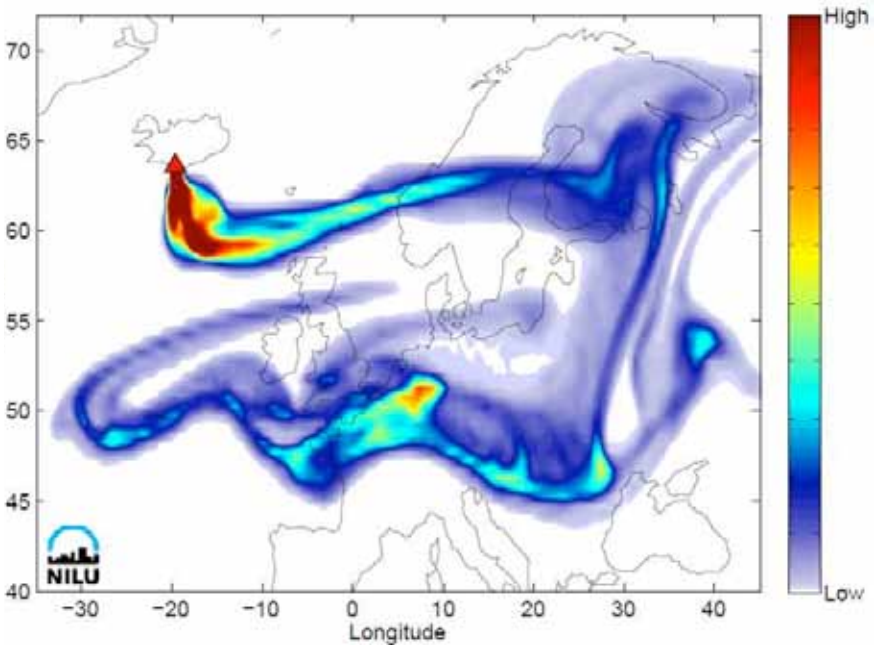

Fig 6. FLEXPART simulation of the volcanic emission from Eyjafjöll in April 2010. The forecast was issued about one day after the eruption onset, and the figure shows the forecast two days ahead. The volcano is marked by a red triangle. As the emission strength was unknown at the time of the forecast, the concentrations of the volcanic emissions can only be rated from 'high' to 'low' as given by the colour bar. (NILU)

of ash by the volcanic plume. The source strength used was often adjusted subjectively by visual comparison with satellite observations of ash to obtain a reasonable fit with the available observation data. With the recent introduction of specific ash concentration thresholds, however, the ash source term must be known with high accuracy as a function of time and altitude for the entire duration of an eruption. This poses a great challenge since current eruption column models do not fully account for the range of known explosive eruption styles, and the uncertainties on obtained magma discharge are very large for weak plumes. Objective and automatic methods will be needed in the future, to determine the ash source term by combining volcanological *a priori* information, satellite remote sensing and other observational data, and model results. Such objective techniques are commonly known as inverse modelling and data assimilation.

Key parameters needed to characterise the source term are, in order of priority:

i) the total erupted mass (total volume and maximum height of plume);
ii) the particle size distribution of the erupted mass after aggregation;
iii) the grain-size distribution, including vertical distribution and density of the particles.

These parameters should be given as functions of time, as they will change during the course of an eruption.

All these parameters can be estimated from volcanological and local (qualitative) observations combined with *a priori* knowledge from previous eruptions as well as by atmospheric measurements. Ideally, a model should be used to combine the various sources of information in an optimal way.

2.3.2 Timeliness

The greatest danger to aviation occurs immediately after the onset of a volcanic eruption, when no or incomplete warnings are typically available and when model predictions (if available) are least reliable. Immediately after the onset of an eruption, typically nearly no quantitative atmospheric observation data are available and modellers will have to make rough assumptions on the source term, based on volcanological information and local (observer reports, webcams, photographs, thermal infrared cameras, radar, lidar) realtime observations. Later, atmospheric observations can be used to better constrain the source term and, thus, improve the model predictions.

For early provision of reliable model forecasts, it is of great importance to have such observations available as soon as possible after the start of a volcanic eruption. Ideally, such information comes from geostationary satellites which can observe an ash plume at high temporal resolution (e.g. every 15 minutes), if cloud cover permits. In the absence of such observations or in addition, data from polar orbiting satellites may also become available soon after an eruption. However, since there are few overpasses per day and/or spatial coverage is incomplete, the first observations from polar-orbiting satellites may occur many hours or even more than a day (or, considering the possibility of unfavourable viewing conditions during an overpass, occasionally even several days) after an eruption. Other observations (e.g. from lidar and/or weather radar networks, camera-mounted monitoring stations, MISR, etc.) are likely to become available even later (e.g. as an ash plume passes over Europe). Therefore, use of data from geostationary platforms should have the highest priority for operational model predictions.

2.4 Volcanological information, local observations, early warning

Volcanological data may be obtained from studies of past eruptions and monitoring activities. Studies of past eruptions allow identification and characterisation of types of explosive volcanic eruptions and as well to associate a probability of occurrence, whereas monitoring activities can provide information on the physical-chemical parameters which characterise the state of a volcanic system.

At the pre-eruption stage, geophysical data provides information on physical state via elevation in occurrences of volcanic earthquakes (e.g. geodedic measurements/continuous GPS, from seismic stations), elevation changes and ground displacements (e.g. from Envisat-ASAR (ESA), Radarsat-MDA (CSA)), thermal anomalies and gas and aerosol composition retrieval (e.g. from ground- and satellite-based infrared and multispectral spectrometer).

Once a given volcano erupts, it becomes essential to identify the eruption source parameters from volcanological data in order to facilitate reliable ash forecasting, especially in the very early phase when no atmospheric observations are available. The eruption parameters may be evaluated using direct measurements, remote observations and previous studies of eruptions having similar features. In particular, the plume height (the maximum height reached by the eruption column) may be well covered with direct ground-based observations (e.g. surveillance cameras and webcams, photo pictures, thermal infrared cameras) and satellite imageries. If radar or lidar instruments are available, it may be also possible to retrieve column height variations in real time.

The grain-size distribution is difficult to estimate *a priori*. Sizes and morphological features of tephra particles are related to different explosive dynamics and may vary from one eruption to another, or even across different phases of the same eruptive event. Similarly, both sphericity and density of the particles depend on the type and intensity of explosive activity. However, to improve model forecasting, an analysis of the physical properties of volcanic ash is essential. The volcanological community should make an effort to get available data into a database, not only for assessing mass, but also to provide *a priori* information that will be useful for later remote sensing retrieval activities. Nonetheless, every volcano may produce eruptions with different features that should also be included in this study. During an eruption, volcanologists could choose from the information obtained by the monitoring system, input parameters belonging to a given typology with similar features of the ongoing eruption. Techniques of data assimilation and inverse modelling could be also used.

Explosive volcanic eruptions generate ash-laden jets that emerge from the vent at speeds typically on the order of 100 to several hundred m s^{-1}. The ash is generated by fragmentation: the magma is transformed into a gas jet bearing particles with a range of characteristic sizes from the order of 10 cm down to the order of a micron. The transfer of heat from the hot fragments to the air and subsequent conversion of heat to mechanical (and potential) energy is a function of the actual grain size distribution in the erupted mixture, which in turn controls the vigour of the mixing and the strength of ensuing convection. It is the heated atmosphere that provides the buoyancy to the convective region of the column and enables it to rise in the stratified atmosphere until it reaches a maximum height and then spreads out at its level of neutral buoyancy. The difference between the maximum height and the level of neutral buoyancy depends on the momentum the plume possesses (this could be evaluated using doppler radars installed near the volcanic vent, e.g. Dubosclard et al. 2004) when it first attains the neutral buoyancy level. This is valuable information for determining plume heights.

The height reached in the atmosphere by a plume is fundamentally related to the flux of material that is ejected at the vent, i.e. the thermal power liberated at the source. At the low end, source mass fluxes can be of the order of $10^4 - 10^5$ kg s^{-1} (which was roughly the case for the Eyjafjöll plume), but at the high end they can be 10^9 kg s^{-1}, or even higher – a huge variation. Weak plumes may plausibly be treated as a source of particles that is relatively passive from the point of view of atmospheric circulation; this will not be the case for a very strong plume.

The coarsest particles tend to be deposited close to the vent and the finer (i.e. ash-grade) particles carried away by the plume and then atmospheric currents to large distances so that reconstruction of the total grain size distribution is an arduous task. The Eyjafjöll eruption showed two major complications with respect to this generic analysis (which is based on a strong plume in a quiescent atmosphere), namely that the plume was weak and hence strongly bent over by the wind, and secondly that the mass flux at the vent was being partitioned at the source. This partitioning is not uncommon in relatively weak subglacial Icelandic eruptions. It is also more common when the magma composition is basaltic rather than silicic, because the former magma type is more fluid and fragmentation is hence less efficient. Unless good constraints are available from observations at the source to quantify roughly this mass partitioning, it becomes another source of uncertainty.

For weak eruptions such as that of Eyjafjöll, the effects of crosswind and mass partitioning at the source between various components introduce significant complications. The details of the particle size distribution are harder to know because these depend on the intensity of the fragmentation process and how it proceeds. More detailed information can be found in Annex 2b.

2.5 Inverse modelling and data assimilation

So far, satellite products such as ash cloud/column estimates from the IR split window signal have mostly been visually compared to provide confidence levels for the forecasts. In order to fully and quantitatively extract the information from observations, techniques such as inverse modelling and data assimilation have been developed. Inverse modelling means to find optimum values of parameters that are used as input by a model so that the model output best matches the observations. In the context of volcanic ash modelling, this applies especially to determination of the ash mass emission flux. Data assimilation refers to the (quasi-)continuous use of observational data to create initial conditions for sequences of model runs. In each assimilation step, a forecast from the previous model run is used as a first guess, which is then modified to be in (better) agreement with the observations. Modern data assimilation techniques such as variational data assimilation use methodologies that are very similar to that for inverse modelling (Elbern et al., 2007). Data assimilation has been normal practice for a long time in operational weather forecasting, but is only now emerging for atmospheric constituents (e.g. Hollingsworth et al., 2008) and has not yet been used for volcanic ash plume modelling.

Inverse modelling has been applied to derive quantitative vertical profiles of the mass emission in an explosive volcanic eruption for SO_2. The technique was developed for the Jebel at Tair 2007 eruption (Eckhardt et al., 2008) and further investigated for the Kasatochi 2008 eruption (Kristiansen et al, 2010). This method uses total column values of SO_2 from different satellite platforms and sensors for a few hours to days after the eruption (Stohl et al., 2005). The transport and deformation pattern of the SO_2 cloud is caused by the variable winds in the atmosphere. The vertical wind shear allows determination of a vertical emission profile even though the satellite data used did not have any vertical resolution. The method could in principle be applied to ash as well, as retrievals of ash mass column values are possible. A major complication is, however, the influence of the particle size distribution on both the atmospheric

transport and the optical properties used in the retrieval. Furthermore, an extended eruption over many weeks as it occurred at Eyjafjöll in spring 2010 requires a modified, more complex inversion approach and increases computation requirements significantly.

This method obviously has an important potential for improving volcanic ash forecasts, including unmonitored volcanoes. While substantial further development will be needed, it could be used in real time at the VAACs to update continuously the source term (and, thus, model predictions of ash dispersion) as satellite remote sensing data becomes available.

Data assimilation systems have potential to improve the accuracy of simulations in order to track the movement of volcanic ash over several days. Satellite data have the unique property of covering the whole volcanic plume or at least (per scene) large parts, cloud cover permitting. With lidars, detailed ash height information is made available, if the ash cloud is identified properly. A best means for quantification of ash mass is given by airborne *in situ* measurements, allowing for considerably improved expectations for skillful inversion results. Several research groups have experience with assimilating satellite observations of ozone and nitrogen dioxide in air quality models, but very little has been done so far for volcanic sulphur dioxide emissions, and nothing on volcanic ash.

It is therefore important to assess the available satellite observations as well as ground-based observations that could be of use in data assimilation, and develop observation operators (relationship between the model variable and the actual observation). These observations can then be tested in existing systems and the experience gained should be transferred to the operational centres. A special aspect of this assimilation strategy should be emission source inversion. Traditional atmospheric data assimilation uses the observations to adjust the atmospheric fields every 12 hours or so, but for strong sources like volcanoes it is mandatory to adjust the source term itself as well. The full problem to be solved is therefore a combined inversion/data assimilation task. An initial set of observations to assess for possible data assimilation should include data from ceilometer/lidar networks and available satellite data. For the

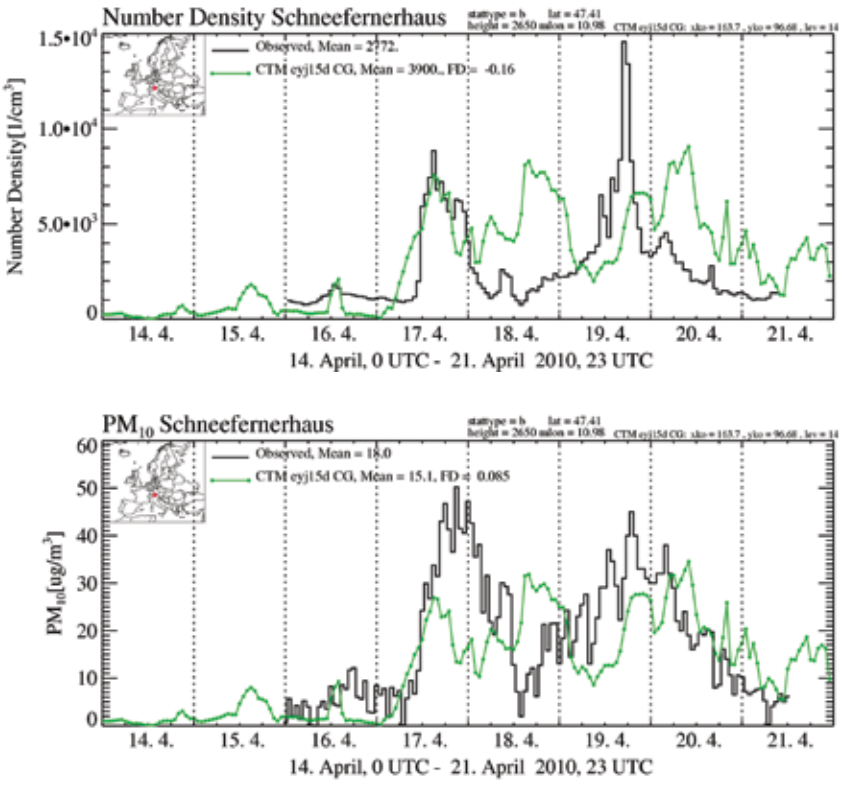

Fig 7. Intercomparison of model forecasts with actual ground-based measurements of the Eyjafjöll volcanic ash cloud. The graph shows time series of observed number densities of particles larger than 10 nm (black line) during 14–21 April 2010 at Zugspitze (southern Germany, ~2900m altitude) and modelled particulate matter (PM) number density (green, top panel), and for PM_{10} (green, bottom panel). Model simulations by EURAD-IM, RIU. Observations courtesy MOHP, German Weather Service (RIU)

latter, it can be expected that SO_2 from SCIAMACHY, GOME-2, OMI, and IASI, and aerosol products from MODIS, MISR, CALIPSO, PARARSOL, AIRS, IASI, SEVIRI, and OMI can be used. However, this list is by no means exhaustive.

It has proved difficult to make definitive statements about ash cloud extent from any one single observational source. There is a need to integrate all observing sources in NRT (if possible) to have a best estimate picture of geographical coverage, height and depth, and concentration. No single source or even multiple observation source can give us all this at present. Integrated ground-based systems (e.g. lidar, ceilometers, research aircraft, aerosol sondes etc.) combined with satellite observations ingested into data assimilation schemes are likely to provide improved initial conditions of both eruption conditions and plume extent. However, it must also be considered that many observation systems (e.g. ceilometers, lidar) do not provide direct estimates of volcanic ash mass and their assimilation into models may be difficult or will require additional uncertainties. Furthermore, timeliness of provision is an issue, as mentioned before, and observations should be available before an ash plume arrives in a busy air space or populated area.

2.6 Ensemble forecasts

The transition from a zero-tolerance flight policy to threshold-based flight ban areas in the presence of limited knowledge calls for probabilistic forecasts. Error sources, most prominently the volcanic emission profiles and composition, must be expressed in terms of discrete or continuous probability densities. Likewise, meteorological forecasts, especially cloud cover, cloud types and precipitation characteristics, are another source of uncertainties. Ensemble-based simulation is a key technique to address estimated uncertainties. Ensembles could be based on existing meteorological ensemble forecasts (e.g. the ensemble prediction system at ECMWF) to address the uncertainty in forecasted wind patterns, but should also place a special focus on uncertainty in the source term. For the latter, observational evidence will play a key role in estimating the uncertainties in, for instance, emission heights and emission mass. Variations in emission information can then be incorporated into the numerical model initial conditions, in a similar way to how uncertainty is introduced in initial conditions of atmospheric wind, temperature and pressure.

The experience from operational meteorology will be important in understanding how best to represent ensemble (or potentially multimodel ensemble) information in terms of discrete or continuous probability densities.

It is important for customer communities (aviation authorities and airlines) to have information delivered from a single authoritative provider, to ensure consistency and clarity of message and consequent reduction in uncertainty in response action.

2.7 Detailed plume modelling

To date, only meso-scale or large-scale models are used to predict the volcanic ash dispersion in real time. These models ignore the small-scale processes in the eruption plume itself, which actually determine the eruption plume height and are decisive for aerosol coagulation (and, thus, aerosol size distribution). Specialised models exist, such as ATHAM (Active Tracer High Resolution Atmospheric Model) (e.g. Oberhuber et al., 1998), which simulates the processes in the volcanic eruption column in great detail, given a specified mass flux of pyroclastic material. In future, it could also lead to improvements of the large-scale ash dispersion predictions if small-scale eruption column models were embedded in the larger-scale dispersion models.

References

Andronico, D., Scollo, S., Cristaldi, A., Caruso, S. (2008). The 2002–03 Etna explosive activity: tephra dispersal and features of the deposit. J. Geophys. Res. doi:10.1029/2007JB005126.

Barsotti, S., Neri, A., Scire, J.S. (2008). The VOL-CALPUFF model for atmospheric ash dispersal: 1. Approach and physical formulation, J. Geophys. Res., 113, B03208, doi:10.1029/2006JB004623.

Bitar, L., Duck, T.J. Kristiansen, N.I., Stohl, A. and Beauchamp S. (2010): LIDAR observations of Kasatochi volcano aerosols in the troposphere and stratosphere. J. Geophys. Res., in press.

Bonadonna, C., Macedonio, G., Sparks, R.S.J. (2002). Numerical modelling of tephra fallout associated with dome collapses and Vulcanian explosions: application to hazard assessment on Montserrat. In: Druitt, T.H., Kokelaar, B.P. (Eds.), The Eruption of Soufrière Hills Volcano, Montserrat, from 1995 to 1999. Memoir. Geological Society, London, pp. 517–537.

Bonadonna, C., Phillips, J.C., Houghton, B.F. (2005). Modeling tephra sedimentation from a Ruapehu weak plume eruption. J. Geophys. Res. 110, B08209. doi:10.1029/2004JB003515.

Carazzo, G., Kaminski, E. and Tait S. (2008). On the rise of turbulent plumes: quantitative effects of variable entrainment for submarine hydrothermal vents, terrestrial and extra-terrestrial explosive volcanism. Journal of Geophysical Research v.113, doi:10.1029/2007JB005458.

Cioni, R., Longo, A., Macedonio, G., Santacroce, R., Sbrana, A., Sulpizio, R., Andronico, D. (2003). Assessing pyroclastic fall hazard through field data and numerical simulations: Example from Vesuvio. J. Geophys. Res., 108(B2), 2063, doi:10.1029/2001JB000642.

Costa, A., Macedonio, G., Folch, A. (2006). A three dimensional Eulerian model for transport and deposition of volcanic ashes. Earth Planet. Sci. Lett. 241, 634–647.

Costa, A., Folch, A., Macedonio, G. (2010). A Model for Wet Aggregation of Ash Particles in Volcanic Plumes and Clouds: I. Theoretical Formulation. J. Geophys. Res., 115, B09201, doi:10.1029/2009JB007175.

D'Amours, R., Malo, A., Servranckx, R., Bensimon, D., Trudel, S. and Gauthier-Bilodeau J.-P. (2010): Application of the atmospheric Lagrangian particle dispersion model MLDP0 to the 2008 eruptions of Okmok and Kasatochi volcanoes. J. Geophys. Res., 115, D00L11, doi:10.1029/2009JD013602.

Draxler, RR, Hess GD. (1998). An overview of the HYSPLIT-4 modelling system for trajectories, dispersion and deposition. Australian Meteorological Magazine 47: 295–308.

Dubosclard, G., Donnadieud, F., Allard, P., Cordesses, R., Hervier, C., Coltelli, M., Privitera, E., Kornprobst, J. (2004). Doppler radar sounding of volcanic eruption dynamics at Mount Etna. Bull. Volcanol. 56, 398–411.

Eckhardt, S., Prata, A.J., Seibert, P., Stebel, K. and Stohl A. (2008): Estimation of the vertical profile of sulfur dioxide injection into the atmosphere by a volcanic eruption using satellite column measurements and inverse transport modelling. Atmos. Chem. Phys., 8, 3881–3897.

Elbern, H., Strunk, A., Schmidt, H. and Talagrand, O. (2007). Emission rate and chemical state estimation by 4-dimensional variational inversion, Atmos. Chem. Phys, 3749–3769.

Fero, J., Carey, S.N., Merrill, J.T. (2008). Simulation of the 1980 eruption of Mount St. Helens using the ash-tracking model PUFF. J. Volcanol. Geotherm. Res. 175 (3), 355–366.

Folch, A., Costa, A. and Macedonio G. (2009): FALL3D: A computational model for transport and deposition of volcanic ash. Computers and Geosciences 35, 1334–1342.

Hoffmann, A., Ritter, C., Stock, M., Maturilli, M., Eckhardt, S., Herber, A. and Neuber R. (2010). LIDAR measurements of the Kasatochi aerosol plume in August and September 2008 in Ny-Alesund, Spitsbergen, J. Geophys. Res., in press.

Hollingsworth, A., Engelen, R.J., Textor, C., Benedetti, A., Boucher, O., Chevallier, F., Dethof, A., Elbern, H., Eskes, H., Flemming, J., Granier, C., Kaiser, J.W., Morcrette, J.J., Rayner, P., Peuch, V-H., Rouil, L., Schultz, M., Simmons, A. and the GEMS consortium (2008). Toward a monitoring and forecasting system for atmospheric composition, The GEMS Project. Bull. Amer. Meteor. Soc., 89, 1147–1164, doi:10.1175/2008BAMS2355.1

Jones A.R., Thomson D.J., Hort M. and Devenish B. (2007). 'The U.K. Met Office's next-generation atmospheric dispersion model, NAME III', in Borrego C. and Norman A.-L. (Eds) Air Pollution Modeling and its Application XVII (Proceedings of the 27th NATO/CCMS International Technical Meeting on Air Pollution Modelling and its Application), Springer, pp. 580–589.

Josse, B., Simon, P. and Peuch, V.-H. (2004). Rn-222 global simulations with the multiscale CTM MOCAGE. Tellus 56B, 339–356.

Kristiansen, N.I., Stohl, A., Prata, A.J., Richter, A., Eckhardt, S., Seibert, P., Hoffmann, A., Ritter, C., Bitar, L., Duck, T., Stebel K. (2010): Remote sensing and inverse transport modeling of the Kasatochi eruption sulfur dioxide cloud. J. Geophys. Res., 115, D00L16, doi:10.1029/2009JD013286.

Langmann, B., (2000). Numerical modelling of regional scale transport and photochemistry directly together with meteorological processes. Atmos. Environ. 34, 3585–3598.

Langmann, B., Varghese, S., Marmer, E., Vignati, E., Wilson, J., Stier, P., O'Dowd, C.D., (2008). Aerosol distribution over Europe: A model evaluation study with detailed aerosol microphysics. Atmos. Chem. Phys., 8, 1591–1607

Morton, B.R., Taylor, G.I. and Turner, J.S. (1956) Turbulent gravitational convection from maintained and instantaneous sources. Proc. Royal Soc. Lond. v.234, 1–23.

Oberhuber, J.M., Herzog, M., Graf H.F. and Schwanke K. (1998): Volcanic plume simulation on large scales, J. Volcanol. Geotherm. Res. 87, 29–53.

Prata, A.J., Carn, S. A., Stohl, A., and Kerkmann, J. (2007). Long range transport and fate of a stratospheric volcanic cloud from Soufriere Hills volcano, Montserrat. Atmos. Chem. Phys., 7, 5093–5103.

Ryall D.B., Maryon R.H. (1998). Validation of the UK Met. Office's NAME model against the ETEX dataset. Atmos. Environ. 32(24): 4265–4276.

Searcy C., Dean K.G., Stringer W. (1998). PUFF: a volcanic ash tracking and prediction model. J Volcanol Geotherm Res 80:1–16

Stohl, A., Hittenberger, M. and Wotawa G. (1998). Validation of the Lagrangian particle dispersion model FLEXPART against large scale tracer experiments. Atmos. Environ. 32, 4245–4264.

Stohl, A., Forster, C., Frank, A., Seibert, P. and G. Wotawa P. (2005): Technical Note: The Lagrangian particle dispersion model FLEXPART version 6.2. Atmos. Chem. Phys. 5, 2461–2474.

Wang, X., Boselli, A., D'Avino, L., Pisani, G., Spinelli, N., Amodeo, A., Chaikovsky, A., Wiegner, M., Nickovic, S., Papayannis, A., Perrone, M.R., Rizi, V., Sauvage, L. and Stohl A. (2008). Volcanic dust characterization by EARLINET during Etna's eruptions in 2001–2002. Atmos. Environ. 42, 893–905.

Webley, P.W, Dean, K., Bailey, J.E., Dehn J. and Peterson R. (2009). Automated forecasting of volcanic ash dispersion utilizing virtual globes. Journal Natural Hazards, Vol. 51, 345–361

Witham C.S., Hort M.C., Potts R., Servranckx R., Husson P., Bonnardot F. (2007). Comparison of VAAC atmospheric dispersion models using the 1 November 2004 Grimsvötn eruption. Meteorol Appl 14:27–38.

Ash-rich and collapsing phreatomagmatic eruption column at 18:32 on 16 April seen from Skógar; view is to the Northwest. (Á. Höskuldsson)

Question 3:

What are the observations VAACs need and what are the implications for future satellite observing systems (e.g. MetOp, MTG, post-EPS, ADM, EarthCARE, Sentinels)?

Prata, A.J., Aminou D., Buongiorno F., Carboni E., Fehr T., Mannstein H., Munro R., Remedios J., and Thorsteinsson H.

3.1 VAAC requirements and the ash concentration threshold

Satellite data can be used in a variety of ways to assist with Volcanic Ash Advisory Centre (VAAC) operations. Prata and Tupper (2009) have recently summarised the status of the science surrounding ash identification from satellites and the aviation problem in a special issue of *Natural Hazards*. Papers within this issue go into the details of the various techniques and research areas contributing to VAAC operations. Table 2 shows some of the requirements and parameters identified as potentially measurable from satellites.

VAACs operate under the auspices of ICAO and most are co-located with Meteorological Watch Offices (MWOs) within operational meteorological centres. MWOs immediately advise VAACs when a volcanic eruption occurs and request a series of actions and advice from the VAAC. This advice includes ash advisories in text and optionally in a graphical format. By international agreement, the current system does not require graphics in the form of ash

Requirement	Parameters
Operational data provision	— Standardised volcanic ash product — Realtime — Nowcasting — Transmission in real time — Timing (5 min warning)
Repetition rate	— 15 mins or better
Data latency	— ?
Early warning	— Gas emissions (SO_2, CO_2, HCl, HF) — Deformation — Hot spot detection
Detection	— Ash/no-ash and/or SO_2 — Quantitative estimation
Source parameters	— Realtime information — Size distribution (particle effective radius, shape) — Mass flux — Water vapour and temperature profile
Validation	— Dispersion models — Spatial dimension — Concentration — Size distribution — SO_2 and/or ash
End of eruption	— ?

Table 2. VAAC requirements and associated parameters that could be measured by satellite instruments.

concentration plots. Most VAACs have the capability to run sophisticated atmospheric dispersion models and these are used to provide forecasts of the movement and position of volcanic ash clouds at agreed time intervals, typically with a 6 h forecast time.

Generation of the ash advisories requires use of as much information as possible from diverse sources, including and probably most importantly from satellite instruments. Information from ground-based observers, pilots, and volcanological observatories are also vital in developing the ash advisory. Here we concentrate on the use of satellite data.

Almost all VAACs rely heavily on access to realtime satellite imagery to identify and locate volcanic clouds. The primary data types used are images, visible and infrared, with animation if available. Interpreting these data requires a high degree of meterological skill and training. Good observational meteorologists are able to use context and experience to identify and interpret volcanic features within satellite images. At this stage of analysis the interpretation must be done rapidly and is often subjective, depending on exactly what data are available (e.g. rapid scan geosynchronous data, or less frequent polar orbiting data). Locations of volcanic features within images are compared with the output of dispersion models and an estimate of the extent and location of the volcanic hazard is made. The feature is defined by a polygon with a small number of sides, and typically three height intervals are specified. Often it is possible to subjectively utilise the model trajectory with the information from the satellite image to estimate the vertical layer of the atmosphere most affected. However, when there is no wind shear, or winds are blowing in similar directions and speeds but at different heights, the height identification can be ambiguous. At many VAACs the use of satellite data stops at this point. Some VAACs can go further by using cloud shadows in visible imagery to estimate volcanic cloud heights, or use thermal images to determine cloud-top temperatures that can be interpreted to cloud-top heights by use of a nearby contemporaneous radiosounding. Very few VAACs make use of any satellite data in their operations, other than geosynchronous meteorological imagery (e.g. SEVIRI, GOES and MTSAT) and polar orbiting operational sensors, such as the NOAA/AVHRRs. These data are images; at most, the only quantitative processing done is to convert the thermal imagery into brightness temperatures. For VAACs that do make use of the thermal brightness temperatures, the brightness temperature difference image (BTD) based on the 'reverse absorption' effect (Prata, 1989a, b) at 11 μm and 12 μm (sometimes referred to as the 'split-window'), are found to be particularly useful for identifying ash. Table 3 lists some of the methods used to detect ash from current satellites.

In Europe, EUMETSAT have provided a 'dust' RGB composite image based on imagery with channels centred at 8.6, 10.8 and 12 μm. This RGB imagery has

Name	Principle	Reference
RA	2-band IR (11 and 12 μm)	Prata (1989a,b)
Ratio	2-band IR (11 and 12 μm)	Holasek and Rose (1991)
4-band	IR + visible	Mosher (2000)
TVAP	3-band IR (3.9, 11 and 12 μm)	Elrod et al. (2003)
PCI	Multi-band principal components	Hilger and Clark (2002a,b)
WVC	2-band IR + water vapour correction	Yu et al. (2002)
RAT	3-band IR (3.9, 11 and 12 μm)	Pergola et al. (2004)
3-band	3-band (IR + visible)	Pavalonis et al. (2006)
RA=Reverse Absorption; TVAP=Three band Volcanic Ash Product; PCI=Principal Components; WVC= Water Vapour Correction method; RAT=Robust AVHRR Technique.		

Table 3. The main satellite-based methods for detecting and discriminating volcanic ash clouds.

VAAC	GEO Satellite(s)	Temporal Refresh	Spectral Capabilities	Next Generation GEO Satellite
Anchorage	GOES-11	30 minutes	Split-window	GOES-R (2015)
Buenos Aires	GOES-12 GOES-13 MSG	15 minutes 180 minutes 15 minutes	No split-window No split-window Advanced	GOES-R (2015)
Darwin	MTSAT FY2D FY2E	60 minutes 60 minutes 60 minutes	Split-window Split-window Split-window	Similar to GOES-R from JMA (2020?) and **FY4A from China (2014)**
London	MSG	15 minutes	Advanced	**MTG (~2018)**
Montreal	GOES-11 GOES-13	30 minutes 15 or 30 minutes	Split-window No split-window	GOES-R (2015)
Tokyo	MTSAT FY2D FY2E	30 minutes 60 minutes 60 minutes	Split-window Split-window Split-window	Similar to GOES-R from JMA (2020?) and **FY4A from China (2014)**
Toulouse	MSG	5 or 15 minutes	Advanced	**MTG (~2018)**
Washington	GOES-11 GOES-12 GOES-13 MSG	30 minutes 15 minutes 15 or 30 minutes 15 minutes	Split-window No split-window No split-window Advanced	GOES-R (2015)
Wellington	MTSAT GOES-11	60 minutes 180 minutes	Split-window Split-window	Similar to GOES-R from JMA (2020?) and GOES-R (2015)

Table 4: An overview of the geostationary satellite capabilities is shown as a function of VAAC. The table summarises the temporal and spectral capabilities (those relevant to volcanic ash remote sensing) of each instrument that covers each VAAC area of responsibility. In addition, future geostationary satellite capabilities are summarised. Next generation satellites that include a hyperspectral sounding capability are shown in **bold**.

proved very useful for identifying volcanic clouds, but it does not discriminate between ash and SO_2 (the channel at 8.6 µm is affected by SO_2 absorption). Also, to untrained users the imagery can be confusing, and a high reliance must be placed on context and movement in the images to properly identify volcanic features. Nevertheless, these RGB composites are now widely used and have proved helpful.

In the last three years or so, data from research satellites have become increasingly available within a timeframe that is useful for VAAC procedures. For example, OMI and GOME-2 SO_2 data products can be accessed via web pages and these are found to be very helpful in identifying volcanic clouds, because measuring SO_2 from space is much easier than identifying ash, which is the major hazard to aviation. SO_2 and ash do not always travel together and on occasion little SO_2 is emitted by a volcano, making the use of SO_2 problematic as a proxy for ash. Table 4 shows the current and near future satellite capabilities available to VAACs.

Annex 3a shows some example satellite images of volcanic ash clouds, SO_2 and the aerosol index (a measure of absorption of UV light by particles).

Prior to 21 April 2010, all VAACs provided ash advisories without the need to quantify the amount or concentration of ash. Advice was given based upon the observation of ash in the atmosphere, and subsequent modelling based on a standard volcanic source strength, dispersed by measured winds. Thus there was no requirement for quantitative volcanic ash products from satellite data, although much research had been done on this topic and many such products were available to the research community. A new limit was imposed at a level of 2 mg m^{-3}, such that areas identified with levels exceeding this would be deemed 'no fly zones'. This new limit is only applicable for eruptions within the jurisdiction of the London VAAC and no such limit has been sanctioned by

ICAO. It is unclear whether the limit will be accepted throughout the nine VAAC regions, or indeed whether this limit will be increased or decreased after review.

The imposition of a limit implies that the dispersion model is capable of providing a contour showing ash concentrations, and, in particular, that a level of 2 mg m^{-3} can be delineated. In order to be able to do this, accurate information on the volcanic source (e.g. the mass flux, vertical distribution of mass, the column height and the particle size distribution) is needed. Generally this kind of information is not readily available even at the most advanced and well-instrumented volcano observatories. Without the volcano source information, the only other means to constrain the dispersion model concentrations is through direct measurement. Downwind measurements of the plume concentration can be made using ground-based, balloon-borne, airborne and satellite-based instruments.

3.2 Infrared satellite measurements

Satellite measurements of ash mass loadings are currently available from instruments on board both polar orbiting and geosynchronous platforms. Notably among these for Europe are: AVHRR, (A)ATSR, SEVIRI, AIRS and IASI. These instruments have thermal channels at 11 and 12 µm that are necessary to detect and quantify volcanic ash. It is not at all difficult to detect a mass loading of 2 g m^{-2}, which translates to an ash concentration of 2 mg m^{-3} for an ash layer of 1 km thickness. The reverse absorption method is described in "Annex 3b: The reverse absorption algorithm", and an example is shown of the sensitivity of the method to ash concentrations of 2 mg m^{-3}.

Horizontal resolution can be an issue, but generally speaking the spatial resolutions of most of today's operational and research satellite instruments are sufficient for detecting most hazardous volcanic clouds. Horizontal resolutions of 1–10 km are adequate. Vertical resolution is important but most satellite instruments can only provide column estimates. This appears to be a large gap in the capability of current satellite instruments to address the volcanic ash problem.

IRS spectral range should be extended to provide coverage of SO_2 features to add a night-time SO_2 observation capability from GEO.

3.3 UV and visible light measurements from satellites

Other current satellite instruments can be used to provide validation of some of the parameters required for accurate retrieval of ash mass loadings, but it is necessary to be clear which satellite data are of primary importance and which are secondary. Most of the instruments using visible radiation as a source are of secondary importance, for two reasons. First, these instruments can only measure when the Sun is above the horizon and therefore cannot be used in an operational volcanic ash hazard identification system. Second, these instruments are not optimised for measuring the 1–10 µm-sized particles that are responsible for causing engine damage in commercial jets. However, they are capable in some cases of providing cloud-top heights and can provide aerosol optical depth measurements, which may be used for validation.

Because of the nature of volcanic activity (unpredictable, sporadic and often in remote locations) it is easy to see the importance of satellite measurements. VAACs require near continuous observations and require data in a rapid manner.

Summarising these points for the UV/VIS sensors:

— Geosynchronous observations are preferred, but full disc coverage is important to provide information for the full area covered by the London and Toulouse VAACs.

— Spatial resolution should be as good as possible also for the LEO instruments e.g. GOME-2 (the current safety margin is 60 km which is smaller than the current GOME-2 ground pixel).

— Data access should be fast and easy also for ESA/EUMETSAT missions/ instruments.

— VAACs are concerned with ash, which is not a standard product from UV/VIS sensors. However, SO_2 is useful as its identification is fast and unambiguous and because SO_2 emissions often precede eruptions. The absorbing index (AI)-type products that are produced from UV/VIS are qualitative but fast and much less affected by clouds than current ash products from imagers.

— UV/VIS data should not be ignored as it can provide rapid and easy-to-interpret information on volcanic eruptions.

3.4 Precursor and early warnings

Early warnings and early readiness in the event of an eruption will rely on the expertise and active involvement of volcanic observatories. Seismicity, seismic mapping, crustal deformation and gaseous release are only a few types of observation that help observatories to prepare the operational community for the onset of an ash eruption. Increased density of ground sensors in the vicinity of volcanoes will help researchers to better map and understand their volcanoes.

Remote sensing with interferometric SAR (InSAR) observations (e.g. Envisat-ASAR, Terra-SAR/TanDEM-X, Radarsat) has also revolutionised the detection of ground deformation. InSAR observations are today an important and accepted tool in the early detection of magma injection and in mapping the underlying structure of a volcano. A policy of regular (weekly/monthly) and openly-available InSAR observations of volcanoes will greatly aid understanding of eruptions.

Remote sensing of thermal anomalies, especially in the SWIR, can give signs of an impending eruption as well as serving as a negative plume indicator (it is an optically-thin source). Volcanologists have expressed that higher spatial resolution in thermal imaging will be an important future improvement.

The majority of volcano observatories and the ICAO have a relatively simple and straightforward system of four levels, increasing from ‘non-eruptive’ (usually green or white), through ‘elevated unrest’ (yellow), ‘heightened unrest’ (orange) to ‘eruption underway’ (red).

These stages of disaster management are most useful for disaster managers but volcano observatories tend to structure the evolving stages of their requirements slightly differently, thus three observation scenarios can be distinguished:

— Identification of phenomena
Locating and identifying potentially-hazardous or important features such as fumaroles, lava domes, lava flows and crater lakes, and establishing ‘background’ levels of activity.

— Monitoring of expansion/development of phenomena
Collection of a time series of data that chronicles changing levels of activity from background to hazardous levels. Time frames for such monitoring vary widely from days to years. Such data can help in modelling possible impacts of future hazardous events.

— Generation of hazards
Identifying where hazards are being generated and areas impacted or likely to be impacted can help with search and rescue or damage assessment. Impacts and extents are essential to understanding major events – often close access is impossible during or shortly after major volcanic events. Data can be used to improve future models of hazards and their impacts.

Ash clouds are generated by explosive volcanic eruptions. In order to mitigate the volcanic risk and therefore increase the preparedness for a possible volcanic event, satellite systems should be equipped with suitable instrumentation to support the monitoring of precursors, especially for volcanoes which lack of adequate ground monitoring systems.

To accomplish these tasks the current planned missions should be integrated with instruments that may furnish, by means of systematic observations, information on the variation of key volcanic parameters:

— Thermal anomaly detection and analysis in the pre-eruptive periods

— Changes in gas emission composition and volcanic aerosol concentrations in permanent degassing plumes from summit craters or fumarole fields

— Deformation of the surface by means of SAR images and GPS

Focusing on points 1 and 2, Table 5 summarises the observational objectives and the related measurements.

Table 5: Volcanic precursor observation objectives and measurements

Objective	Related Quantitative Measures
Correlation between thermal precursors and eruptive activity	— % of thermal anomalies that precede eruptions as a function of anomaly area and intensity, for a given volcano — Rate of increase/decrease of anomaly intensity/flux as a function of eruption duration/volume/flux
Correlation between gas emissions from permanent degassing plumes (summit craters and fumarole fields) and volcanic eruptive activity	— Rate of increase/decrease of SO_2, CO_2, H_2O (primarily) concentration/flux in pre-eruptive periods and during eruptive activity
Correlation between volcanic aerosols from permanent degassing plumes (summit craters and fumaroles fields) and volcanic ash plumes emitted during the eruptive activity	— Changes in the aerosol concentrations in pre-eruptive periods, aerosol optical thickness variation in function of time
Temporal, spatial, energetic, and instrumental limits on remote thermal anomaly detection	— Required sampling frequency for >90% detection certainty as a function of anomaly intensity, instrumental resolution, and $NE\Delta T_I$ (instrumental)
Sensitivity of detection thresholds to intrinsic and extrinsic variables	— $NE\Delta T_X$ (scene noise relative to the anomaly) as a function of scene roughness, roughness, topography, temperature, emissivity, atmospheric water vapour, cloud cover, volcanogenic emissions, seasonal variables
Global Thermal Anomaly Catalogue (GTAC)	— Geographical information system locations of anomalous pixels as a function of time referenced by radiant intensity and/or time at the surface (atmospherically-corrected/T/E-separated) or at the instrument.
Systematic surveys of all eruptions	— Time-series distribution of radiant intensity/flux of thermal anomalies as a function of time/distance from the eruption apex and/or vent.

Satellite – Sensor	TIR Spatial Resolution	Night/Day	Revisiting Time	# TIR bands	SWIR bands
MSG – SEVIRI	3 to 5 km	D,N	Geostationary (15 min)	5	1
NOAA – AVHRR	1.1 km	D,N	12 hr	2	1
METOP – AVHRR-3	1.1 km	D,N	Daily	2	1
TERRA, AQUA – MODIS	1.1 km	D,N	Daily	10	4
ERS-1 – ATSR ERS-2 – ATSR-2	1 km	D,N	3 to 5 days	2	1
Envisat – AATSR	1 km	D,N	3 to 5 days	2	1
LANDSAT – TM / ETM	120m / 60m	D, [N]	16 days	1	2
TERRA – ASTER	90m	D	16 days	5	6
Sentinel-2 – MSI	30-60 m	D [N]	5 day (2 satellites)	0	3
Sentinel-3 – SLST	500-1km	D,N	2 days (2 satellites)	2	3

Table 6: Sensors, resolutions, revisit times and bands available from current and some proposed satellite instruments that are useful for early warning/precursors

3.5 Sensor requirements for precursor/early warnings

The current missions and the near-future missions (ESA/EUMETSAT, Sentinels) will ensure observation with a high repetition cycle both for observing lava flows (SWIR/MIR) and ash cloud (TIR) events (see Table 6). Nevertheless it is obvious that there is an observational gap for TIR/MIR multispectral sensors at high spatial resolution, which are needed to locate the specific thermal anomalies and small gas emissions to monitor the pre-eruptive phases of volcanoes.

A specific goal could be achieved by combining future systems (Sentinels) with high spectral capabilities (sounders, spectrometers) and high global coverage (geosynchronous) with polar orbiting systems with a repetition cycle between 3–16 days (systematic acquisitions not on demand) and spatial resolution between 30–60 m. Spectral coverage could be a select number of spectral channels suitable for volcanic observations. The available detector technology and payload design may permit development of a class of small sensors that could fly in missions that are already scheduled.

3.6 Global and regional systems

It is worth reflecting on the fact that many of the already-highlighted limitations in ash aerosol observations, such as obscuring clouds and a lack of direct measurements, are in fact very common limitations within meteorology and Earth observations in general. The May 26–27 workshop at ESRIN highlighted the importance of diversity in observations and focus. Gaps in observations of the atmosphere are a reality that we must learn to deal with by thinking big.

Meteorological organisations have long since recognised the importance of sharing data and working together through comprehensive networks of weather observations, common standards, and sometimes common processing facilities. International bodies such as the WMO, EUMETNET, ICAO and EUMETSAT are instrumental in uniting countries in their effort to share data when monitoring the atmosphere. It is also natural that these bodies take it onto themselves to establish and improve standards and guidelines on ash.

The ultimate goal is to realise a comprehensive observation system with the ability to detect ash in multiple Earth locations and under varied atmospheric conditions. Also needed is the ability to share data and products effectively

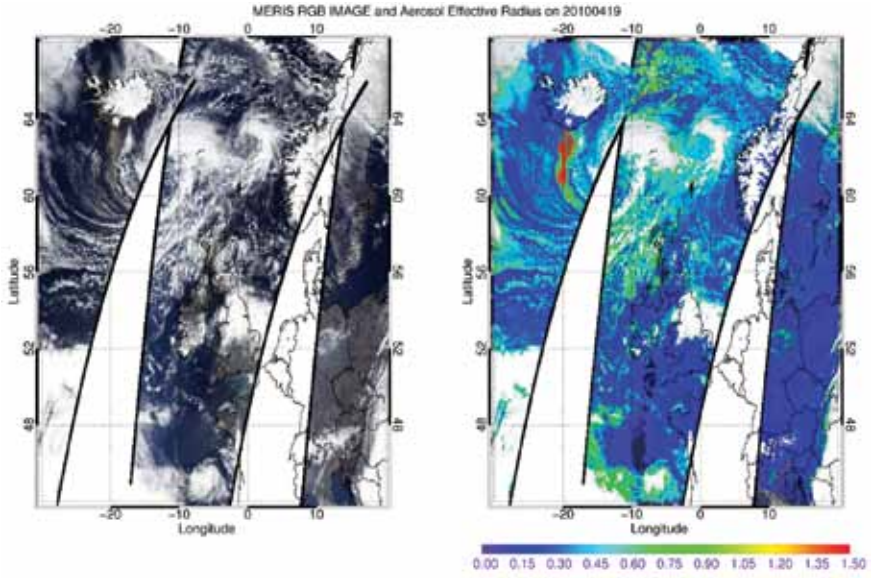

Fig 8. The Red-Green-Blue composite image (left) shows the ash plume from Iceland's Eyjafjöll volcano and clouds, as seen by Envisat's Medium Resolution Imaging Spectrometer (MERIS) on 19 April 2010. The right image shows the retrieved aerosol effective radius (indicating the ash cloud in red). (W. von Hoyningen-Huene)

and in a timely manner. To ensure good progress, meteorology, volcanology and the satellite agencies will need to establish a formal forum to interact on a broad range of topics, ranging from ground instrument financing to data access policies and standards. Long-established international cooperations on a broad range of observations within meteorology give good hope for success.

A comprehensive operational observation system for ash needs to combine both geostationary and polar orbiting observatories. It would therefore be most advantageous if detailed sensitivity to ash aerosol were to be made an official specification in future meteorological satellite sensors.

3.7 Conclusions

— The combination of ash load (and concentration) derived from IASI, AIRS and other instruments with a high spectral resolution in the thermal IR in combination with the VA detection and tracking in SEVIRI is a promising technique for ash cloud monitoring. It would provide quantitative information in a way that allows monitoring of ash clouds and SO_2 with a high temporal resolution in a nowcasting mode, day and night.

— The operational meteorological satellites (MTP) will provide these capabilities also in future ("Annex 3c: Future ESA/EUMETSAT satellite missions"). Nevertheless, it is important to validate the derived quantitative observations by *in situ* measurements. Due to the change from zero tolerance to an ash threshold value, the validation has become more important than before.

— For future systems the possibility of direct assimilation of radiances into weather forecast models should be kept in mind.

— Two primary ESA satellite missions (EarthCARE and ADM-Aeolus) are likely to contribute useful information for monitoring ash clouds. These are described in Annex 3c, and a list of future systems useful for the ash problem is provided in Table 3c1 of Annex 3c.

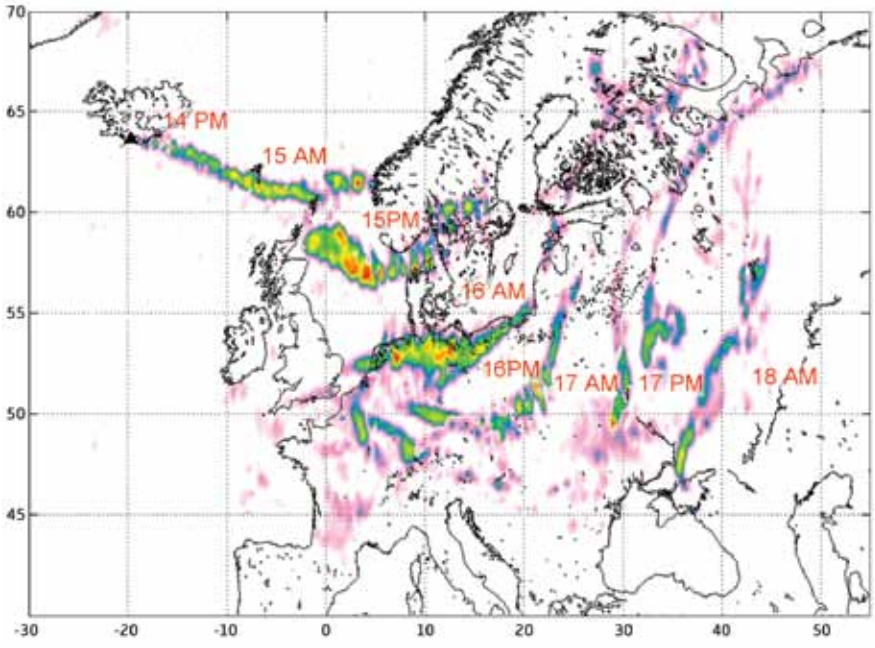

Fig 9. Integrated plot of the Infrared Atmospheric Sounding Interferometer (IASI) ash radiance index for 14–18 April 2010. The overpass times are around 9:30 a.m. and 9:30 p.m. (L. Clarisse, ULB)

3.8 Future missions needed

Geostationary imagery and sounding from UV to TIR (like MTG), polar orbiting scanning lidars (future), and polar orbiting stereo-viewing imagers (like MISR) are the optimum combination to retrieve ash clouds from space.

Nevertheless such an optimal satellite observing system will be only one component of a global end-to-end monitoring/forecasting system, which will also include ground-based measurements (e.g. lidar, radar, ceilometers, radiometers), airborne measurements, and several operational and R&D modelling capabilities worldwide.

Annex 3a shows some examples of current satellite data that are capable of observing ash clouds. These examples have been chosen because the data identify volcanic substances (either ash or SO_2) as opposed to aerosols (e.g. AOD).

References

Barton IJ, Prata AJ, Watterson IG, Young SA (1992) Identification of the Mount Hudson volcanic cloud over SE Australia. Geophys Res Lett 19:1211–1214

Bernard A, Rose WI (1984) The injection of sulfuric acid aerosols in the stratosphere by the El Chichon volcano and its related hazards to the international air traffic. Nat Hazards 3(1):59–67. doi:10.1007/ BF00144974

Bluth GJS, Schnetzler CC, Krueger AJ, Walter LS (1993) The contribution of explosive volcanism to global atmospheric sulphur dioxide concentrations. Nature 366:327–329

Carn SA, Krueger AJ, Krotkov NA, Gray MA (2004) Fire at Iraqi sulfur plant emits SO_2 clouds detected by Earth Probe TOMS. Geophys Res Lett 31:L19105. doi:10.1029/2004GL020719

Carn SA, Krotkov NA, Yang K, Hoff RM, Prata AJ, Krueger AJ, Loughlin SC, Levelt PF (2007) Extended observations of volcanic SO_2 and sulphate aerosol in the stratosphere. Atmos Chem Phys Discuss 7:2857–2871

Carn SA, Prata AJ, Karlsdottir S (2008) Circumpolar transport of a volcanic cloud from Hekla (Iceland). J Geophys Res 113. doi:10.1029/2008JD009878

Casadevall TJ (1994) The 1989/1990 eruption of Redoubt Volcano Alaska: impacts on aircraft operations. J Volcanol Geotherm Res 62(30):301–316

Casadevall TJ, Delos Reyes PJ, Schneider DJ (1996) The 1991 Pinatubo eruptions and their effects on aircraft operations. In: Newhall CG, Punongbayan RS (eds) Fire and mud: eruptions and lahars of Mount Pinatubo, Philippines. Philippines Institute of Volcanology and Seismology, Quezon City, University of Washington Press, Seattle, pp 625–636

Clerbaux C, Hadji-Lazaro J, Turquety S, George M, Coheur P-F, Hurtmans D, Wespes C, Herbin H, Blumstein D, Tournier B, Phulpin T (2007). The IASI/MetOp I mission: first observations and highlights of its potential contribution to GMES. COSPAR Inf Bull 2007:19–24

Constantine EK, Bluth GJS, Rose WI (2000). TOMS and AVHRR sensors applied to drifting volcanic clouds from the August 1991 eruptions of Cerro Hudson. In: Mouginis-Mark P, Crisp J, Fink J (eds) AGU Monograph 116—Remote Sensing of Active Volcanism, pp 45–64

Eckhardt S, Prata AJ, Seibert P, Steibel K, Stohl A (2008) Estimation of the vertical profile of sulfur dioxide injection into the atmosphere by a volcanic eruption using satellite column measurements and inverse transport modeling. Atmos Chem Phys Discuss 8:3761–3805

Eisinger M, Burrows JP (1998) Tropospheric sulfur dioxide observed by the ERS-2 GOME instrument. Geophys Res Lett 25(22):4177–4180

Ellrod GP, Connell BH, Hillger DW (2003) Improved detection of airborne volcanic ash using multispectral infrared satellite data. J Geophys Res 108(D12):4356. doi:10.1029/2002JD002802

Fleming EL, Chandra S, Shoeberl MR, Barnett JJ (1988) Monthly mean global climatology of temperature, wind, geopotential height and pressure for 0–120 km. National Aeronautics and Space Administration, Technical Memorandum 100697, Washington, DC

Guffanti M, Albersheim S (2008) The United States national volcanic ash operations plan for aviation. Nat Hazards Special Issue: Aviation hazards from volcanoes. doi:10.1007/s11069-008-9247-1

Hanstrum BN, Watson AS (1983) A case study of two eruptions of Mount Galunggung and an investigation of volcanic eruption cloud characteristics using remote sensing techniques. Aust Meteorol Mag 31:131–177

Hillger DW, Clark JD (2002a) Principal component image analysis of MODIS for volcanic ash. Part I: most important bands and implications for future GOES imagers. J Appl Meteorol 41:985–1001

Hillger DW, Clark JD (2002b) Principal component image analysis of MODIS for volcanic ash. Part II: simulation of current GOES and GOES-M imagers. J Appl Meteorol 41:1003–1010

Holasek RE, Rose WI (1991) Anatomy of 1986 Augustine volcano eruptions as recorded by multispectral images processing of digital AVHRR weather satellite data. Bull Volcanol 53:42–435.

Holasek RE, Woods AW, Self S (1996) Experiments on gas-ash separation processes in volcanic umbrella clouds. J Volcanol Geotherm Res 70:169–181.

Krotkov NA, Carn SA, Krueger AJ, Bhartia PK, Yang K (2006) Band residual difference algorithm for retrieval of SO_2 from the Aura Ozone Monitoring Instrument (OMI). IEEE Trans Geosci Remote Sens 44(5):1259–1266.

Krueger AJ (1983) Sighting of El Chichon sulfur dioxide clouds with the nimbus 7 total ozone mapping spectrometer. Science 220:1377–1379.

Krueger AJ, Walter LS, Bhartia PK, Schnetzler CC, Krotkov NA, Sprod I, Bluth GJS (1995) Volcanic sulfur dioxide measurements from the total ozone mapping spectrometer instruments. J Geophys Res 100(D7):14057–14076.

Krueger AJ, Schaefer SJ, Krotkov N, Bluth GJS, Baker S (2000). Ultraviolet remote sensing of volcanic emissions. In: Mouginis-Marks PJ, Crisp JA, Fink JH (eds) Remote sensing of active volcanism. Geophys Monogr Ser 116:2543, AGU, Washington, DC.

Malingreau J, Kaswanda P (1986) Monitoring volcanic eruptions in Indonesia using weather satellite data: the Colo eruption of July 28, 1983. J Volcanol Geotherm Res 27(1–2):179–194.

Matson M (1984) The 1982 El Chichon volcano eruptions—a satellite perspective. J Volcanol Geotherm Res 23:1–10.

Miller TP, Casadevall TJ (1999) Volcanic ash hazards to aviation. In: Sigurdsson H, Houghton B, McNutt SR, Ryman H, Stix J (eds) Encyclopedia of volcanoes. Academic Press, San Diego, pp 915–930.

Mosher FR (2000) Four channel volcanic ash detection algorithm, Preprint Volume. 10th Conference on Satellite Meteorology and Oceanography, Long Beach, California, 9–14 January, 2000, pp 457–460.

Pavolonis MJ, Feltz WF, Heidinger AK, Gallina GM (2006) A daytime complement to the reverse absorption technique for improved automated detection of volcanic ash. J Atmos Oceanic Technol 23:1422–1444.

Pergola N, Tramutoli V, Marchese F, Scaffidi I, Lacav T (2004) Improving volcanic ash cloud detection by a robust satellite technique. Remote Sens Environ 90:1–22.

Pieri D, Ma C, Simpson JJ, Hufford G, Grindle T, Grove C (2002) Analyses of in-situ airborne ash from the February 2000 eruption of Hekla volcano, Iceland. Geophys Res Lett 29:16. doi:10.1029/2001GL013688.

Prata AJ (1989a) Observations of volcanic ash clouds using AVHRR-2 radiances. Int J Remote Sens 10(4–5):751–761.

Prata AJ (1989b) Radiative transfer calculations for volcanic ash clouds. Geophys Res Lett 16(11): 1293–1296.

Prata AJ, Grant IF (2001) Retrieval of microphysical and morphological properties of volcanic ash plumes from satellite data: application to Mt. Ruapehu, New Zealand. Q J R Meteorol Soc 127(576B): 2153–2179.

Prata AJ, Kerkmann J (2007) Simultaneous retrieval of volcanic ash and SO_2 using MSG-SEVIRI measurements. Geophys Res Lett 34:L05813. doi:10.1029/2006GL028691.

Prata AJ, Bluth GJS, Rose WI, Schneider DJ, Tupper AC (2001) Comments on Failures in detecting volcanic ash from a satellite-based technique. Remote Sens Environ 78:341–346.

Prata, A. J., and Tupper, A. T., (2009) Aviation hazards from volcanoes: the state of the science, Nat Hazards doi: 10.1007/s11069-009-9415-y.

Prata AJ, Rose WI, Self S, O'Brien DM (2003) Global, long-term sulphur dioxide measurements from TOVS data: a new tool for studying explosive volcanism and climate. In: Volcanism and the Earth's atmosphere, Geophysical Monograph 139 AGU, pp 75–92.

Prata AJ, Carn SA, Stohl A, Kerkmann J (2007) Long range transport and fate of a stratospheric volcanic cloud from Soufriere Hills volcano, Montserrat. Atmos Chem Phys 7:5093–5103.

Richardson AJ (1984) El Chichon volcanic ash effects on atmospheric haze measured by NOAA-7 AVHRR data. Remote Sens Environ 16:157–164.

Richter A, Wittrock F, Burrows JP (2006) SO_2 measurements with SCIAMACHY. In: Proceedings of the first conference on atmospheric science, Frascati, Italy, 8–12 May 2006. ESA SP-628.

Rose WI, Delene DJ, Schneider DJ, Bluth GJS, Kruger AJ, Sprod I, McKee C, Davies HL, Ernst GJ (1995) Ice in the 1994 Rabaul eruption: implications for volcanic hazard and atmospheric effects. Nature 375:477–479.

Sawada Y (1987) Study on analysis of volcanic eruptions based on eruption cloud image data obtained by the Geostationary Meteorological Satellite (GMS). Technical reports of the Meteorological Research Institute, vol 22, 335 pp.

Sawada Y (1996) Detection of explosive eruptions and regional tracking of volcanic ash clouds with geostationary meteorological satellites (GMS). In: Scarpa R, Tilling RI (eds) Monitoring and mitigation of volcano hazards. Springer-Verlag, Berlin, Heidelberg, pp 299–314.

Schneider DJ, Rose WI, Kelley L (1995) Tracking of 1992 eruption clouds from Crater Peak of Mount Spurr volcano, Alaska, using AVHRR. US Geol Surv Bull 2139:27–36.

Schneider DJ, Rose WI, Coke LR, Bluth GJS (1999) Early evolution of a stratospheric volcanic eruption cloud as observed with TOMS and AVHRR. J Geophys Res 104(D4):4037–4050.

Simkin T, Seibert L (1994) Volcanoes of the world, 2nd ed. Geoscience Press, Tucson

Simpson JJ, Hufford G, Pieri D, Berg J (2000) Failures in detecting volcanic ash from a satellite-based technique. Remote Sens Environ 72:191–217.

Simpson JJ, Hufford G, Pieri D, Servranckx R, Berg J (2002) The February 2001 eruption of Mount Cleveland, Alaska: case study of an aviation hazard. Weather Forecast 17:691–704.

Thomas W, Erbertseder T, Ruppert T, Van Roozendael M, Verdebout J, Balis D, Meleti C, Zerefos C (2004) On the retrieval of volcanic sulfur dioxide emissions from GOME backscatter measurements. J Atmos Chem 50:295–320. doi:10.1007/s10874-005-5079-5.

Torres O, Bhartia PK, Herman JR, Ahmad Z, Gleason J (1998) Derivation of aerosol properties from satellite measurements of backscattered ultraviolet radiation: theoretical basis. J Geophys Res, 103(D14):17099–17110.

Tupper A, Carn SA, Davey J, Kamada Y, Potts RJ, Prata AJ, Tokuno M (2004) An evaluation of volcanic cloud detection techniques during recent significant eruptions in the western ring of fire. Remote Sens Environ., 91:27–46.

Urai M (2004) Sulfur dioxide flux estimation from volcanoes using advanced spaceborne thermal emission and reflection radiometer—a case study of Miyakejima volcano, Japan. J Volcanol Geotherm Res., 134(1–2):1–13.

Van Geffen J, Van Roozendael M, Di Nicolantonio W, Tampellini L, Valks P, Erbetseder T, Van der A (2007) Monitoring of volcanic activity from satellite as part of GSE PROMOTE. Proceedings of the first conference on atmospheric science, Frascati, Italy, 8–12 May 2006. ESA SP-628.

Watkin SC (2003) The application of AVHRR data for the detection of volcanic ash in a volcanic ash advisory centre. Meteorol Appl 10:301–311.

Wen S, Rose WI (1994) Retrieval of sizes and total masses of particles in volcanic clouds using AVHRR bands 4 and 5. J Geophys Res 99(D3):5421–5431.

Witham CS, Hort MC, Potts R, Servranckx R, Husson P, Bonnardot F (2007) Comparison of VAAC atmospheric dispersion models using the 1 November 2004 Grimsvötn eruption. Meteorol Appl 14: 27–38.

Yu T, Rose WI, Prata AJ (2002) Atmospheric correction for satellite-based volcanic ash mapping and retrievals using split window IR data from GOES and AVHRR. J Geophys Res 107(D16):4311. doi:10.1029/2001JD000706.

Part 4:
Recommendations

G.M. Doherty, Brenguier J.L., Brunner D., Buongiorno M.F., Carboni E., Clerbaux C., Corradini S., De Leeuw G., Elbern H., Engelen R., Fritzsche P., Gobbi G.P., Holmlund K., Höpfner M., Husson P., Kahn R., Malingreau J.P., Mannstein H., Munro R., Papineau N., Pergola N., Prata A.J., Remedios J., Richter A., Rix M., Rose W., Schneider D., Seibert P., Stammes P., Theys N., Thomas W., Watson I.M., Zehner, C.

R1: Access to all data sources for volcanic plume observations in Europe should be accelerated, improved and open.

R1.1: Obstacles to data access should be identified and reviewed, and appropriate measures taken to reduce known problems and delays.

R1.2: Data access to existing observing systems (including ESA and EUMETSAT) should be improved for
- Near-realtime delivery
- Full and open access

R1.3: Pathways to collect and integrate critical data from ground-based and airborne European and national networks and facilities should be established and expanded
- e.g. EARLINET, AERONET, MPLNet, GAW, ACTRIS, EUFAR, IAGOS
- National lidar and ceilometer networks, surface air quality sites such as EMEP (EU), IMPROVE (USA), WMO-GAW, etc.

R1.4: National authorities should share their databases, to allow transnational evaluation of operational dispersion models.

R1.5: An inventory of relevant satellite observing capabilities should be established and updated annually.

R1.6: An Eyjafjöll eruption database of all observations and products from the April–May 2010 event should be established for research purposes, to enable modelling, research, development, data assimilation, inverse modelling, model comparison.

R1.7: Data from future research missions (e.g. ADM, EarthCARE) should be made available as quickly as possible, and ideally in near-real time.

R1.8: Users should consider all relevant satellite data, not only European sources. e.g. Japanese missions.

R1.9: Access to timely data from volcano observatories should be improved.

R2: Existing observation capabilities within Europe should be further consolidated and enhanced by combining satellite, airborne and ground-based systems for detecting and characterising volcanic ash clouds.

R2.1: Existing Pan-European ground-based observation networks should be extended to be adequate for volcanic plume detection and for generation of a 4-D map of ash distribution.
- National Ceilometer networks
- Lidar sites in each country (Raman, polarisation, multiwavelength)
- Measurement stations at high altitudes

R2.2: Timely and coordinated deployment and reporting should be assured for national research aircraft within Europe
- Research aircraft operations are integrated in the framework of the European Network EUFAR, but decisions to deploy are made nationally.
- Note: Research aircraft from Switzerland, Germany, UK, France and Spain contributed actively to monitoring the plume and to the decision process. These are not operational, but can be made ready within 1–2 days, with *in situ* and remote sensing (lidar, radar) capabilities. They are useful for monitoring plume extent with high horizontal and vertical resolutions. They can sample ash particles to characterise scattering properties and density. They cannot (because manned) sample ash plume core. Thus, they cannot provide accurate measurements of mass concentration.

R2.3: Sub-orbital platforms should be investigated for detailed particle microphysical and optical measurements to support satellite retrieval products.

R2.4: Operational radiosondes should be extended with particle/ash measurements (e.g. backscatter sondes) for this type of event.

R2.5: A suitable (multiwavelength, polarisation) airborne lidar should be deployed on a high-altitude aircraft to measure the vertical distribution of the source, in order to constrain the plume evolution modelling.

R2.6: UAS (MALE and mini-UAS) should be deployed for *in situ* measurements to monitor and measure the vertical and horizontal distribution of the ash plume over closed airspace.

R3: Actions should be taken to ensure that accurate and timely data are available from volcano observatories or monitoring stations situated near to volcanoes.

R3.1: Capabilities should be ensured for measurements close to the volcano to characterise the ash column, in the early stages and throughout the eruption
- Collection of ash samples from near-source to a distance of n-days
- Refractive index measurements
- Size distribution
- Density measurements of ash particles
- Vertical profile
- Phase function

R3.2: Frequent measurements with radar, webcams, IR and UV cameras and Sun photometers should be made close to the volcano from an early stage of an eruption, to get plume height information.

R3.3: UAS (MALE and mini-UAS) should be deployed for *in situ* measurements
- for research on plume initial development
- in conjunction with dropsondes
- to characterise precisely the eruption source and plume during eruption, to initialise meteorological dispersion models

R4: Concerted developments should be undertaken to integrate existing advanced retrieval methods into operational systems.

R4.1: Crisis response based on proven operational methods should be progressively improved by the best scientific and technological advances.

R4.2: The performance of measurement systems and accuracy of retrieval algorithms should be reassessed in the light of the new safe ash concentration limits, as measurements will have to provide quantitative information with accuracy limits rather than qualitative ones – these new measurements should be used to reassess the threshold values.

R4.3: New and improved retrievals for volcanic ash should be developed for:
- Ash cloud height
- Ash cloud concentration
- Ash effective radius
- Mass loading

R4.4: Measurements of SO_2 should be given continued attention, notwithstanding the recent focus on the risks posed by volcanic ash
- SO_2 has proven to be a very reliable indicator of volcanic activity
- It is still unclear if ash is the only threat to aircraft or if SO_2/sulfuric acid is also harmful
- Pre-eruptive degassing measurements are potential early warning tools
- SO_2 height should be determined

R4.5: Quantitative ash concentration retrievals should be developed to combine mass loadings from SEVIRI with vertical height extent (e.g. CALIPSO, MISR, AATSR) information or model data.

R4.6: Longwave (IR) and shortwave (UV and VIS) ash cloud observations should be combined to derive particle size distribution.
- Longwaves are mainly sensitive to large particles (> 1 micron)
- Shortwaves are sensitive also to small particles (< 1 micron)

R4.7: Interactions between the research community and VAAC personnel should be enhanced to facilitate usage of new inputs in the operational system (e.g. EARLINET, AERONET, ceilometer networks, new satellite retrievals).

R5: Techniques for assimilation and inversion of satellite data in dispersion models should be further developed and applied to provide quantified ash cloud advisory information.

R5.1: Various observation types (e.g. airborne lidar, satellite-based, ground-based) should be used to constrain the vertical distribution of the source.

R5.2: Further developments should be made of inverse modelling and data assimilation techniques to constrain the source strength and plume extent using satellite observations.

R5.3: Mechanisms should be established for evaluating and adjusting model parameterisations, to respond as rapidly as possible to differences between the aggregated observations and model predictions.

R5.4: Inter-comparisons should be made of model simulations and remote sensing observations of ash clouds, specific volcanic gas phase constituents (e.g. SO_2, sulphuric acid), and related particle formation.

R5.5: Different models should be applied for selected eruptions where the retention of ash and its deposition are very important.

R5.6: Quantitative remote sensing data should be used as near-realtime input to dispersion models.

R5.7: Techniques should be developed to assimilate data from e.g. IASI, AIRS, GOME2, AVHRR, MODIS, SEVIRI and OMI into models to improve ash plume dispersal forecasting. These sensors are already very useful for detecting plumes (alerts).

R6: Relevant satellite observation systems and data products should be formally validated with observations from other sources and should, where appropriate, be certified versus quantitative requirements for volcanic plume monitoring.

R6.1: Data used for validation should be carefully distinguished from (satellite) data used for the early warning and monitoring phase.

R6.2: Satellite retrievals and dispersion model results should be intercompared, e.g.:
- AOD, particle type, effective radius, cloud height and location;
- Height, thickness, backscatter, colour ratio, and depolarisation from Caliop;
- AOD and range of heights from SEVIRI, PARASOL, MISR and AATSR;
- effective radius from SEVIRI, MISR, MODIS, AATSR, MERIS

R6.3: Satellite data should be further validated with ground-based operational measurements.

R6.4: Models should be validated using independent satellite observations
- e.g. MODIS, AATSR, MERIS, MISR, CALIPSO, SEVIRI.

R6.5: Satellite-based limb observations of SO_2 and aerosols in the UT/LS should be used for model validation and better characterisation of vertical transport of volcanic emissions.
- MIPAS and SCIAMACHY limb observations should be included in satellite data sets on volcanic events
- The potential to provide additional information on e.g. volcanic aerosol composition and vertical distribution should be investigated.
- Note: Spatial resolution and coverage of limb observations is insufficient for alerts to VAACs

R6.6: A suite of certified volcanic ash products should be developed, validated and delivered operationally. The minimum product set should include:
- Plume extent, IR optical depth, UV AAI
- Brightness temperature difference; cloud top height
- Ash mass loading; total mass; mean effective particle size
- Note: There is presently a paucity of standardised satellite data products dedicated to the ash problem. However, the necessary tools and techniques are currently available, along with the means for validation.
- Operational SEVIRI products provide visual (RGB) information every 15 minutes. They are very useful for following the plume. Scientific SEVIRI data products provide more information (e.g. height, particle size, AOD, SO2, ice) about the ash plume and should be made operational at a later stage.

R7: Actions should be taken to ensure that planned future European satellites will provide more efficient and guaranteed support for ash cloud related crises: both operational (MTG, Sentinels) and research missions.

R7.1: Infrared observations should be assured as a high priority, because of the need to monitor by night as well as by day.

R7.2: High spectral resolution observations (e.g. IASI, AIRS) should be assured because they can distinguish silicate ash from other airborne particles and provide the possibility to retrieve SO_2 and other volcanic gases.

R7.3: An interferometer on a geostationary platform should be considered high priority (IASI and AIRS have proved useful for monitoring both particles and gases in volcanic clouds).

R7.4: Geostationary imaging capability of MSG/SEVIRI, which is essential for monitoring ash plumes from space, should be maintained.

R7.5: Improved capabilities of MTG for monitoring of volcanic ash, aerosol and SO_2 should be assured
- MTG-FCI 0.4 and 0.5 micron channels for monitoring aerosols
- improved spatial and temporal resolution
- MTG-IRS 800—900 cm^{-1} spectral region for monitoring ash
- as demonstrated by IASI
- with high temporal resolution.

R7.6: The inclusion of a 1200–1400 cm^{-1} band on MTG-IRS should be reconsidered, in order to complement information on SO_2 concentrations from Sentinel-4 UVN.

R7.7: New opportunities for synergistic use of the suite of imagers and sounders on MTG should be considered.

R7.8: Timely geostationary satellite observations should be assured uninterrupted into the future, and enhanced.
- The current 5–15 mins data rate of MSG is adequate
- Note: Timeliness of both IR and visible imagery is critical for early warning (e.g. hot spots) and for plume monitoring.

R7.9: Consistent aerosol information products should be provided from SLST and OLCI on Sentinel-3.

R7.10: Sentinel-4 O2-A band (NIR) channel should be provided at high spectral resolution for vertically-resolved aerosol information.

R7.11: Although spatial resolutions of 1–10 km of current satellite instruments are adequate for monitoring ash clouds, future systems should provide higher spatial resolution (10–100m) data focused on hot spots, for early warning. High temporal resolution (10–15 minutes) is also a key requirement for a warning system.

R7.12: The feasibility should be investigated of using already-planned scientific lidar missions for volcanic ash monitoring.

R7.13: Sentinel-5 Precursor UV monitoring capabilities (ash, AAI, and SO_2) should be exploited for volcanic ash monitoring.

R8: Studies should be made of potential new satellites and instruments dedicated to monitoring volcanic ash plumes and eruptions.

R8.1: Some exploratory studies should be conducted to evaluate the best ways to utilise the data to develop products and investigate synergies between measurements from planned and proposed future missions.

R8.2: Vertical resolution of satellite data is very restricted from current satellite systems. There is an urgent need to gather information on the vertical structure of evolving volcanic clouds. This is best obtained from lidar systems, e.g. Caliop, but the repetition rate is poor. A study should be performed on a spaceborne scanning lidar mission that is adequate for volcanic ash plume monitoring.

R8.3: Feasibility should be investigated of an instrument that can be pointed towards an erupting volcano or evolving volcanic cloud, for higher spatial resolution and greater chance of observation.

R8.4: A small flexible mission dedicated to volcano monitoring should be studied:
- Camera with the right channels and sufficient coverage
- High spatial resolution to see between the clouds
- Agile pointing platform with fast planning
- Simple calibration system
- Stable thermal design
- Aimed at regions outside MTG coverage

R9: Intensive basic research should be conducted on physical, chemical and radiometric properties of volcanic ash, from crater to aged clouds.

R9.1: Refractive index measurements should be made of representative volcanic ash samples, with the accuracy needed for satellite retrieval algorithms.
- At least 10 different ash types (each volcanic eruption is unique)
- Real and imaginary indices
- Particle shape
- Covering UV to thermal IR wavelength range
- Spectral resolution of 0.5 wavenumber

R9.2: Density measurements of ash particles should be made so that optical depth measurements can be translated into mass concentration.

R9.3: The capacity to measure rapidly properties of ash ejected during any future crisis should be improved.

R9.4: Studies of fallout mechanisms are needed, such as ice formation, aggregation and sedimentation processes.
- Why do models keep the ash in the air for longer times than is seen from satellites or from data collected on the ground?

R10: European recommendations and actions should be coordinated with ICAO, the global presiding aviation regulatory authority, and with WMO, the coordinator of the global system of VAACs.

R10.1: A comprehensive observation system should be established, capable of detecting ash in multiple Earth locations under varied atmospheric conditions.

R10.2: Relevant European organisations should further engage in the relevant global frameworks for coordinating observation systems, sharing instruments, algorithms, data and experience amongst the various worldwide actors.

R11: A follow-up workshop should be organised to review progress on these recommendations after one year.

Annex 1a: UK Met Office contribution

A. Broad

1. General remarks: Volcanic ash observation and monitoring capability

Observations of volcanic eruptions are at present used in three main ways:

— Observing the eruption

— Observing the movement and extent of the ash cloud:

  — height
  — thickness/depth
  — location
  — concentrations

— Validation of numerical model predictions of ash cloud extent

2. General remarks: Current lessons learned from the Eyjafjöll eruption

— One of the largest uncertainties has been information on the status of the eruption for model initialisation. This leads to discrepancies in model outputs and is a key recommendation going forward: consistency in model initialisation and sharing of information on initialisation.

— A second big uncertainty has been obtaining information on ash cloud concentrations. Aircraft, primarily research facilities with appropriate instrumentation, have been a key tool but have been unable to fly through thick ash due to engine manufacturer constraints.

— It proved difficult to make definitive statements about ash cloud extent from any one single observational source. There is a need to integrate all observing sources in NRT (if possible), to have a best-estimate picture of geographical coverage, height and depth, and concentration. No single source or even multiple observation sources can give us all this at present.

— Exchange of information and sharing of best practices is vital and all will need to learn lessons from the recent eruption.

2.1 Observing the eruption

The largest uncertainty in the ability of numerical models to predict the spread of volcanic ash, and hence to advise aviation regulators, is in observations of the eruption itself:

— How high is the ash being expelled to?

— What concentration of ash is being expelled?

Current observations come from a range of sources: satellite (height & spatial distribution of the main plume), laser cloud base recorders (LCBR) and lidar systems (both detecting ash cloud height and depth), seismic (how active is the volcano) and human (height and concentrations).

These have been coordinated by the Icelandic Meteorological Organisation (IMO) through its official role as an IAVW (International Airways Volcano Watch).

3. Volcanic ash cloud observations

Observations are required of the ash cloud (directly or indirectly through other aerosols or column-integrated products): its geographical coverage, cloud height and vertical depth, and the concentration of ash within the cloud.

3.1 Satellite

The following satellite products are routinely generated in NRT and provide the basis for satellite detection:

- Products based on 15-minute SEVIRI data from Meteosat-9, including the following:
  - Two-channel BTD product based on 10.8 µm – 12.0 µm (thresholds kept under review to maximise useful signal);
  - Three-channel BTD product based on the two-channel version but using also SEVIRI 8.7 µm data to further exclude false alarm pixels;
  - 'Dust' RGB based on SEVIRI channels. Also a variant of this product, with some colour scale manipulation to allow better colour discrimination (following inputs from H-P Roesli, EUMETSAT);
  - HRV imagery, in particular at the dawn & dusk periods, when low Sun angles sometimes reveal the ash plume;
  - Cloud Top Temperature (CTT) and Cloud Top Height (CTH) based on multispectral analysis.

- Products based on AVHRR / MODIS direct broadcast data from polar-orbiting satellites (currently MetOp-A, NOAA-15, -16, -17, -18, -19, FY-1D, TERRA, AQUA), including the following:
  - Two-channel BTD products based on the same theory as the SEVIRI product described above;
  - False-colour RGB products (based on VIS channels) which sometimes shows the ash plume, especially if dense and especially at low Sun angles.

- Products based on IASI global coverage data from MetOp-A including the following:
  - SO_2 plume detection product.

In addition, products generated externally, most on an experimental or ad hoc basis, are routinely monitored to check their availability with appropriate timeliness, and also to check the information revealed by them, for possible future case studies and product improvements. These products include:

- Multispectral SEVIRI data analysis provided by Mike Pavolonis at CIMSS/SSEC at: *http://cimss.ssec.wisc.edu/goes_r/proving-ground/geocat_ash/loops/iceland.html*

— Expedited analysis of CALIPSO data from NASA LARC at: *www-calipso.larc.nasa.gov/products/lidar/browse_images/show_date.php?s=expedited&v=V2-02&browse_date=2010-04-20*

— Analysis of OMI data from AURA by NOAA/NESDIS at: *http://satepsanone.nesdis.noaa.gov/pub/OMI/OMISO2/iceland.html*

Limitations

— Satellite products are most useful where there are significant concentrations of volcanic ash, although for certain phases of the 2010 event, clear signals at long downwind ranges have been readily detected;

— Quantitative estimates of plume concentration are problematic;

— Products are affected by the presence of underlying, overlying or shrouding clouds, especially ice clouds.

3.2 Meteorological research aircraft

The UK has been operating two research aircraft, Germany one aircraft, and France one to two aircraft, since mid-April. The aircraft have aerosol remote sensing instrumentation (lidars – see below) as well as aerosol sampling instruments to measure concentrations and particulate characteristics.

These aircraft have proved to be invaluable during the 2010 Icelandic volcano eruption and have provided some of the most reliable, real-time information about ash cloud extent and concentrations.

Limitations

— They are not operational and need to be made airborne with the correct instrumentation at short notice.

— There are too few of them and thus spatial coverage is limited.

— They are subject to exactly the same problems as other aircraft and therefore cannot fly too close to dense areas of ash cloud to sample concentrations due to aviation safety considerations (engine ingestion of volcanic ash).

— Insurance difficulties to gain clearance to fly in dangerous conditions.

— The instrumentation that has been developed is of a research nature and also has its limitations. Further refinement of the instrumentation maybe necessary.

3.3 LIDARs (LIght Detection And Ranging)

Although generally operated by the research community and therefore not always available operationally, the most effective surface-based measurement systems for detecting the presence of volcanic plumes are lidar systems. They emit pulses of laser light and detect the backscattered signal.

Limitations

— They detect everything in the atmosphere, including low- and high-level cloud as well as volcanic ash. Using different observing channels (and other

observations), cloud and aerosol can be distinguished, although volcanic ash can not be specifically identified with complete certainty.

— Lidar signals cannot penetrate through thick clouds, so low-level clouds can obscure detection of aerosol/ash plumes higher up in the atmosphere.

3.4 Laser Cloud Base Recorders

Laser cloud base recorders (LCBRs – also known as ceilometers) are simple, low-power forms of lidars designed to measure the height of cloud bases. They can be retuned to measure aerosol layers and changes in aerosol concentration, and hence ash cloud.

Limitations

— Usually they are tuned to detect clouds in support of operational weather forecasting.

— Like lidars, LCBR signals are unable to penetrate cloud.

— Depending on the type of instrument, the height range to be monitored spans from near-ground levels up to 15 km in the atmosphere.

— LCBRs are unable to detect information to indicate particle size and shape.

— The raw data must be analysed by LCBR experts. The raw data is not routinely recorded or transmitted from the instruments because of limitations on communication bandwidth, although this is currently being addressed in Germany.

3.5 Lightning location

The ash plumes from some volcanic eruptions produce frequent lightning discharges in the immediate vicinity of the volcano, which are an indication that an eruption is taking place and generating ash clouds to sufficient altitude to trigger lightning events.

Limitations

— Subjective information on the magnitude of eruption activity only.

— Not systematic: does not apply to ALL eruptions.

3.6 Aerosol probes on board UAVs

Particle measurement system (PMS) probes are frequently fitted to aircraft and can measure aerosol particle size, from which it can be deduced whether the particle is volcanic ash or not. They can be mounted on UAV (Unmanned Aerial Vehicle) aircraft.

Limitations

— Data not available in real time: size distributions are derived in research mode, requiring laboratory analysis

— Expensive option compared to other technologies as probes can frequently be irreparably damaged when UAV returns to surface.

— Small UAVs have a limited flight range and can only operate at relatively low altitudes, below ~16 000 ft (4.9 km).

— Operations can be limited to designated areas such a military firing ranges.

3.7 Aerosol sondes

Particle measurement system (PMS) probes have been developed which can fly together with balloon-mounted meteorological radio-sondes. These can also measure aerosol particle characteristics from which it can be deduced whether the particle is volcanic ash or not and an estimate made of the concentration levels.

Limitations

— Development of the capability is ongoing and only a small number of the probes exist.

4. Volcanic ash cloud modelling

The Met Office's capability to predict the transport and spread of pollution is delivered by the NAME (Numerical Atmospheric-dispersion Modelling Environment) computer model. The model began development following the Chernobyl accident in 1986 and since that time it has been used to model a wide range of atmospheric dispersion events, including previous volcanic eruptions and the Buncefield explosion in 2005. In addition to its role as an emergency response guidance tool, the model is used for routine air quality forecasting and meteorological research activities. NAME provides a flexible modelling environment able to predict dispersion over distances ranging from a few kilometres to the whole globe, and for time periods from minutes upwards.

For forecasts that have been initialised consistently there has been remarkably good comparison between VAAC predictions (London, Toulouse and Montreal) and other models that are applicable to the eruption (NILU and the GMES MACC products coordinated by ECMWF).

Note: There needs to be proper interpretation of products from different models as there are not direct one-to-one comparisons. For instance, certain models provide total-column SO_2: a single, vertically-integrated product which gives the boundaries of an aerosol closely related to volcanic ash. The VAACs provide thresholds of ash concentration at a number of different layers in the atmosphere.

5. London VAAC official role and Met Office response to regulators

5.1 Met Office: London VAAC role

The Met Office's role throughout the eruption has been defined by its internationally-designated remit as a Volcanic Ash Advisory Centre (VAAC). The Met Office provides this service in accordance with the requirements of the International Civil Aviation Organisation (ICAO). In this context, the official VAAC advisories for the extent of the Eyjafjöll eruption follow worldwide ICAO

rules and show a single value for ash concentration taken to be the threshold of the fly/no-fly zone for safety purposes: 2 mg m^{-3}.

5.2 Official VAAC product

The official VAAC product is produced operationally by forecasters based on a 'safe' threshold value of 200 microgrammes of ash per cubic metre.

The Met Office London VAAC products are based on 6-hour averages and on averages over three flight layers: 0 to 20 000 feet (FL 000 to FL 200), 20 000 to 35 000 feet (FL 200 to 350), and 35 000 to 55 000 feet (FL 350 to FL 550).

5.3 Supplementary products: red, grey and black areas

At the request of the CAA in the UK the Met Office has added new, supplementary products to the official VAAC advisories which can be found at the Met Office website:
www.metoffice.gov.uk/corporate/pressoffice/2010/volcano/forecasts.html

The outer edges of the **red zones** on these charts represent the standard threshold (200 µg of ash per cubic metre) as used in the official VAAC products.

The **grey areas** represent ash concentrations that are 10 to 20 times the standard (red) threshold, representing an ash concentration of 2000–4000 µg m^{-3}. To operate in this new zone, airlines need to present the CAA with a safety case that includes the agreement of their aircraft and engine manufacturers.

The **black areas** represent ash concentrations that are 20 times the standard (red) threshold and twice the grey threshold (concentrations greater than 4000 µg m^{-3}. These are areas within which engine manufacturer tolerances are exceeded.

Note: Each model forecast of the extent of the ash cloud assumes that the volcano will continue to erupt at the same intensity for the duration of the forecast period. During the course of the Eyjafjöll eruption, the volcano's activity did not remain constant for more than a couple of days.

6. Suggestions for improvements in non-satellite volcano observation networks

6.1 Draft recommendations to the UK network

The UK Met Office, in coordination with research communities, is developing a set of recommendations for improvements to the UK network. These are:

— Proposed operational high power lidar network;

— Improved access to LCBR data;

— New research aircraft: a dedicated small twin-engined aircraft that is instrumented and ready to go at a moments notice with the capability to respond quickly to any pollution emergency or air quality incident;

— Improved aerosol sonde capabilities and UAVs.

These will be coordinated and integrated with any European network enhancements.

6.2 Current draft European suggestions

The European Commission have prepared an information note for all Commission Directorates ("The impact of the volcanic ash cloud crisis on the air transport industry," 27 April 2010 Assessment of risks). The Information Note states (paragraph 43):

— *"The "lessons learnt" show the need to accelerate ongoing research and development:*

— *"to improve data collection and modeling [sic] methodologies such as satellite observation and imagery, atmospheric in situ measurements, dispersion models etc.*

— *"to ensure that they fill the identified gaps of data and information needs and in order to support a robust and more detailed risk assessment.*

— *"to envisage new actions including the adoption of the latest technology such as unmanned aircraft vehicles (UAV) for atmospheric measurements, complementing or replacing the traditional in-situ measurements with balloons."*

7. Developments in support of volcanic ash and gas monitoring using satellite data

7.1 Met Office Volcanic Ash developments already performed or under way

MSG/SEVIRI

1. A new MSG 3-channel volcanic ash product has been developed and is now in routine production for the Iceland area and also extended to the wider North Atlantic area. The primary motivation was to improve the existing SEVIRI two-channel product and to complement the (very useful) RGB 'Dust' product by providing better discrimination of the plume from surroundings.

2. The algorithm for ash that is being used by EUMETSAT is also being trialled at the Met Office after adjustment of some of the thresholds, but to date a robust product has not been achieved.

AVHRR and MODIS on polar orbiters

3. The ash signal threshold (brightness temperature difference) for the two-channel volcanic ash products has been adjusted to reduce the number of 'false alarm pixels'.

4. Increased frequency and coverage of the two-channel volcanic ash polar products have been implemented, by:

    — Including products based on MODIS on Terra and Aqua (tuning work still in progress)
    — Looking at other polar orbiter imagers (e.g. FY-1D)

Other data sources

5. Known sources of alternative data generated in research mode are being investigated, which may be considered for operational implementation at the London VAAC but, in the short term, have been made available by links to external sites. Some examples are:

   — LATMOS IASI data SO_2 at: *http://cpm-ws4.ulb.ac.be/Alerts/index.php?NewYear=2010&NewMonth=05&sel_day=0*
   — MODIS aerosol optical depths at: *http://lance-modis.eosdis.nasa.gov/*
   — Imager data from GOSAT at *www.gosat.nies.go.jp/eng/related/201004.htm*

7.2 Future developments

Short-term

— Initial demonstration of quantitative ash cloud products from MSG:

   — Ash cloud height – using standard or slightly revised SEVIRI cloud-top height scheme,
   — Ash column amount – using standard or slightly revised SEVIRI cloud emissivity scheme, then converting emissivity to optical depth, and thence to estimate of ash column amount. (This estimate can only be expected to be accurate when the transmittance is in the range ~0.2–0.8.)

— Initial investigation into ash detection using IASI (on same platform as AVHRR and with higher spectral resolution but with lower spatial resolution). Comparison with collocated AVHRR products and proposals for quantitative product development.

Possible within one year

— Further development of Meteosat and AVHRR/MODIS ash-detection imagery products, e.g. fewer false alarms.

— Improved retrieval of ash cloud height, optical depth and ash concentration from Meteosat and Polar imagery.

— Determination of minimum threshold of ash detection with Meteosat and AVHRR/MODIS.

— Further development of ash cloud quantification from IASI. If successful, extension to AIRS could be investigated to improve temporal coverage.

— Investigation of SO_2 products: MSG/SEVIRI (based on 7.3 micron channel signal), MetOp/IASI and Aqua/AIRS (based on spectral features around 7 and 8 microns).

— Study of other potentially useful products, currently available in research mode – see (5) above. Identify those that might be useful to the VAAC, and work with data providers to make products available in near-real time.

Longer term developments

— Exploit other new operational sensors as they become available (e.g. NPP carrying VIIRS, CrIS and OMPS, from late 2011. VIIRS will gives MODIS-like capability.

— Exploit other research sensors as they become available:

  — ACE
  — EarthCARE

— Doppler wind lidar – ADM/Aeolus from 2013.

— Exploit Meteosat Third Generation (subject to final approval) from ~2017, carrying MTG-FCI (SEVIRI follow-on) and MTG-IRS (advanced IR sounder).

— Review post-EPS and Sentinel-5 payloads to ensure a good capability to monitor volcanic ash and gases from at least one of these platforms.

Annex 1b: The European Aerosol Research Lidar Network (EARLINET)[1]

I. Mattis, G. Pappalardo

1. Introduction

EARLINET is the first tool capable of doing 4-dimensional aerosol measurements. It was established in 2000 to derive a comprehensive, quantitative, and statistically-significant database for the aerosol distribution on the continental and long-term scale (Bosenburg et al, 2003; Pappalardo et al., 2010). A lot of other effort has been made in the past to measure the horizontal, vertical and temporal distribution of the aerosol particles on a global scale. Passive remote sensing instruments aboard satellites or ground-based sun photometers usually cannot measure the vertical layering of aerosol plumes. Vertically-resolved lidar measurements are therefore an indispensable tool to study the vertical structure of the aerosol field, and its temporal development. Unfortunately, single ground-based lidar observations cannot detect the horizontal variability of the aerosol field, and lidars aboard aircraft cannot perform process studies or long-term measurement series. Only coordinated network observations of lidars can overcome these problems.

All EARLINET stations measure simultaneously on a predefined schedule at least three times a week, e.g. Monday afternoon and Monday and Thursday after sunset. This data set is used to obtain unbiased data for climatological studies. The increasing number of automated EARLINET lidars drastically improves the overall measurement time. Additionally to these regular measurements, coordinated network observations are performed to address specific important events such as Saharan dust storms, forest fires, volcanic eruptions (Pappalardo et al., 2004a; Wang et al, 2008), and photochemical smog. All measured profiles are stored in a centralised database with a standardised data format, which allows easy access to the complete data set for further scientific studies.

Coordinated network activity for observation of the Eyjafjöll ash plume over Europe started at 15 April 2010. Almost all EARLINET stations started intensive measurements and observed the evolution of the ash plume until 24 April. The plume first reached the stations Cabauw and Hamburg during the morning hours of 16 April. Later that day the layer arrived at Leipzig and Munich at between 2.5 and 6 km altitude. The optical depth of this first plume at 500 nm was up to 0.7. Ash mass concentrations were of the order of 1000±350 µg m^{-3} in the centre of the main ash layer (Ansman et al., 2010). Later the ash plume was diluted and distributed over almost all Europe, e.g. it reached Italy on 19 April and Greece on 21 April.

A second event was observed over Portugal and Spain (6 May) and then over Italy (8 May) and Greece (10 May). The volcanic plume was then observed again over Southern Germany on 11 May.

Detailed daily reports with summaries of the EARLINET observations were submitted to WMO.

[1] The EARLINET-ASOS project is funded by the EC under grant RICA-025991. ESA financial support under ESTEC Contract No. 21487/08/NL/HE and ESRIN Contracts No. 21769/08/I-OL and 22202/09/I-EC is gratefully acknowledged.

2. Instrumentation

Fig 1b1 illustrates the locations of the lidar stations that participate in EARLINET. Detailed locations and contact information can be found at *www.earlinet.org*.

Three of the stations operate fully-automated lidars on the basis of round-the-clock observations. There are nine simple backscatter lidars. Eighteen of the EARLINET stations operate Raman lidars that allow for the independent retrieval of profiles of the particle extinction and backscatter coefficients (Ansman et al., 1992). The particle extinction-to-backscatter (lidar) ratio contains information on particle size and particle light-absorption and thus allows for a rough separation among different aerosol types. Nine multi-wavelength Raman lidar stations belong to EARLINET. These lidars allow for the retrieval of three backscatter coefficients at wavelengths 355 nm, 532 nm, and 1064 nm, plus two extinction coefficients and lidar ratios at 355 nm and 532 nm. The wavelength dependence of the backscatter and extinction coefficients and of the lidar ratios allow for a more detailed differentiation of aerosol types (Müller et al., 2007).

Within EARLINET, inversion algorithms were developed to obtain microphysical aerosol properties such as effective radius, volume- and surface-area concentration, and real and imaginary parts of the complex refractive index from multi-wavelength Raman lidar information (Müller et al., 1999; Böckmann, 2001; Böckmann et al., 2005). Backscatter coefficients at three wavelengths plus extinction coefficients at two wavelengths are the minimum required input data for such inversion schemes (Veselovskii et al., 2002).

There is a rigorous quality assurance programme for instruments (Matthias et al., 2004) and evaluation algorithms (Böckmann et al, 2004; Pappalardo et al., 2004b). In 2006 the EC-funded infrastructure project European Aerosol Research Lidar Network: Advanced Sustainable Observation System (EARLINET-ASOS) was launched. The main concerns of EARLINET-ASOS are the development of tools for the automatisation and homogenisation of the lidar systems and the development of a centralised and homogenised data analysis (Amodeo et al., 2007).

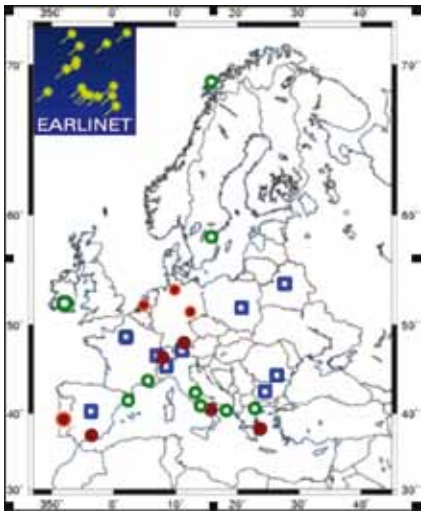

Fig 1b1. Locations of the lidar stations of the EARLINET consortium in June 2010. Open squares indicate simple backscatter lidars; open circles show Raman lidar stations; and solid circles indicate multi-wavelength Raman lidar stations.

3. Separation of aerosol types

EARLINET extends from the Mediterranean in the south to Andøya north of the Arctic circle. There are midlatitude marine stations like Bilthoven, Cabauw and Hamburg, and lidar sites with continental climate like Belsk and Minsk. The Mediterranean Sea is covered by three Spanish stations in the west, four sites in Italy, and two Greek stations in the east of the Mediterranean. Because of this large geographical extent, EARLINET can study a variety of aerosol types under different meteorological and climatological conditions. There are very clean conditions in Andøya. There are EARLINET sites in relatively clean areas like Cabauw as well as in the highly-polluted megacity Athens.

Several times a year, mineral dust plumes are transported from the Saharan region and across Europe. Also detected are smoke plumes from European forest fires, mainly inside the planetary boundary layer (PBL), and in the free troposphere (FT) from sources in North America or Siberia. Differences can be observed between fresh anthropogenic pollution in the highly-industrialised regions of western Europe, e.g. in the PBL over Leipzig, anthropogenic pollution in less developed areas, e.g. the Balkan, and aged anthropogenic pollution from the east coast of North America, which is advected to Europe in the FT.

Table 1b1 provides an overview which combinations of measured optical data allow for a separation of the usual aerosol types over Europe (Müller,

Table 1b1: Possible aerosol type differentiation from lidar measurements.

Directly-measured quantities	Successive separation into aerosol types, for the ideal case that there are no other aerosol types or mixtures of aerosol types
1-β + 1-α	A-K
1-β + 1-α + 1-δ	A, F, G, H, I, J, K | B, C, D, E
2-β + 1-α + 1-δ	A, K, F, G, H | I, J | B, C, D | E
3-β + 1-α + 1-δ	A, K | F, G, H | I | J | B, C | D | E
2-β + 2-α + 1-δ	A | K | F, G | H | I | J | B | C | D | E
3-β + 2-α + 1-δ	A | K | F | G | H | I | J | B | C | D | E microphysical retrieval of spherical particles
3-β + 2-α + 2-δ	(limited) microphysical retrieval of mineral dust particles

personal communication, undated). The complete differentiation between all usual aerosol types is possible only in the case of a combination of profiles of backscatter coefficients at three wavelengths, extinction coefficients at two wavelengths, and a particle depolarisation profile. Such data sets are provided by the nine multi-wavelength Raman lidars in EARLINET.

The optical properties of the first, highly-concentrated aerosol plume from the Eyjafjöll eruption (as observed over Leipzig and Munich) were similar to the optical properties of fresh Saharan dust. The extinction-to-backscatter ratios ranged from 55–60 sr. The values of the particle depolarisation ratio at 532 nm were close to 35% and thus they were slightly higher than the ones for pure Saharan dust (25%–35%). The values of the ash-related Ångström exponents in the short wavelength range were 0–0.1 and thus larger than the values of about 0.7 that are typically observed for Saharan dust layers over Leipzig. Also in this case, a separation of the optical signature of the ash plume from the signatures of other aerosol types was only possible by a combination of the extinction-to-backscatter ratio, the depolarisation ratio and the multi-wavelength information (Ångström exponent).

4. EARLINET – satellite and global scale

EARLINET represents an optimal tool to validate CALIPSO lidar data and to provide the necessary information to fully exploit the data produced from that mission. In particular, aerosol extinction and lidar ratio measurements, provided by the network, are important for the aerosol retrievals from the backscatter lidar (CALIOP) on board CALIPSO. EARLINET started correlative measurements for CALIPSO on 14 June 2006, at the beginning of the operational period of CALIOP (Pappalardo et al., 2010); these correlative measurements are still in progress.

EARLINET will contribute also to future satellite missions with lidar on board such as ADM-Aeolus and EarthCARE. Each of these missions will have on board a High Spectral Resolution Lidar at 355 nm, able to give independent measurements of aerosol extinction and backscatter coefficient in the UV. The multi-wavelength EARLINET data will be very useful to validate these missions and also to give the conversion factors that allow integration of the aerosol data at 532 nm and 1064 nm from CALIPSO with the measurements at 355 nm from ADM-Aeolus and EarthCARE.

At a global scale, within the Global Atmosphere Watch (GAW) aerosol programme, EARLINET also strongly contributes to the implementation of GALION, the GAW Aerosol Lidar Observation Network (Bösenberg and Hoff, 2008).

Annex 1c: Report on the Falcon flight of 19 April 2010

U. Schumann, H. Schlager, B. Weinzierl, O. Reitebuch, A. Minikin, H. Huntrieser, T. Sailer, H. Mannstein[1]

Abstract

A successful Falcon measurement flight was performed on 19 April 2010 to probe plumes over Germany from the Eyjafjöll volcano eruption. Layers of volcanic ash were detected by lidar and probed *in situ* with aerosol instruments. Under suitable viewing conditions, the ash layer was visible as a brownish layer. The horizontal and vertical distributions of the volcano layers were variable. In the plume layers, particles larger than 3 µm were detected at concentrations not present in the free troposphere during unpolluted conditions. The concentrations of large particles measured in the volcano layers are comparable to concentrations measured typically in Saharan dust plumes but smaller compared to particle concentrations in the polluted boundary layer. An estimation of the particle mass concentration in the volcanic ash plume, probed as part of a vertical profile over Leipzig at about 4 km altitude, yielded 60 µg m^{-3}.

After the flight the Falcon was inspected. No damage was found during initial inspections, including of the engines (after boroscopy) and windows. Further engine inspection continued for some time. Silver foils attached to under-wing stations showed no visible impact from volcanic ash.

1. Flight route and meteorological situation

The flight route is shown in Fig 1c1. Takeoff and landing in Oberpfaffenhofen were at 14:12 UTC and 17:53 UTC, respectively. The flight route was from Oberpfaffenhofen to Leipzig, Hamburg, Bilthoven (Netherlands), Stuttgart and back to Oberpfaffenhofen. The Falcon was mainly cruising at 8 km altitude for lidar observations. Vertical flight profiles were performed at Leipzig and Stuttgart. Near Aachen the Falcon climbed to 11 km for measurements in the stratosphere.

During the flight, air masses with aged volcanic emissions were measured in the southern and middle part of Germany (Fig 1c3). These air masses first arrived in Germany on 16 April (originating from the first strong volcanic eruption on 14–15 April) but then circulated around a high pressure system over France before arriving in Germany a second time on the 19 April (~4–5 days old).

Fig 1c1. Flight route of the DLR Falcon on 19 April 2010

2. Visual and Meteosat impressions of the volcanic aerosol layer

During the flight, volcanic ash layers were clearly visible as shown in Figure 1c2. This picture was taken from the Falcon over Leipzig at around 15 UTC, where the volcanic ash layer had a vertical depth of about 2 km. The volcanic ash plume was also visible by Meteosat (Fig 1c4).

Fig 1c2. Picture taken on board the DLR Falcon near Leipzig on 19 April 2010

[1] DLR-Institut für Physik der Atmosphäre, Oberpfaffenhofen, 20 April 2010

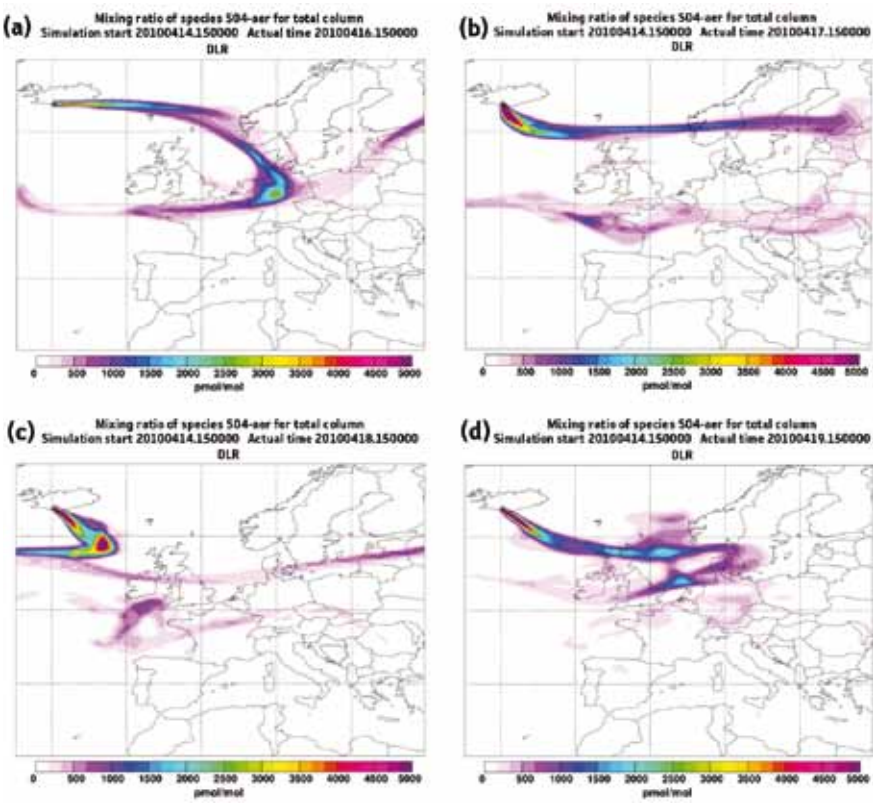

Fig 1c3. FLEXPART simulations of the time evolution of an aerosol tracer released from the Iceland volcano (release rate inferred from MSG observations) from 14 April 2010. Total columns (pmol/mol) on 16 April, 15 UTC (a), 17 April, 15 UTC (b), 18 April, 15 UTC (c), and 19 April, 17 UTC (d) (conditions during the Falcon flight).

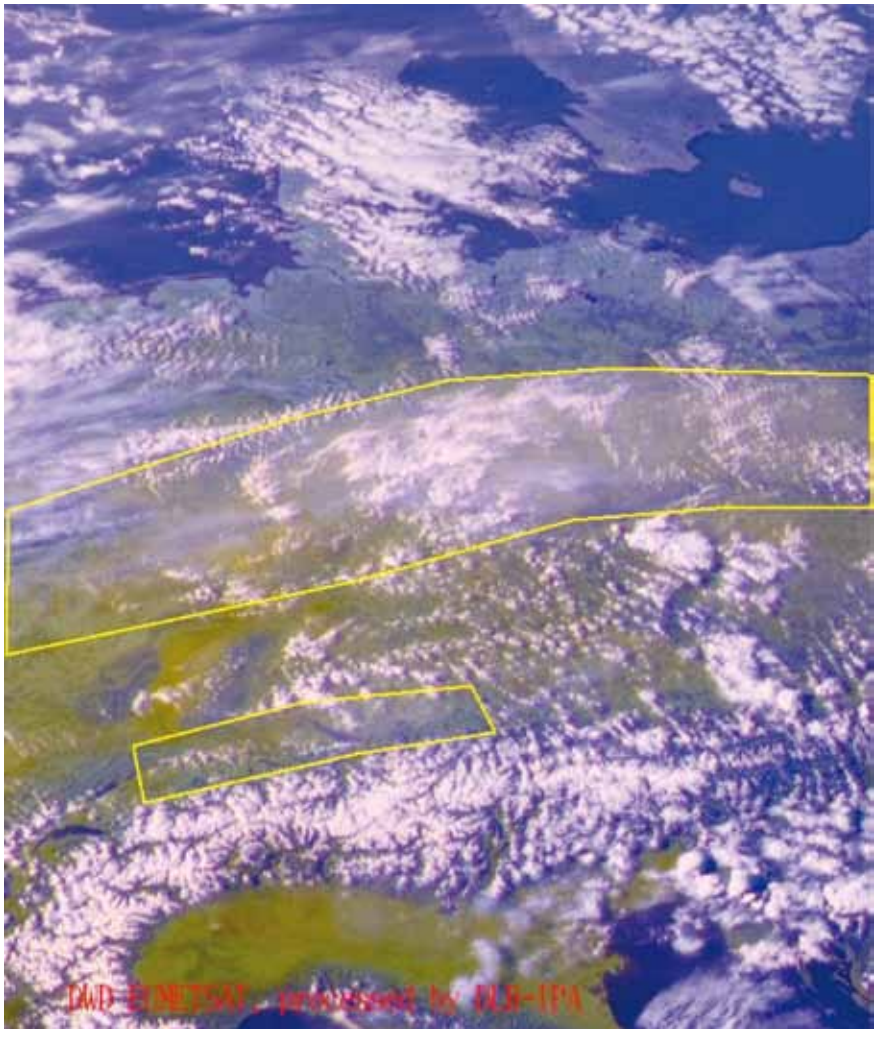

Fig 1c4. False colour composite including information from the Meteosat-SEVIRI high resolution visible channel with a resolution of 1 km at the sub-satellite point. Due to the low Sun at 1600 UTC, aerosol layers become visible mainly due to a reduction of the contrast of surface features. The yellow polygons enclose areas showing such a reduced contrast, not only in this image but also in the time series. A distinction between the ash layers and boundary layer pollution is not possible, but trajectory analysis indicates a good agreement to the aerosol from the Eyjafjöll volcano eruption from 14 April 2010.

3. Lidar results

Measurements of aerosol and particle layers (upper and lower boundary, height, horizontal extent) were performed with a 2-µm lidar. The quicklooks made during the flight show clearly elevated particle layers above the atmospheric boundary layer. The lidar detected several layers of higher particle content at altitudes between 3.5 km to 6 km. Near Munich two layers of 500–1000 m thickness were observed. Near Leipzig these two layers were partly combined into one layer of 2 km thickness. In general, the layers were horizontally and vertically very inhomogeneous and changed their properties on scales of 100–200 km. The particle concentrations in the elevated layers (above 3.5 km) were lower compared to the particle concentration in the boundary layer (below 3 km). In northern Germany (around Hamburg) no particle layers were observed above the boundary layer. Quicklooks of lidar vertical cross sections are shown in Figures 1c5 to 1c7.

Note: These figures are quicklooks, and hence show the scanning mode oscillations of about 45 s.

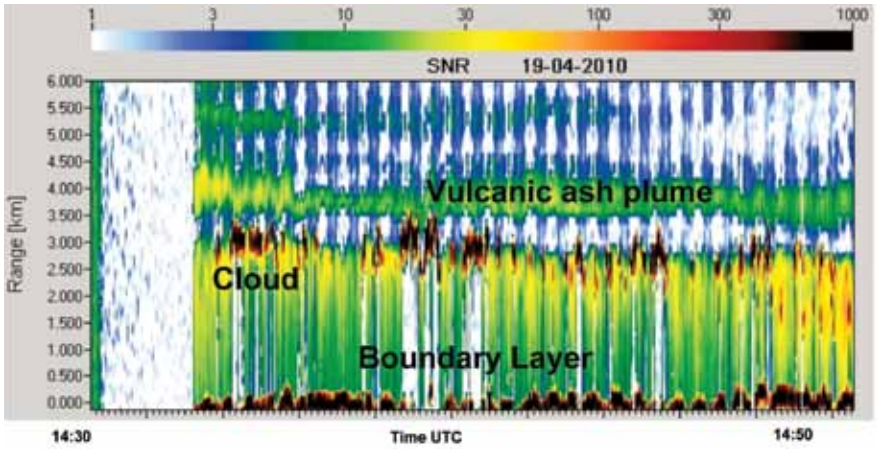

Fig 1c5. Quicklook from 2-µm lidar measurements from Falcon flight on 19 April 2010 showing signal-to-noise ratio (SNR) shortly after takeoff from Oberpfaffenhofen, from 14:30–14:50 UTC going north for 20 minutes (about 200–240 km flight track). Red/black shows high SNR from clouds (around 3 km) and ground (0 km); blue/green shows layers with aerosol; white/blue indicates noise (no valid data); two layers of higher aerosol level are visible at 4 km and 5.5 km.

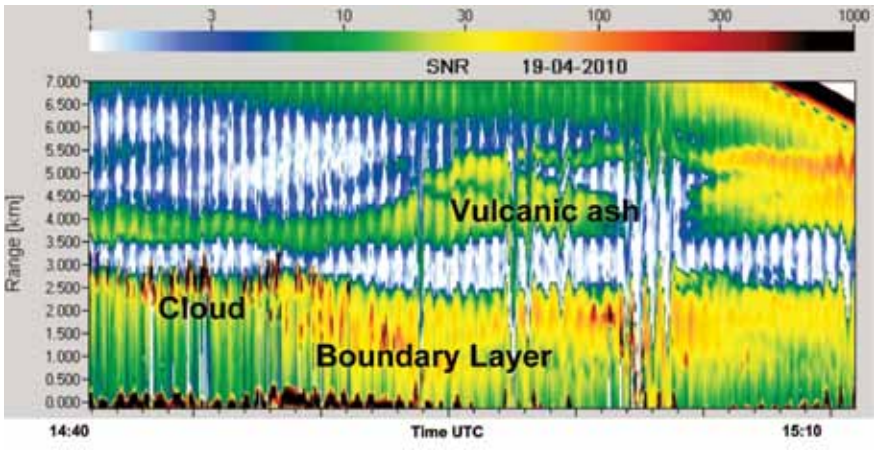

Fig 1c6. Quicklook from 2-µm lidar measurements from Falcon flight on 19 April 2010 showing SNR over 30 minutes south of Leipzig and around Leipzig from 14:40–15:10 UTC. Red/black shows high SNR from clouds (around 3 km) and ground (0 km); blue/green shows layers with aerosol; white/blue indicates noise (no valid data); the two layers of higher aerosol level (at left) at 4 and 5.5 km merge into one layer of almost 2 km thickness (at right).

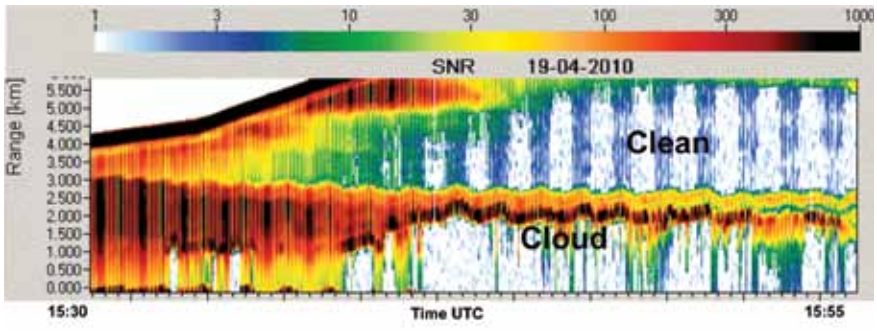

Fig 1c7. Quicklook from 2-µm lidar measurements from Falcon flight on 19 April 2010 showing SNR over 25 minutes from Leipzig to Hamburg from 15:30-15:55 UTC. Red/black shows high SNR from clouds (around 2 km); above the clouds (>3 km) no aerosol layers are visible (middle to right side of figure).

4. Results from *in situ* measurements

Figures 1c8 to 1c10 depict the time series of *in-situ* measurements recorded during the flight.

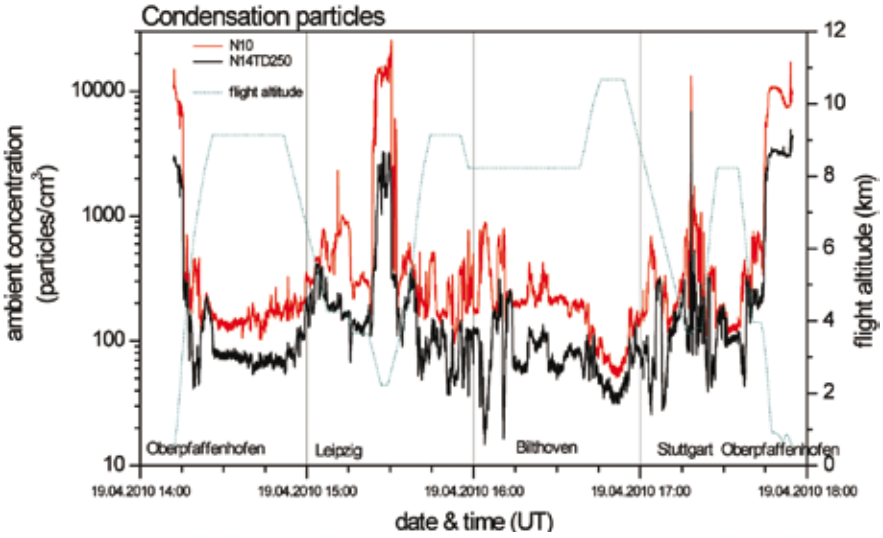

Fig 1c8. Time series of total particle fine number concentration (N10) and total non-volatile particle fine number concentration (N14TD250) measured during the research flight.

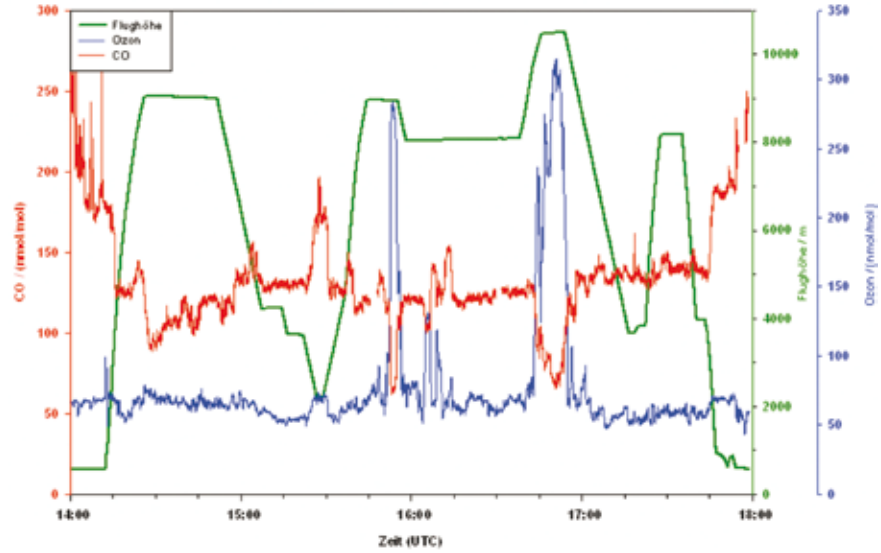

Fig 1c9. Time series of carbon monoxide (CO) and ozone (O_3) during the Falcon flight on 19 April 2010.

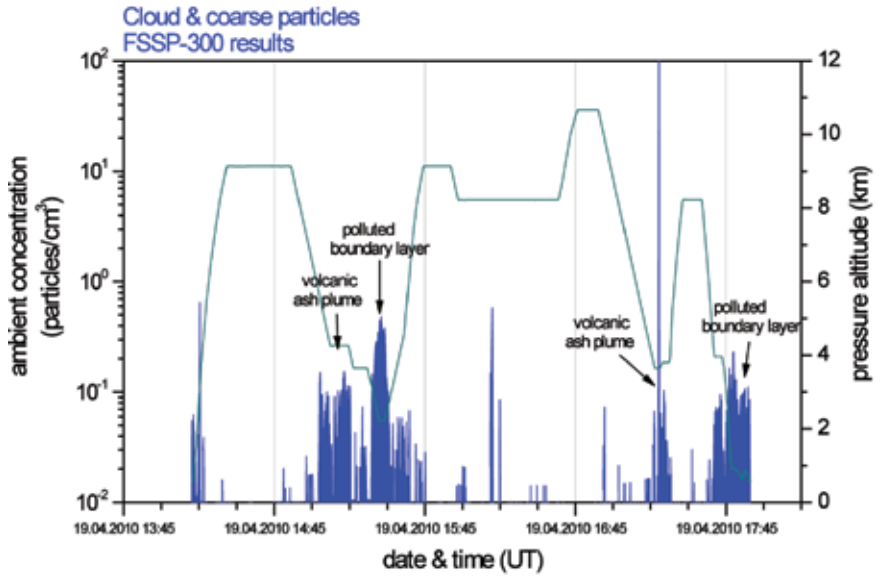

Fig 1c10. Time series of super-micron particle number concentrations measured during the research flight (FSSP-300, channels 18–31; assuming the refractive index of ammonium sulphate; this corresponds to the size range of approximately 3–20 µm).

In Fig. 1c8, total particle number concentrations in the size range 10 nm to 2.5 µm are shown in red; non-volatile particles (dust/ash, black carbon, or sea salt) in black; and the flight altitude in green. Fig. 1c9 displays volume mixing ratio of carbon monoxide (CO) and ozone (O_3). Fig. 1c10 shows the number concentrations of super-micron particles.

The ash plume was probed at an altitude of 3.8–5.8 km during the descent over Leipzig, between 15:00 and 15:15 UTC. Furthermore, it was again probed near Stuttgart at an altitude of 3.8 km around 17:20 UTC. In the volcanic ash plume the total aerosol concentration is enhanced, as well as the number of super-micron particles (3–20 µm) which normally are not present at these altitudes in the free troposphere. No signatures in CO and ozone are observed. The boundary layer extends up to 3 km and is quite polluted (total fine particles >15 000 particles per cm^3; CO up to 200 nmol per mol). Furthermore, the number concentration of super-micron particles is enhanced. Because of the high CO values the boundary layer is likely to be dominated by urban pollution. A contribution of volcanic aerosol can not be excluded due to the high super-micron particle concentration.

The volcanic ash plume over Leipzig is also nicely illustrated in the vertical profile measurements (Figure 1c11, left).

Figure 1c11 (right) shows an intercomparison of coarse mode particle concentration measured in fresh Saharan dust plumes (aerosol optical depth 0.4 – 0.6) and coarse mode particle concentration measured in the volcanic ash plume measured over Leipzig (red symbol). The coarse mode particle concentrations in the volcanic ash plume measured on 19 April 2010 (age: 4–5 days) is in the range seen in Saharan dust plumes.

The particle number size distribution in the volcanic ash plume over Leipzig is shown in Figure 1c12. It is a composite of three laser aerosol spectrometers (optical particle counters), a PCASP-100X and a FSSP-300, both mounted under the aircraft wings, and a Grimm-OPC 1.129 mounted in the cabin. PCASP and OPC data agree well in the overlapping size range. It is currently unknown if the FSSP-300 data in the size range of 3–4 µm could be affected by some overcounting due to electronic noise.

The conversion of the physical raw data of these instruments into size information depends on the assumption of the refractive index of the measured particles. The refractive index is connected to the chemical composition and structure of the aerosol particles and is unknown for this particular aerosol

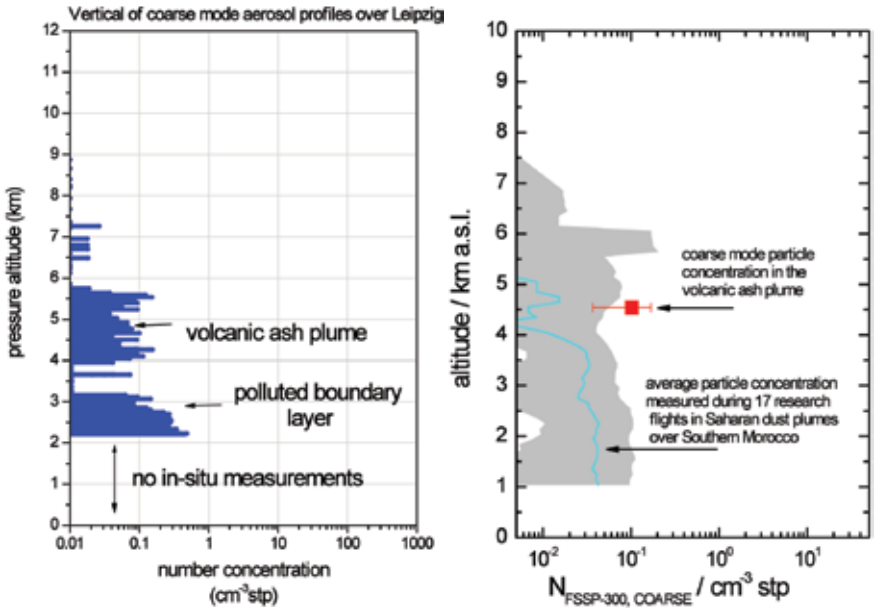

Fig 1c11 (Left) Vertical profile of coarse mode particles (3–20 µm) measured over Leipzig. (Right) Intercomparison of coarse mode particle concentration measured in fresh Saharan dust plumes (aerosol optical depth 0.4–0.6) and coarse mode particle concentration measured in the volcanic ash plume measured over Leipzig (red symbol). The blue line shows the median particle concentration in the Saharan dust plumes, and the grey shaded area represents the range within 10- and 90-percentile values. All values in this graph are given for STP conditions (273.15 K, 1013.25 hPa).

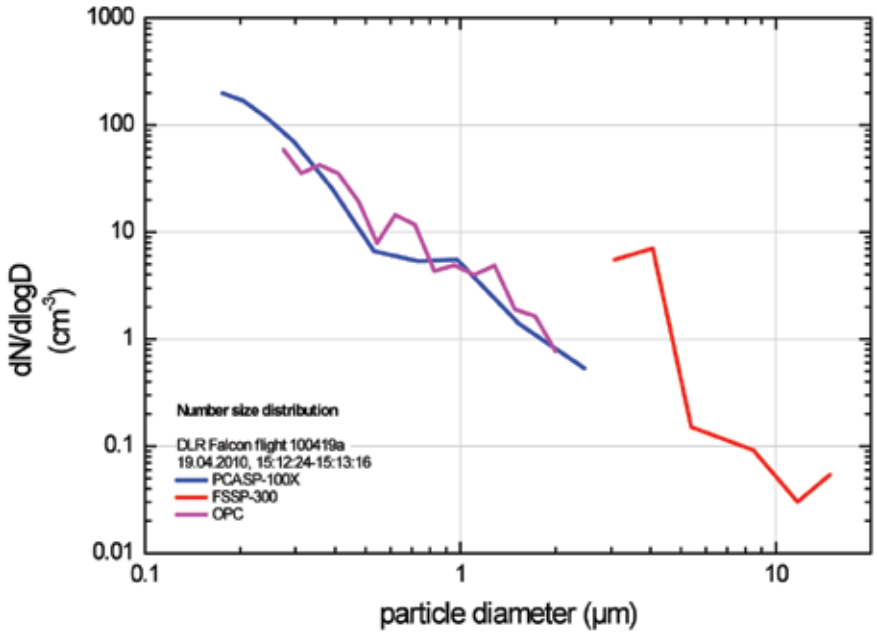

Fig 1c12. Preliminary aerosol number size distribution in the volcanic ash plume over Leipzig at 4.3 km pressure altitude.

layer. The general effect is: If particles contain absorbing material, the particle size derived from the same raw data signal is larger. This is critical in particular for the large particles of around micron size which dominate the total volume of the aerosol population. For this preliminary analysis, a refractive index value in the coarse particle size range was used according to published data for volcanic particles (but not knowing if the particles investigated are of the same type). Therefore, the data here have to be used with care because of possible systematic errors.

Given these constraints, the total particle volume can be derived from the particle number size distribution. This in turn can be converted into a mass concentration if the particle density is known.

Assuming a particle density of 2 g cm^{-3} our current best estimate for the particle mass concentration in the ash plume over Leipzig is 60 µg m^{-3}. The error is difficult to estimate without further analysis but at least a factor of two uncertainty should be assumed. It is possible that higher concentrations occur in other parts of the plume. In fresh volcanic plumes the concentrations will be much higher.

Annex 1d: The role of ground-based meteorological radars within volcanic ash observation and monitoring capability

F.S. Marzano, E. Picciotti, and G. Vulpiani

1. Introduction

Volcanic ash is a natural hazard whose effects have been well documented. It is a hazard to aircraft operations, and the threat to public safety posed by volcanic ashfall is significant. Given these hazards, timely detection and tracking of the ash plume is essential to a successful warning process, particularly during and immediately following an eruptive event.

As pointed out by UK Met Office, the largest uncertainty in the ability of numerical models to predict the spread of volcanic ash, and hence to advise aviation regulators, is in observation of the eruption itself:

i) How high is the ash is being expelled?

ii) What concentration of ash is being expelled?

Observations listed by the UK Met Office came from a range of sources: satellite (height & spatial distribution of the main plume), laser cloud base recorders (LCBR) and Light Detection And Ranging (Lidar) systems (both detecting ash cloud height and depth), seismic (how active is the volcano) and human (height and concentrations).

The use of **ground-based meteorological microwave radars** should be added to this list. Their role within the volcanic ash monitoring network is the topic of this contribution.

2. Ground-based radars and remote sensing of ash clouds

A variety of satellite techniques have been successfully used to track volcanic ash clouds; however, these techniques have certain limitations in both spatial and temporal resolution. Issues involving the detection of ash clouds using infrared brightness temperature differencing, a commonly-used method, have been addressed, suggesting several scenarios where effective infrared satellite detection of volcanic ash clouds may be compromised. The brightness temperature differencing, also known as the 'split-window' method, was shown to be subject to errors when the volcanic plume lies over a very cold surface, or when the plume lies above a clear land surface at night where strong surface temperature and moisture inversions exist. Ground-based microwave instrumentation, such as Global Positioning System (GPS) receivers and wind profiler radars, may play a complementary role for monitoring volcanic cloud evolution, even though their operational utility is limited by the relatively small spatial coverage. On the other hand, ground-based lidar optical systems may show a higher sensitivity to ash content than microwave instruments, but counterbalanced by stronger path attenuation effects.

Ground-based microwave radar systems can have a valuable role in volcanic ash cloud monitoring, as evidenced by available radar imagery. These systems represent one of the best methods for realtime and areal monitoring of a volcano eruption, in terms of its intensity and dynamics. The possibility of monitoring 24 hours a day, in all weather conditions, at a fairly high spatial resolution (less than a few hundred metres) and every few minutes after and during the eruption is the major advantage of using ground-based microwave

radar systems. They can provide data for determining the ash volume, total mass and height of eruption clouds.

There are still several open issues with the microwave weather radar capabilities of detecting and quantitatively retrieving ash cloud parameters. A major limitation in the exploitation of microwave weather radars for volcanic eruption monitoring is the exclusive use of operational weather radars for clouds and precipitation observation. Several unknowns may also condition the accuracy of radar products, most of them related to the microphysical variability of ash clouds due to particle size distribution, shape and dielectric composition. Some of them have been analysed in previous works (Marzano et al., 2005, 2006a), where the sensitivity of microwave radar response to particle ash distribution and wavelength was investigated using ad hoc, physically-oriented random schemes of eruptive ash cloud volumes. Fine-sized ash, medium-sized ash and lapilli were distinguished with mean diameters of about 0.01 mm, 0.1 mm and 1 mm, respectively, and concentrations of up to few tens of grams per cubic metre. The electromagnetic behaviour of pure and porous ash particles was also modelled, and its impact on the radar reflectivity signature was analysed for fine ash, medium ash and lapilli. No particle aggregation mechanisms and effects were considered in these works.

Indeed, the aggregation of volcanic ash particles within the eruption column of explosive eruptions has been observed at many volcanoes. Recent satellite observations of ash clouds provide strong indirect evidence that ice may be present on ash particles. The aggregation influences the residence time of ash in the atmosphere and the radiative properties of the 'umbrella' cloud (i.e. ash at the height of neutral buoyancy, spreading horizontally and vertically). Numerical experiments are helpful for exploring processes occurring in the eruption column. Some advanced plume models can simulate the interactions of hydrometeors and volcanic ash, including aggregate particle formation within a rising eruption column (Marzano et al., 2008, 2010b).

In order to quantitatively evaluate the ash retrieval by weather radars, a prototype algorithm for volcanic ash radar retrieval (VARR) has recently been formulated and discussed (Marzano et al., 2006b, 2010b). Starting from measured single-polarisation reflectivity, the estimation method is based on two cascade steps: i) a classification of eruption regime and volcanic ash category; ii) estimation of ash concentration and fall rate. The expected accuracy of the VARR algorithm estimates is evaluated on synthetic data sets. A minimum detectable reflectivity analysis is also accomplished for various ash classes and for some available radar systems at S, C and X band.

3. Sensitivity of ground-based radar to volcanic ash particles

A common question is about the sensitivity of ground-based meteo-radars to volcanic ash particles. Radar systems are often thought to be sensitive to particles above a few millimetres such as lapilli and ballistic particles, but this is fundamentally incorrect or, at least, incomplete. As shown below, the correct answer should take into account the distance of the radar antenna from the volcano vent and the acquisition mode, as received power decreases with the inverse square of the distance and the signal is enhanced if long pulses and space-time averaging are performed.

In order to test ground-based meteorological radar sensitivity, a simplified simulation environment is proposed such that a Gaussian-shaped range profile of volcanic ash concentration has been generated. The radar site has been located at the origin of the coordinate system and the volcanic ash cloud peak has been assumed to be at a distance d between 30 and 300 km, depending on the pulse repetition frequency (PRF). Note that for PRF=250 Hz, the maximum range r_{max} = 600 km, whereas for PRF=2500 Hz it is r_{max} = 60 km. The radial

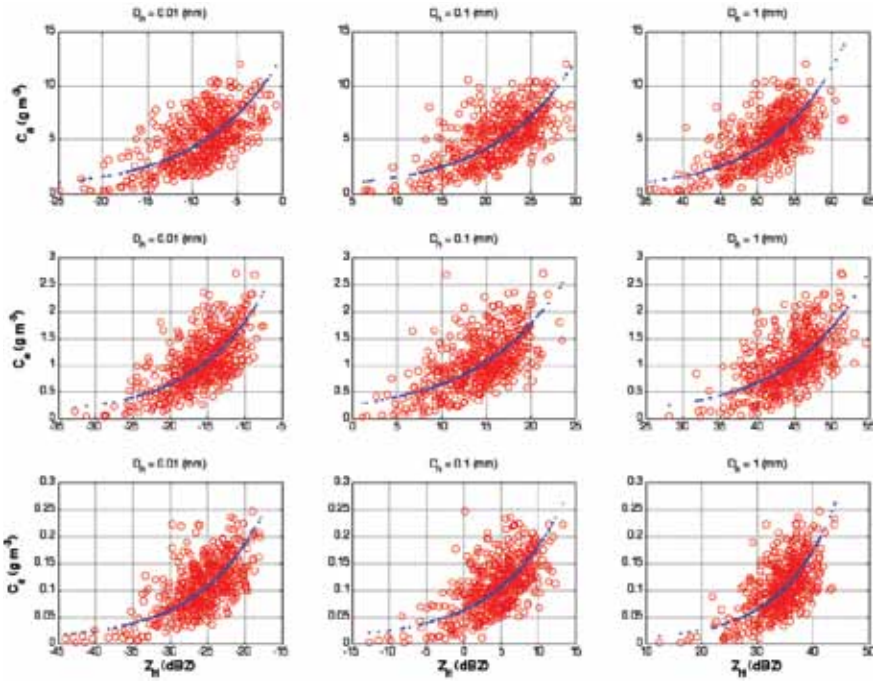

Fig 1d1. Statistical relationship between ash concentration, C_a, and radar reflectivity, Z_{Hm}, for each ash concentration class (intense, moderate and light at upper, middle and lower row panels) and ash size class (fine ash, coarse ash and lapilli at left, middle and right column panels). Regression curves are shown by dotted lines (from Marzano et al., 2006b).

resolution has been assumed equal to 300 m (i.e. impulse duration τ = 2 μs). A range extension of 20% of the peak distance has been assumed for every synthetic ash cloud, together with an ash concentration random variation having a standard deviation equal to 10% of the maximum value of the ash profile in order to generate concentration range gradients. The choice of a Gaussian-shaped range profile is quite arbitrary, but it is intended to reproduce scenarios where the ash content decreases either downwind or upwind, increasing its extension as the ash cloud is advected far from the volcano vent.

The peak concentration of each ash cloud has been set up in order to reproduce the average values of light, moderate and intense concentration classes and distinguishing between fine ash, coarse ash and lapilli (gross ash). As a synthesis of available volcanic information, within each class we have supposed a random distribution for:

i) ash particle diameter with average values equal to 0.01 mm, 0.1 mm and 1 mm for fine, coarse and lapilli ash;
ii) ash concentration with averages equal to 0.1 g m^{-3}, 1 g m^{-3} and 5 g m^{-3} for light, moderate and intense concentration regimes.

The ash density has been set at an average value of 1 g cm^{-3}. Figure 1d1 depicts the output example of this randomisation procedure for the nine ash classes, in terms of ash concentration C_a versus synthetic measured reflectivity Z_{Hm}.

At all considered frequency bands, Rayleigh scattering conditions have been assumed, and this implies that radar reflectivity is equal for all the bands (Marzano et al., 2006a). An example of these synthetic ash cloud range profiles is illustrated in Figure 1d2, where the eruption cloud with a peak at 60 km is sketched for all nine ash classes in terms of comparison between the simulated ash-reflectivity response and the Minimum Detectable Z-Reflectivity (MDZ) for the considered radar systems in Table 1 at C- and X-band (Marzano et al., 2006b).

Some conclusions, constrained to the considered radar systems, can be drawn from this MDZ analysis.

i) For C-band systems, detection of a fine ash signal larger than MDZ seems to be possible only in cases of very *intense* concentration. On the other hand, for coarse and gross ash the radar is able to detect ash particles with a reflectivity larger than zero.

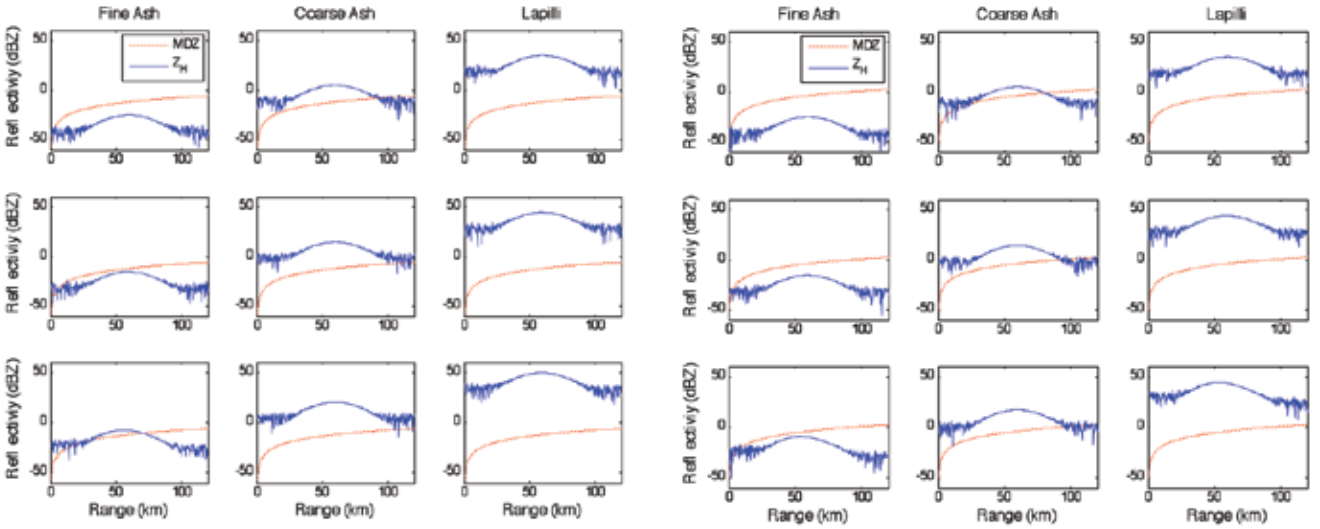

Fig 1d2. (Left) Reflectivity response and minimum detectable reflectivity (MDZ) for ash cloud range profiles with a concentration peak at 60 km at C-band for a light (top row), moderate (middle row) and intense (bottom row) concentration and fine (left column), coarse (middle column) and lapilli (right column) ash size classes. (Right) Same as in left, but at X-band (from Marzano et al., 2006b).

ii) For X-band radar, there is a lower sensitivity to ash content, fine ash never being detected and coarse being detected only with a moderate concentration regime. The chosen X-band system is evidently penalised by characteristics worse than the other two radars (see Table 1d1).

iii) For simulations at S-band, results are slightly worse than at C-band and intermediate with respect to X-band.

iv) From results with ash cloud peaks at 30, 120 and 240 km, the increase of the range between the radar and ash cloud (from 30 to 240 km) obviously leads to a worse ash sensitivity of microwave radar response. Of course, by halving the distance, MDZ is decreased by 6 dB, and by radially averaging reflectivity data, MDZ decreases because the received power is proportional to the impulse duration τ.

4. Ground-based radar applied to volcanic ash monitoring

The potential of radar data in observing volcanic ash clouds has been analysed using some case studies in which a volcano eruption happened near an available weather radar:

— Grímsvötn eruption in 2004, analysed together with the Icelandic Met Office (IMO) (for details, see Marzano et al., 2006b, 2010a);
— Augustine eruption in 2006, analysed together with the USGS Alaska Volcano Observatory (for details, see Marzano et al., 2008, 2010b).

Table 1d1. Three radar systems at S-, C- and X-band and their technical characteristics (from Marzano et al., 2006b)

RADAR SYSTEM CHARACTERISTICS	Radar S band	Radar C-band	Radar X-band
Band	S	C	X
Frequency Range	2.70 – 2.90 GHz	5.45 – 5.82 GHz	9.375 GHz
Transmit Peak Power	600 kW	250 kW	50 kW
RF Pulse Width	0.8 to 2 ms	0.5 to 2 ms	0.5 to 2.0 ms
PRF	250 – 5000 Hz	250 – 2500 Hz	250 – 2500 Hz
Antenna Gain	45 dB	45 dB	41.6 dB
Polarisation	Linear H	Linear H	H and V
Half-power Beamwidth	1.0 degree	1.0 degree	1.3 degrees
Sensitivity (MDS)	-113 dBm	-113 dBm	-112 dBm
Receiver Noise Figure	2 dB	2 dB	2.3 dB

4.1 Grímsvötn, Iceland, 2004

Grímsvötn is one of the most active volcanoes in Iceland, with a ~62 km^2 caldera covered by 150 m to 250 m-thick ice. Its highest peak, Grímsfjall, on the southern caldera rim, reaches an elevation of 1722 m. Volcanic eruptions, numbering several per century, are phreatomagmatic because of the ice cover, and they usually persist for days to weeks. Geothermal activity continuously melts the overlying ice, and meltwater accumulates in a sub-glacial lake within the caldera until the surrounding ice is breached. Volcanic eruptions in Grímsvötn often coincide with 'jökulhlaups' (glacier bursts). On the morning of 1 November 2004, a jökulhlaup tremor was observed on the seismic records at the Grímsfjall station. The Grímsvötn eruption started in the evening of 1 November and was observed by a C-band weather radar located in Keflavik, Iceland. The first plume detected by the Keflavik radar was at 23:05 UTC on 1 November. Lightning over Grímsvötn, which accompanied the rising plume, was eventually seen at about 03:00 UTC, but darkness and weather conditions prevented visual observation of the eruption site. The eruption on the night of 2 November was followed by frequent plumes. The last one, detected by the weather radar, was at 08:30 UTC on 3 November. After this time, the plume was too low to be detected by the radar (reaching 6 km height or less). Radar volume scans were continuously acquired and data were made available every half an hour from 23:00 on 1 November until 06:00 on 2 November. Reflectivity data were radially averaged to 2 km in order to increase the measurement sensitivity (equal to about –5 dBZ at around a 260 km range). Considering the distance of about 260 km between the Keflavik radar and the Grímsvötn volcano, volcanic ash clouds can only be detected at heights over about 6 km using the minimum elevation of 0.5°. This means that the volcanic eruption cloud cannot be detected between the Grímsvötn summit at 1725 m and 6000 m altitude. By comparing this range with the expected freezing level (around 1350 m) and considering the phreatomagmatic nature of Grímsvötn eruptions, the formation of ice particles and combination processes within the ash plume such as ice nucleation around ash nuclei were predicted.

4.2 Augustine, Alaska, 2006

The Augustine volcano is 1260 m high (4134 ft) and is a conically-shaped island stratovolcano located in the southern Cook Inlet, about 290 km (180 mi) southwest of Anchorage, Alaska. The Augustine volcano is the most active volcano in the Cook Inlet region, with five significant eruptions (1883, 1935, 1963-64, 1976, 1986) prior to 2006. These eruptions were primarily explosive events that produced volcanic ash clouds at their onset, followed by the emplacement of summit lava domes or flows. The explosive phase of the 2006 eruption consisted of thirteen discrete vulcanian explosions from 11 to 28 January 2006, with seismic durations that ranged from one to eleven minutes. These violent explosive events are characterised by the ballistic ejection of volcanic blocks and bombs, the emission of volcanic ash, and accompanied by an atmospheric pressure wave. Cloud heights during this phase varied from 7.5 km to 14 km above sea level. The character of the eruption changed to a more continuous ash emission phase from 28 January to 2 February, producing ash plumes at lower altitudes (less than 4 km above sea level). The ability of the NEXRAD radar to provide near-realtime updates on the position and altitude of volcanic ash clouds was vital in providing timely and accurate forecasts and warnings.

One of the most significant contributions made by the radar data was in short-term aviation forecasting. Radar cross-sections were routinely used for diagnosing the vertical disposition of ash clouds during each event. These observations, in tandem with pilot reports, were used to ascertain the vertical

extent of the ash clouds and issue timely advisories to the aviation community. The ability to track the volcanic ash in the short term was also vital to issuing timely and location-specific volcanic ashfall advisories. The ability to monitor the movement of the volcanic ash cloud on a minute-by-minute basis was essential, given the close proximity of Augustine to settlements around the Cook Inlet region. In addition, marine weather statements were issued, alerting mariners to the potential hazards posed by the volcanic ash. The VARR retrieval procedure was applied to WSR-88D S-band radar data available during the eruption of the Augustine volcano on 13 January 2006.

5. Preliminary conclusions

The major advantage of using ground-based microwave radar systems is the possibility of monitoring 24 hours a day, in all weather conditions, at a fairly high spatial resolution; and every few minutes after the eruption. The latter can be crucial for monitoring the volcano from its eruption early-stage near the volcano vent, dominated by lapilli and blocks of tephra, to the ash-dispersion stage up to few hundreds of kilometres away, dominated by the transport and evolution of coarse and fine ash particles. Of course, the sensitivity of the ground-based radar measurements will decrease as the distance to the ash cloud increases, so that for distances greater than about 50 km, fine ash might become 'invisible' to the radar. Nonetheless, radar observations can be complementary to satellite, lidar and aircraft observations. Moreover, radar-based measurements such as the realtime erupted volcanic ash concentration, height, mass and volume can be used to initialise dispersion model inputs.

Due to logistics and the space–time variability of volcanic eruptions, a useful radar system for detecting ash clouds would be a portable X-band weather Doppler polarimetric radar. This radar system might satisfy technological, economical and new scientific requirements to detect ash clouds. The siting of the observation system, which is problematic for a fixed radar system (as the volcano itself may cause a beam obstruction and the plume may advect in unknown directions), can be easily solved by resorting to portable systems.

An overall algorithm for X-band radar polarimetric retrieval of volcanic ash clouds from measured dual-polarisation reflectivity can be devised by extending the VARR approach. It can be based on four steps:

i) monitoring of the active volcano through a method based on analysis of reflectivity radar data–time series associated with *in situ* information and satellite-derived products;
ii) tracking of the ash plume based on a pattern-matching approach applied to radar images;
iii) classification of the ash plume through a method based on the vectorial Bayesian theory;
iv) retrieval of the ash concentration and fall rate from the measured reflectivity through parametric models. The expected accuracy of the VARR algorithm estimates can be evaluated using a synthetic data set. In order to quantitatively evaluate the ash detectability by weather radars, a sensitivity analysis can be preliminarily performed by simulating a synthetic ash cloud and varying ash concentration and size as function of the range.

A conclusion is that dual-polarisation ground-based weather radars can be successfully used for dynamic volcanic ash cloud monitoring and quantitative retrieval of ash category, concentration and fall rate. Of course, the expected accuracy is conditioned by the microphysical assumptions, chosen to constrain the inverse problem, even though the Bayesian retrieval approach can easily ingest the knowledge of these uncertainties within the

VARR scheme. It is intuitive and has been here demonstrated that the radar detectability of moderate-to-low concentration fine ash is improved if, for the same configuration, the available peak power is higher, the radial resolution is larger and the observation distance is shorter.

Further work is needed to assess the VARR potential using experimental campaign data. Future investigations should be devoted to the analysis of the impact of ash aggregates on microwave radar reflectivity and on the validation of radar estimates of ash amount with ground measurements where available. The last task is not an easy one as the ash fall is dominated by wind advection and by several complicate microphysical processes. This means that what is retrieved within an ash cloud may be not representative of what is collected at ground level in a given area. Spatial integration of ground-collected and radar-retrieved ash amounts may be considered, in order to carry out a meaningful comparison.

6. References

Amodeo A. et al., (2007). "Optimization of lidar data processing: a goal of the EARLINET-ASOS project," SPIE 6750(6750-14).

Ansmann A., U. Wandinger, M. Riebesell, C. Weitcamp, & W. Michaelis (1992). "Independent measurement of extinction and backscatter profiles in cirrus clouds by using a combined Raman elastic-backscatter lidar," Appl. Opt. 31, pp. 7113–7131.

Ansmann A., M. Tesche, S. Gross, V. Freudenthaler, P. Seifert, A. Hiebsch, J. Schmidt, U. Wandinger, I. Mattis, D. Müller, M. Wiegner, (2010). The 16 April 2010 major volcanic ash plume over central Europe: EARLINET lidar and AERONET photometer observations at Leipzig and Munich, Germany, Geophys. Res. Lett, 37, L13810, doi: 101029/2010GL043809.

Böckmann C., (2001). "Hybrid regularization method for the ill-posed inversion of multiwavelength lidar data to determine aerosol size distribution," Appl. Opt. 40, pp. 1329–1342.

Böckmann C., J. Bösenberg, U. Wandinger, A. Ansmann, V. Amiridis, A. Boselli, A. Delaval, F. De Tomasi, M. Frioud, I. Grigorov, A. Hågård, M. Horvat, M. Iarlori, L. Komguem, S. Kreipl, G. Larchevêque, V. Matthias, A. Papayannis, G. Pappalardo, F. Rocadenbosch, A. Rodrigues, J. Schnaider, V. Shcherbakov, and M. Wiegner, (2004). "Aerosol lidar intercomparison in the framework of EARLINET: 2. Aerosol backscatter algorithms," Appl. Opt. 43, pp. 977–989.

Böckmann C., I. Mironova, D. Müller, L. Schneidenbach, and R. Nessler, (2005). "Microphysical aerosol parameters from multiwavelength lidar," J. Opt. Soc. Am. A 22, pp. 518–528.

Bösenberg, J et. al,. (2003). "EARLINET: A European Aerosol Research Lidar Network to Establish an Aerosol climatology," Tech. Rep. 348, Max-Planck-Institut für Meteorologie, Hamburg.

Bösenberg, J. and R. Hoff (2008). GAW Aerosol Lidar Observation Network (GALION), WMO GAW Report 178, WMO, Geneva, Switzerland.

Marzano F.S., Picciotti, E., Ferrauto, G., Vulpiani, G., and Rose, W. I. (2005) "Volcanic ash remote sensing by ground-based microwave weather radar," in Proc. General Assem. EGU, Vienna, Austria, . 25–29, pp. 212–215. Wien (A).

Marzano F.S., Barbieri, S., Vulpiani G. and Rose, W.I. (2006a). "Volcanic cloud retrieval by ground-based microwave weather radar", IEEE Trans. Geosci. Rem. Sens., vol. 44, no. 11, pp. 3235-3246.

Marzano F.S., Vulpiani, G., and Rose, W. I. (2006b). "Microphysical Characterization of Microwave Radar Reflectivity Due to Volcanic Ash Clouds", IEEE Trans. Geosci. and Rem. Sens., vol. 44, pp. 313-327.

Marzano F.S., Marchiotto, S., Barbieri, S., Schneider, D., Textor C. and Giuliani, G. (2008). "Ground-based radar remote sensing of explosive volcanic ash eruptions: numerical models and quantitative applications", Proc. of USE of Remote Sensing Techniques (USEReST) for Monitoring Volcanoes and Seismogenic Areas, Naples, Italy, November 11-14.

Marzano F.S., Barbieri, S., Picciotti E. and Karlsdóttir, S. (2010). "Monitoring sub-glacial volcanic eruption using C-band radar imagery", IEEE Trans. Geosci. Rem. Sensing, vol. 58, no. 1, pp. 403-414.

Marzano F.S., Marchiotto, S., Barbieri, S., Textor C. and Schneider, D. (2010b). "Model-based Weather Radar Remote Sensing of Explosive Volcanic Ash Eruption", IEEE Trans. Geosci. Rem. Sensing, vol 48, no. 10, pp.3591-3607, doi:10.1109/TGRS.2010.2047862.

Matthias V., J. Bösenberg, V. Freudenthaler, A. Amodeo, D. Balis, A. Chaikovsky, G. Chourdakis, A. Comeron, A. Delaval, F. de Tomasi, R. Eixmann, A. Hågård, L. Komguem, S. Kreipl, R. Matthey, I. Mattis, V. Rizi, J. Rodriguez, V. Simeonov, and X. Wang, (2004). "Aerosol lidar intercomparison in the framework of the EARLINET project. 1. Instruments," Appl. Opt. 43, pp. 961–976.

Müller D., U. Wandinger, and A. Ansmann, (1999). "Microphysical particle parameters from extinction and backscatter lidar data by inversion with regularization: theory," Appl. Opt. 38(12), pp. 2346–2357.

Müller D., A. Ansmann, I. Mattis, M. Tesche, U. Wandinger, D. Althausen, and G. Pisani, (2007). "Aerosol-type-dependent lidar ratios observed with Raman lidar," J. Geophys. Res. 112(D16202). doi:10.1029/2006JD008292.

Müller D. , Leibniz Institute for Tropospheric Research Leipzig, Germany, personal communication

Pappalardo G., A. Amodeo, L. Mona, M. Pandolfi, N. Pergola, V. Cuomo, (2004a). Raman lidar observations of aerosol emitted during the 2002 Etna eruption, Geophys. Res. Lett., 31, doi:10.1029/2003GL019073.

Pappalardo G., A. Amodeo, M. Pandolfi, U. Wandinger, A. Ansmann, J. Bösenberg, V. Matthias, V. Amiridis, F. deTomasi, M. Frioud, M. Iarlori, L. Komguem, A. Papayannis, F. Rocadenbosch, and X. Wang, (2004b). "Aerosol lidar intercomparison in the framework of the EARLINET project. 3. Raman lidar algorithm for aerosol extinction, backscatter, and lidar ratio," Appl. Opt. 43, pp. 5370–5385.

Pappalardo G., U. Wandinger, L. Mona, A. Hiebsch, I. Mattis, A. Amodeo, A. Ansmann, P. Seifert, H. Linné, A. Apituley, L. Alados Arboledas, D. Balis, A. Chaikovsky, G. D'Amico, F. De Tomasi, V. Freudenthaler, E. Giannakaki, A. Giunta, I. Grigorov, M. Iarlori, F. Madonna, R.-E. Mamouri, L. Nasti, A. Papayannis, A. Pietruczuk, M. Pujadas, V. Rizi, F. Rocadenbosch, F. Russo, F. Schnell, N. Spinelli, X. Wang, and M. Wiegner, (2010), EARLINET correlative measurements for CALIPSO: First intercomparison results, J. Geophys. Res., 115, D00H19, doi:10.1029/2009JD012147.

Veselovskii I., A. Kolgotin, V. Griaznov, D. Müller, U. Wandinger, and D. N. Whiteman, (2002). "Inversion with regularization for the retrieval of tropospheric aerosol parameters from multiwavelength lidar sounding," Appl. Opt. 41, pp. 3685–3699.

Wang, X., et al., (2008). Volcanic dust characterization by EARLINET during Etna's eruptions in 2001-2002, Atmos. Env., 42, pp. 893–9056.

Annex 2a: Description of some European ash transport models

A. Stohl, F. Prata, H. Elbern, S. Scollo and S. Varghese

1. London VAAC model

The Met Office's ability to predict the transport and spread of pollution is delivered by the NAME (Numerical Atmospheric-dispersion Modelling Environment) computer model. The model began development following the Chernobyl accident in 1986 and since that time it has been used to model a wide range of atmospheric dispersion events, including previous volcanic eruptions and the Buncefield explosion in 2005. In addition to its role as an emergency response guidance tool, the model is used for routine air quality forecasting and meteorological research activities. NAME provides a flexible modelling environment that is able to predict dispersion over distances ranging from a few kilometres to the whole globe, and for time periods from minutes upwards.

NAME is a 'Lagrangian' particle model which calculates the dispersion of pollutants by tracking model 'particles' through the modelled atmosphere (Jones et al. 2007). The process is initiated by the emission of model particles into the atmosphere. NAME has the flexibility to specify point or extended sources at any location in the atmosphere, together with relevant source parameters such as the mass emission rate, emission velocity and temperature. Once emitted, particles move in a manner determined by the meteorology, which is input separately to the model. NAME uses meteorological parameters derived from the main Met Office weather forecast model MetUM (the Met Office Unified Model). The most important parameters are the wind speed and direction, which vary in all three dimensions and in time. However other meteorological parameters are used by NAME, such as the vertical temperature profile (which determines the atmospheric stability with respect to vertical motion) and the height of the atmospheric boundary layer (which is important for predicting the short-term spread of pollutants emitted at the surface, as well as sedimentation). NAME includes a model for deep convective transport. In addition to the movement of particles by the prescribed meteorological winds, the particle motion also has a random component to represent the effects of atmospheric turbulence.

Once emitted and being transported by atmospheric motions, pollutants in NAME simulations can also be removed from the model atmosphere by several processes; i) fall out due to gravity, ii) impaction with the surface, iii) washout, where the pollutant is 'swept out' by falling precipitation, and iv) rainout, where the pollutant is absorbed directly into cloud droplets as they form. In addition each model 'particle' can have its own characteristics, for example, particles can represent different compounds or chemicals, and they can have real and different particulate sizes. NAME also includes a chemistry scheme for common atmospheric chemical components.

2. Toulouse VAAC model

MOCAGE-accident is a specific version of the *MOCAGE (Modèle de Chimie Atmosphérique à Grande Echelle)* three-dimensional chemistry and transport model developed by Météo-France. It is tuned for the transport and diffusion of accidental release from the regional to the global scale. Only dynamic and physical processes are taken into account, excluding chemistry. *MOCAGE-accident* runs in offline mode, using Météo-France ARPEGE or ECMWF/IFS

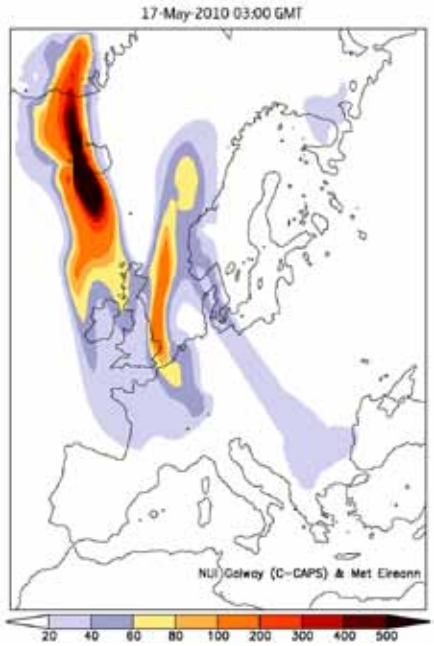

Fig. 2a1. REMOTE model forecast of volcanic ash column burden distribution (mg m^{-2}) for 17 May, 2010, 03:00 GMT simulated with available information of Eyjafjöll volcano source parameters.

operational NWP products as dynamic forcings. Meteorological forcings (hydrostatic winds, temperature, humidity and pressure) feed the advection scheme, as well as the physical parameterisations. They are considered every six hours, and are linearly interpolated to yield hourly values, consistent with the time-step for advection; smaller time-steps are used for physical processes, but the meteorological variables are kept constant over each hour.

MOCAGE-accident can be run for an emission taking place everywhere over the globe. In the operational configuration, it has a 0.5° horizontal resolution and 47 hybrid (σ,P) levels from the surface up to 5 hPa, with approximately seven levels in the planetary boundary layer, 20 in the free troposphere and 20 in the stratosphere. In this way, the model can consider emissions in the first metres above the surface as well as over thousands of kilometres up to the stratosphere. When the pollutant is volcanic ash, sedimentation of the particles is taken into account in addition to processes represented for tracers. *MOCAGE-accident* can also be run in 'inverse' mode in order to provide information on the origin of an air-mass arriving at a given point in space and time.

3. Other European plume models

Various European research groups are capable of running volcanic ash plume simulations, sometimes even in an operational fashion. Within the GMES framework, the MACC and PASODOBLE projects run global and regional models. These models were designed for monitoring atmospheric composition in general, but can be used for specific issues like volcanic eruptions as well. The MACC systems are also capable of using data assimilation to constrain the model forecasts. The global MACC model is based on the ECMWF IFS model which uses semi-Lagrangian transport on a reduced Gaussian grid. As an instant action shortly after the eruption, the MACC global model simulated the plume by a total column tracer proxy. The European continental scale model EURAD-IM (EURopean Air pollution Dispersion-Inverse Model), which features full gas phase and aerosol particle dynamics and chemistry, displayed ash plume simulations for over a month with 15 km horizontal resolution. This model proved to be easily adaptable to volcanic ash and gas eruption modelling, including full gas phase chemistry and aqueous phase chemistry, as well as aerosol dynamics and chemical formation, dry and wet removal, and cloud interaction. For variational inverse modelling, adjoint components of principal process modules are available and applied for source strength inversion with air quality conditions (Elbern et al., 2007). It is clearly desirable, for ash quantification, to know which fraction of remotely-sensed aerosol is due to sulphates or the non-ash component. This however, requires an observing network, which is usually unavailable apart from well-compiled measurement missions. Coupling with a meteorological model (MM5 and WRF), consistent vertical winds are available. A remarkably good agreement with modelled and lidar-observed height levels could be demonstrated. Once *in situ* observations were available from GAW Zugspitze observatory, quantitative simulations could be provided (Figure 7 on page 34).

FLEXPART is a Lagrangian particle transport model (LPDM), similar to the NAME model used at the London VAAC. FLEXPART calculates the trajectories of tracer particles using the mean winds interpolated from the analysis fields, plus random motions representing turbulence (Stohl et al., 2005). Unlike most other LPDMs, FLEXPART also has a parameter for deep convective transport. FLEXPART also handles wet and dry deposition as well as gravitational settling and can simulate transport of particles of different sizes. FLEXPART was validated with data from continental-scale tracer experiments (Stohl et al., 1998) and has been used in a large number of studies on long-range atmospheric transport. The reference version of FLEXPART can ingest meteorological data from either the European Centre for Medium-Range Weather Forecasts

Model name	Institution	Type of model	Reference
Operational			
NAME	London VAAC	Lagrangian	Ryall and Marion (1998)
HYSPLIT	Washington VAAC + Darwin VAAC + many others	Lagrangian	Draxler and Hess (1998)
PUFF	Alaska Volcano Observatory	Lagrangian	Searcy et al. (1998), Webley et al. (2009)
MLDP0	Montreal VAAC	Lagrangian	D'Amours (2010)
MOCAGE	Toulouse VAAC	Semi-Lagrangian	Josse et al. (2004)
FALL3D	Istituto Nazionale di Geofisica e Vulcanologia, Osservatorio Vesuviano	Eulerian	Folch et al. (2009)
Some R&D models as discussed during the workshop			
FLEXPART	NILU + many others	Lagrangian	Stohl et al. (1998), Stohl et al. (2005)
EURAD-IM	University Cologne	Eulerian	Elbern et al., (2007)
REMOTE	National University of Ireland	Smolarkiewicz Scheme	Langmann et al., (2008)

Table 2a1. Some models used for volcanic ash transport and dispersion forecasts.

or from the National Center for Environmental Prediction's (NCEP) Global Forecast System (GFS) model. There are also many other versions using other meteorological data (e.g. from MM5, WRF, COSMO, etc.). FLEXPART is used by dozens of research groups worldwide and is used operationally for emergency preparedness in Austria and for nuclear explosion source attribution at CTBTO. Simulations of volcanic plume dispersions are described in Prata et al. (2007), Wang et al. (2008), Eckhardt et al. (2008), Bitar et al. (2010), Hoffmann et al. (2010) and Kristiansen et al. (2010).

Another model used for volcanic ash forecasts is the regional scale air-quality/climate model REMOTE (Langmann, 2000; Langmann et al., 2008) at the National University of Ireland, Galway. This hydrostatic three-dimensional model uses the ECMWF meteorology forecast data for boundary forcing every 6 hours. REMOTE is coupled with the gas-phase chemistry (RADM2) and aerosol dynamics modules and has advanced treatment for sedimentation, dry deposition and wet deposition. The input parameters for volcanic ash modelling include plume height, emission rate, vertical distribution of emission, density of ash, distribution in the different size modes and the mode median radius of the particles. The particles are treated as insoluble and are introduced in a log-normal distribution into the different size modes. Figure 2a1 shows a typical forecast of volcanic ash concentration from the REMOTE model.

Various other plume models exist in Europe (e.g. TM4, SILAM) and, while not described in this working paper directly, should be included in collaborative efforts on model improvements.

In Volcanology, there are several tephra dispersal models which have been validated comparing model outputs with field data of tephra deposits. Examples are:

— HAZMAP applied to the vulcanian explosions and dome-collapses from the 1995–1999 eruption of Soufrière Hill Volcano in Montserrat (Bonadonna et al., 2002), to the 79 AD Plinian eruption of Vesuvius (Pfeiffer et al., 2005), and to the 21–24 July 2001 Etna eruption (Scollo et al., 2007).
— TEPHRA (Bonadonna et al., 2005) validated on data of the 17 June 1996 andesitic sub-Plinian eruption of Ruapehu, New Zealand.
— FALL3D (Costa et al., 2006) and VOLCALPUFF (Barsotti et al., 2008) validated using field data of the 21–24 July 2001 Etna eruption.
— PUFF (Searcy et al., 1998) validated comparing model results with the tephra deposit of the 1980 eruption of Mount St. Helens (Fero et al., 2008).

Annex 2b: Physical volcanology

S. Tait

1. Introduction

Explosive volcanic eruptions generate ash-laden jets that emerge from the vent at speeds typically on the order of 100 to several hundred metres per second. The ash is generated by fragmentation: the magma is transformed into a gas jet bearing particles with a range of characteristic sizes from the order of 10 cm down to the order of a micron. The small size of the fragments ensures highly efficient transfer of heat from the hot fragments to the air that is entrained into the jet by vigorous turbulent mixing. It is the heated gas that gives the jet sufficient buoyancy to rise in the stratified atmosphere until it reaches a maximum height, and then spreads out at its level of neutral buoyancy. The difference between the maximum height and the level of neutral buoyancy depends on the momentum the plume possesses when it first attains the neutral buoyancy level. The horizontal part of the flow is a gravity current, known as the umbrella region.

The height reached in the atmosphere by a plume is fundamentally related to the flux of material that is ejected at the vent. For example, the thermal power liberated at the source. At the low end, source mass fluxes can be of the order of 10^5 kg s^{-1} (which was roughly the case for the Eyjafjöll plume) but at the high end can be 10^9 kg s^{-1}), or perhaps even higher – a huge variation. Whereas a relatively weak plume can plausibly be treated as a source of particles that is passive from the point of view of the atmospheric circulation, this will not be the case for a very strong plume.

Maximum plume height, particle loading and particle size distribution are quantities that are not always easy to measure but can be understood in the framework of physical models that fit the existing data quite well. Below are summarised the salient features of the current knowledge of explosive volcanism and the processes by which volcanic ash is produced and injected into the atmosphere. The idea is to give a general framework in which the specific case of the Eyjafjöll can be situated.

2. Fragmentation and particle size distribution

Fragmentation begins in the volcanic conduit through which magma rises to the surface and consequently experiences a continuously decreasing pressure. This leads first to the magma becoming saturated with respect to a volatile phase and then to a progressively greater proportion of these volatiles exsolving from the magma to produce bubbles. Although the mass fraction of volatiles in magma is small (typically a few weight percent), the expansion of the volatile phase under the influence of decompression is such that the volume fraction becomes very large near to the vent, and the bubbles connect and disrupt the magma into fragments. This process proceeds with more and more particle collisions producing a larger and larger fraction of small particles. The lower limit of particle size is determined typically by the smallest bubbles, which by observation are of the order of a micron. Secondary fragmentation processes such as explosive interaction with aquifers or surface water and ice (as in the case of Eyjafjöll) can further enhance the production of fine particles.

The coarsest particles tend to be deposited close to the vent, and the finer particles carried away by the plume and then atmospheric currents to large distances so that reconstruction of the total grain size distribution is an

arduous task. For a few dozen eruption deposits, enough data exists to attempt a reconstruction of the generic features. It has been shown that the grain size populations can be described by a power law in the sense defined below.

Volcanologists adopted a convention from sedimentology and use so-called ϕ units which is based on sieve sizes:

$$\varphi = -\frac{\log d}{\log 2}$$

where d is the maximum length of a fragment in mm. In other words, the particle diameter is 2ϕ in mm. The total mass of particles in the deposit of a given sieve size is found by integration based on observations made at given locations and a simple mathematical description of how the deposit thickness declines with distance from the source and the shape of contours of iso-thickness (called isopachs). It is found that a good mathematical fit to the data is obtained using a power law description. If N ($R > r$) is the number of fragments greater than size r, then

$$N = \lambda . r^{-D}$$

where l is a normalisation constant. If the number of fragments in each sieve class ϕ is called $D(\phi)$, then the data can be described by:

$$\ln_2(\Delta(\phi)) = \ln_2(N_o) - D\varphi$$

where N_o is a normalisation constant. Figure 2b1 shows examples of grain size distributions reconstructed from two deposits. One is from the eruption of 1875 of the Icelandic volcano Askja, and the other is the Hachinohe deposit from northern Honshu in Japan, and they show D values of 3 and 3.5 respectively. Laboratory experiments show that primary breakup leads to D values of 2.5 ± 0.1 and that subsequent repeated or secondary fragmentation processes act to increase D. The range of D values found from deposits that sedimented from eruption columns is typically 3.0 to 3.9. There is a tendency for the smallest particles to be transported away in the atmosphere and not to be preserved in the deposit, but the data that exist are consistent with this approach and it is reasonable to assume that a power law is valid down to the smallest sizes. The high values of D from volcanic deposits indicate that fragmentation is a progressive process. The strong interaction between ice and magma in the Eyjafjöll eruption suggests that the expected D value would be relatively high and the proportion of small particle sizes relatively large.

3. Plume dynamics

Volcanic plumes are driven by the heat transferred from the small particles to atmospheric air that is entrained into the eruption jet by vigorous turbulent mixing. In the case of strong fragmentation and a vigorous eruption, it is reasonable to assume that all of the heat from the magma goes to feeding the plume, and the theory of turbulent jets and plumes can be used to obtain a prediction of the behaviour in the atmosphere. Complications can arise in the exit conditions such as over-pressure that leads to shock waves, but experience has shown that after a relatively brief decompression phase just above the vent, it is reasonably accurate to assume that the plume is a narrow object, in pressure equilibrium with the surrounding atmosphere, which allows important theoretical simplifications.

Three fundamental things affect the height that will be reached in the atmosphere and the concentration of ash present at the top of the plume. These are, the mass flux (Q_o) at the source, the vertical profile of atmospheric

Fig. 2b1. Two examples of power-law size distributions from volcanic eruption deposits.

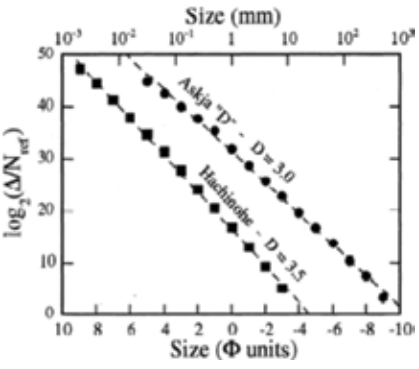

density (S) above the source and the rate of entrainment by turbulent mixing. Although some direct numerical simulations have been carried out firstly in a 2D asymmetric geometry and more recently in 3D, the most efficient models are so-called 'top hat' models in which it is assumed that, at any given height, the jet or plume has characteristic values of radius, vertical velocity and buoyancy (dependent on gas temperature and particle load). These three variables are calculated as a function of height until the vertical momentum drops to zero at the maximum height (H_{max}). These models require an empirical entrainment coefficient (α_e) which, in a first generation of models, was assumed to be a universal constant. In more recent work, validated by comparison with experimental results, it has been shown that the α_e is a variable that depends notably on the buoyancy of the jet via the Richardson Number. This is important because the buoyancy of the jet is negative when it comes out of the vent, becomes positive because of all the entrained and heated air, then negative again between the neutral buoyancy level and the maximum height.

The fundamental dependence of the maximum height reached as a function of the above variables is:

$$H_o = (2.\alpha_e)^{-0.5}.F_o^{0.25}.S^{-0.75} \qquad \text{with} \qquad S = -\frac{g}{\rho_r}.\frac{d\rho_a}{dz}$$

ρ_a and ρ_r are the atmospheric density and a reference density respectively, and z is the vertical coordinate.

One cannot give one universal curve valid for all explosive volcanic eruptions because the atmospheric stratification varies between tropical and polar regions, because the entrainment coefficient varies according to the buoyancy evolution of the plume, and because the amount of volatiles exsolved from the magma varies from case to case. Nevertheless, the general behaviour is well described by the above relationship and calculations in specific cases give good results. Figure 2b2 shows curves relating the mass discharge at the source (Q_o) to the maximum height for different atmospheric stratifications, for a generic situation of a given magma type. This graph shows that volcanic plumes can inject ash into the atmosphere at heights that can range from a few kilometres to a few dozen kilometres, and most importantly that the mass flux of particles and the height of injection are not independent. The mass flux of an explosive eruption determines the environmental impact of an eruption, but it is notoriously hard to measure in real time because of the inherent danger

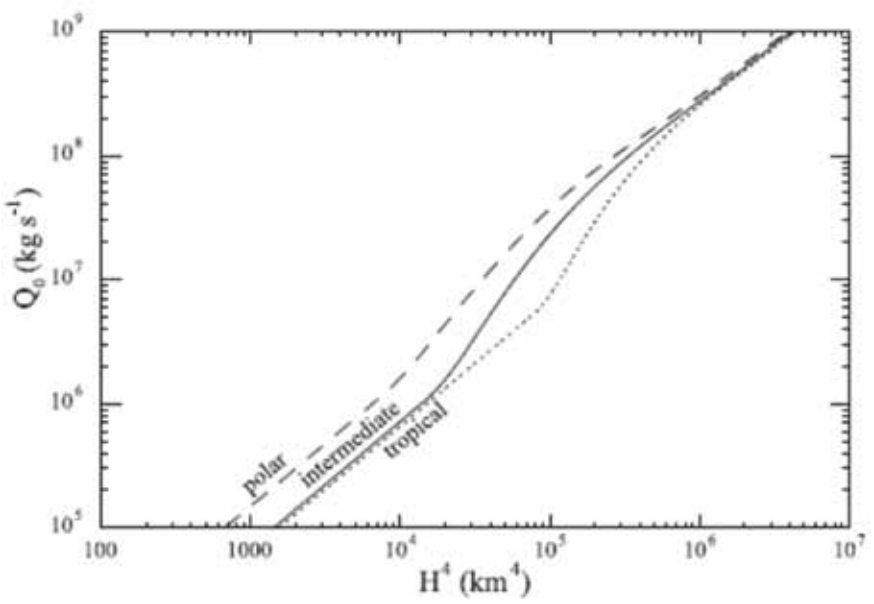

Fig. 2b2. REMOTE model forecast of volcanic ash column burden distribution (mg m^{-2}) for 17 May 2010, 03:00 GMT, simulated with available information on Eyjafjöll volcano source parameters.

of such events. Hence volcanologists typically use the above formalism to measure mass flux indirectly via observations of plume height. In eruptions of known duration and whose total output can be estimated after the fact, an average mass flux can be estimated.

The Eyjafjöll eruption showed two major complications with respect to this generic analysis, which is based on a strong plume in a quiescent atmosphere, namely that the plume was weak and hence strongly bent over by the wind, and secondly that mass flux at the vent was being partitioned at the source: some material dropped back quickly to feed a lava flow on the ground, whereas the rest rose to feed the plume. This partitioning is not uncommon in relatively weak eruptions. It is also more common when the magma composition is basaltic rather than silicic, because the former have less volatiles to exsolve and fragmentation is hence less efficient. Unless good constraints are available from observations at the source to roughly quantify this mass partitioning, it becomes another source of uncertainty. Some idea of the potential quantitative impact of these complications is given in the paragraph below, which discusses the ash loading in the umbrella cloud.

4. Ash loading and umbrella cloud

If the plume is very strong and effectively maintains in suspension the great majority of the ash particles, the ash loading at the top of the plume, and hence in the umbrella cloud as it starts to spread, can be calculated from the model summarised above. The buoyancy of the plume depends fundamentally on two factors: the temperature of the gas and the particle load. Horizontal spreading occurs when the plume reaches its level of neutral buoyancy in the atmosphere. The temperature of the gas is the dominant factor because this is sensitive to the mass (hence heat) flux at the vent. The calculated ash load is shown in Figure 2b3 (for a given magma type, volatile content and exit velocity) as a function of total mass flux, and in Figure 2b4 of the height reached by the plume. Ash load varies but weakly. The typical order of magnitude for the ash load in the umbrella cloud is 1000 mg m^{-3}. These graphs also show the results of some more preliminary calculations in which different percentages of the total mass flux are assumed to be injected into the plume. The reduction in ash loading does not vary exactly linearly with this percentage because all of the

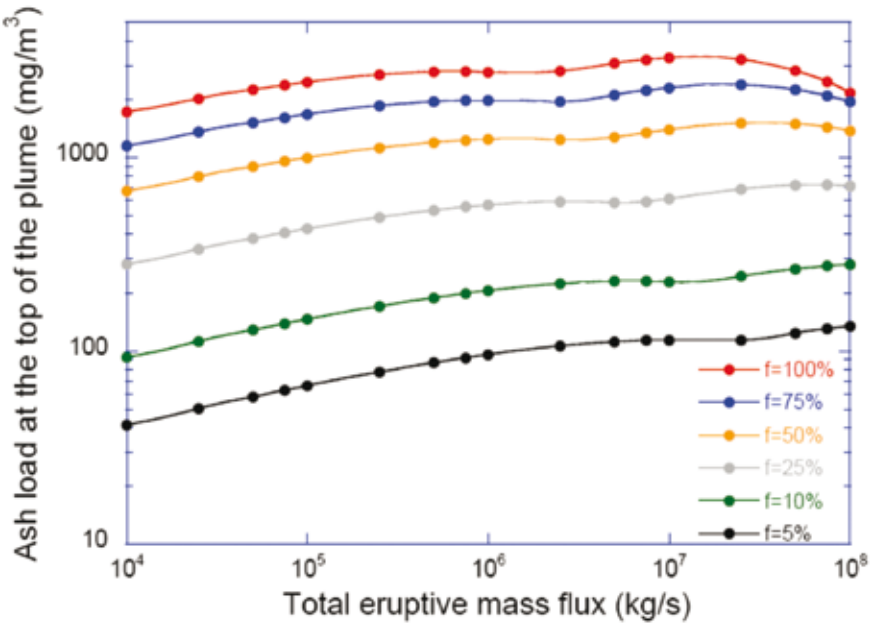

Fig. 2b3. Ash loading in the umbrella cloud near the source as a function of mass flux

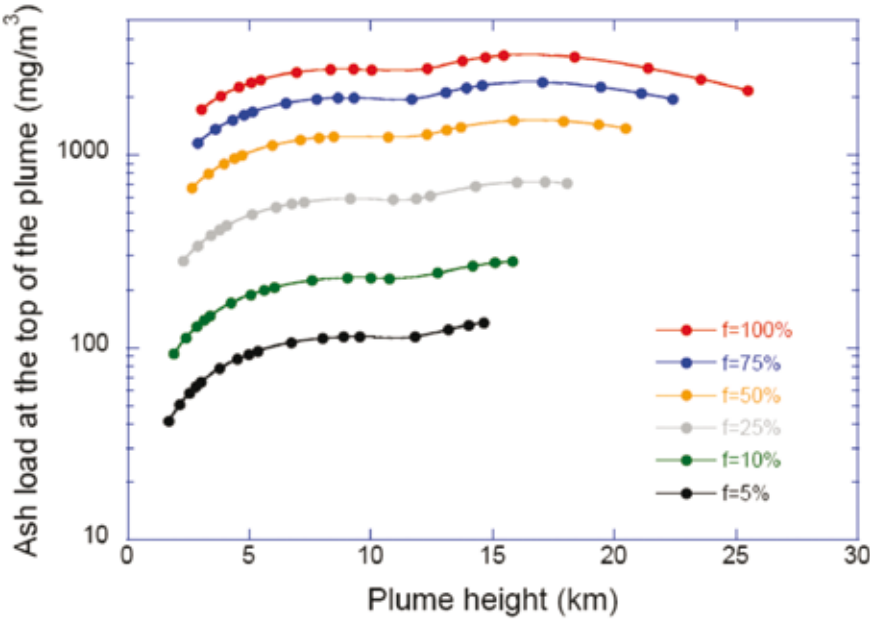

Fig. 2b4. Ash loading in the umbrella cloud near the source as a function of maximum height attained by the plume.

magmatic gas is always assumed to be injected into the plume, and the gas plays a dominant dynamic role. Ash loading drops as the fraction of the total mass flux injected into the plume decreases. Temporal variability in the height of the Eyjafjöll eruption plume may have been due to variations in the mass partitioning at the source, and one would expect that ash loading also varied. These calculations assuming mass partitioning give a preliminary indication of the order of magnitude we should expect and could be refined as necessary.

5. Conclusion

The main message is that relatively robust physical models of eruption columns exist to predict the heights reached in the atmosphere by eruption columns as a function of mass flux at the source. In practice, the mass flux has only been measured accurately for a few test cases of recent eruptions; volcanologists more commonly use column height to estimate the mass flux. Height and mass flux are not independent, but are intrinsically related by the plume dynamics. For strong plumes, the ash loading at the top of the column is also not independent, and the order of magnitude can be estimated within the model framework. For weak eruptions such as that of Eyjafjöll, the effect of crosswind and mass partitioning at the source between a lava flow and the plume introduce significant complications. The details of the particle size distribution are harder to know because these depend on the intensity of the fragmentation process and how it proceeds. Nevertheless a power law distribution for the particle sizes gives a good first order description. Secondary fragmentation processes such as magma–water or magma–ice interaction can significantly shift the size distribution to smaller values, and at present this is difficult to quantify.

The list of references includes some in which recent refinements of eruption models have been introduced which were used in the above discussion. The list also includes some older but more comprehensive reviews of eruption models, and also the pioneering paper by Morton, Taylor and Turner (1956) on rise of a buoyant plume in a stratified environment.

6. References

Andronico, D., Scollo, S., Cristaldi, A., Caruso, S. (2008). The 2002–03 Etna explosive activity: tephra dispersal and features of the deposit. J. Geophys. Res. doi:10.1029/2007JB005126.

Barsotti, S., Neri, A., Scire, J.S. (2008). The VOL-CALPUFF model for atmospheric ash dispersal: 1. Approach and physical formulation, J. Geophys. Res., 113, B03208, doi:10.1029/2006JB004623.

Bitar, L., T. J. Duck, N. I. Kristiansen, A. Stohl, and S. Beauchamp (2010): LIDAR observations of Kasatochi volcano aerosols in the troposphere and stratosphere. J. Geophys. Res., 115, D00L13, doi:10.1029/2009JD013650.

Bonadonna, C., Macedonio, G., Sparks, R.S.J., (2002). Numerical modelling of tephra fallout associated with dome collapses and Vulcanian explosions: application to hazard assessment on Montserrat. In: Druitt, T.H., Kokelaar, B.P. (Eds.), The Eruption of Soufrière Hills Volcano, Montserrat, from 1995 to 1999. Memoir. Geological Society, London, pp. 517–537.

Bonadonna, C., Phillips, J.C., Houghton, B.F., (2005). Modeling tephra sedimentation from a Ruapehu weak plume eruption. J. Geophys. Res. 110, B08209. doi:10.1029/2004JB003515.

Carazzo, G., E. Kaminski and S. Tait (2008). On the rise of turbulent plumes: quantitative effects of variable entrainment for submarine hydrothermal vents, terrestrial and extra-terrestrial explosive volcanism. Journal of Geophysical Research v.113, doi:10.1029/2007JB005458.

Cioni, R., Longo, A., Macedonio, G., Santacroce, R., Sbrana, A., Sulpizio, R., Andronico, D., 2003. Assessing pyroclastic fall hazard through field data and numerical simulations: Example from Vesuvio, J. Geophys. Res., 108(B2), 2063, doi:10.1029/2001JB000642.

Costa, A., Macedonio, G., Folch, A., (2006). A three dimensional Eulerian model for transport and deposition of volcanic ashes. Earth Planet. Sci. Lett. 241, 634–647.

Costa, A., Folch, A., Macedonio, G., (2010). A Model for Wet Aggregation of Ash Particles in Volcanic Plumes and Clouds: I. Theoretical Formulation, J. Geophys. Res., 115, B09292, doi:10.1029/2009JB007175.

D'Amours, R., A. Malo, R. Servranckx, D. Bensimon, S. Trudel, and J.-P. Gauthier-Bilodeau (2010): Application of the atmospheric Lagrangian particle dispersion model MLDP0 to the 2008 eruptions of Okmok and Kasatochi volcanoes. J. Geophys. Res., 115, D00L11, doi:10.1029/2009JD013602.

Draxler RR, Hess GD. (1998). An overview of the HYSPLIT-4 modelling system for trajectories, dispersion and deposition. Australian Meteorological Magazine 47: 295–308.

Dubosclard, G., Donnadieud, F., Allard, P., Cordesses, R., Hervier, C., Coltelli, M., Privitera, E., Kornprobst, J., (2004). Doppler radar sounding of volcanic eruption dynamics at Mount Etna. Bull. Volcanol. 56, 398–411.

Eckhardt, S., A. J. Prata, P. Seibert, K. Stebel, and A. Stohl (2008): Estimation of the vertical profile of sulfur dioxide injection into the atmosphere by a volcanic eruption using satellite column measurements and inverse transport modeling. Atmos. Chem. Phys., 8, 3881–3897.

Elbern, H., A. Strunk, H. Schmidt, and O. Talagrand, (2007). Emission rate and chemical state estimation by 4-dimensional variational inversion, ACP, 3749–3769.

Fero, J., Carey, S.N., Merrill, J.T., (2008). Simulation of the 1980 eruption of Mount St. Helens using the ash-tracking model PUFF. J. Volcanol. Geotherm. Res. 175 (3), 355–366.

Folch, A., A. Costa, and G. Macedonio (2009): FALL3D: A computational model for transport and deposition of volcanic ash. Computers and Geosciences 35, 1334–1342.

Hoffmann, A., C. Ritter, M. Stock, M. Maturilli, S. Eckhardt, A. Herber, and R. Neuber (2010), LIDAR measurements of the Kasatochi aerosol plume in August and September 2008 in Ny-Alesund, Spitsbergen, J. Geophys. Res., 115, D00L12, doi:10.1029/2009JD013039.

Hollingsworth, A., R.J. Engelen, C. Textor, A. Benedetti, O. Boucher, F. Chevallier, A. Dethof, H. Elbern, H. Eskes, J.Flemming, C. Granier, J.W. Kaiser, J. J. Morcrette, P. Rayner, V-.H Peuch, L. Rouil, M. Schultz, A. Simmons, and the GEMS consortium, 2008. Toward a monitoring and forecasting system for atmospheric composition. The GEMS Project. Bull. Amer. Meteor. Soc., 89, 1147–1164, doi:10.1175/2008BAMS2355.1

Jones, A.R., Thomson D.J., Hort M. and Devenish B., (2007). 'The U.K. Met Office's next-generation atmospheric dispersion model, NAME III', in Borrego C. and Norman A.-L. (Eds) Air Pollution Modeling and its Application XVII (Proceedings of the 27th NATO/CCMS International Technical Meeting on Air Pollution Modelling and its Application), Springer, pp. 580–589.

Josse, B., Simon, P. and Peuch, V.-H. (2004). Rn-222 global simulations with the multiscale CTM MOCAGE. Tellus 56B, 339–356.

Kristiansen, N. I., A. Stohl, A. J. Prata, A. Richter, S. Eckhardt, P. Seibert, A. Hoffmann, C. Ritter, L. Bitar, T. Duck, K. Stebel (2010). Remote sensing and inverse transport modeling of the Kasatochi eruption sulfur dioxide cloud. J. Geophys. Res., 115, D00L16, doi:10.1029/2009JD013286.

Langmann, B., (2000). Numerical modelling of regional scale transport and photochemistry directly together with meteorological processes, Atmos. Environ. 34, 3585–3598.

Langmann, B., Varghese, S., Marmer, E., Vignati, E., Wilson, J., Stier, P., O'Dowd, C.D., (2008). Aerosol distribution over Europe: A model evaluation study with detailed aerosol microphysics Atmos. Chem. Phys., 8, 1591–1607

Morton, B.R., Taylor, G.I. and Turner, J.S. (1956) Turbulent gravitational convection from maintained and instantaneous sources. Proc. Royal Soc. Lond. v.234, 1–23.

Oberhuber, J. M., M. Herzog, H. F. Graf and K. Schwanke (1998): Volcanic plume simulation on large scales, J. Volcanol. Geotherm. Res. 87, 29–53.

Prata, A. J., Carn, S. A., Stohl, A., and Kerkmann, J.: Long range transport and fate of a stratospheric volcanic cloud from Soufriere Hills volcano, Montserrat, Atmos. Chem. Phys., 7, 5093–5103, 2007.

Ryall DB, Maryon RH. (1998). Validation of the UK Met. Office's NAME model against the ETEX dataset. Atmos. Environ. 32(24): 4265–4276.

Searcy C, Dean KG, Stringer W (1998) PUFF: a volcanic ash tracking and prediction model. J Volcanol Geotherm Res 80:1–16

Stohl, A., M. Hittenberger, and G. Wotawa (1998): Validation of the Lagrangian particle dispersion model FLEXPART against large scale tracer experiments. Atmos. Environ. 32, 4245–4264.

Stohl, A., C. Forster, A. Frank, P. Seibert, and G. Wotawa (2005): Technical Note: The Lagrangian particle dispersion model FLEXPART version 6.2. Atmos. Chem. Phys. 5, 2461–2474.

Wang, X., A. Boselli, L. D'Avino, G. Pisani, N. Spinelli, A. Amodeo, A. Chaikovsky, M. Wiegner, S. Nickovic, A. Papayannis, M. R. Perrone, V. Rizi, L. Sauvage, and A. Stohl (2008): Volcanic dust characterization by EARLINET during Etna's eruptions in 2001–2002. Atmos. Environ. 42, 893–905.

Webley, P. W, K. Dean, J. E. Bailey, J. Dehn and R. Peterson (2009): Automated forecasting of volcanic ash dispersion utilizing virtual globes, *Natural Hazards*, Vol.51 No. 2, pp345-361, doi:10.1007/s11069-008-9246-2.

Witham CS, Hort MC, Potts R, Servranckx R, Husson P, Bonnardot F (2007) Comparison of VAAC atmospheric dispersion models using the 1 November 2004 Grimsvötn eruption. Meteorol Appl 14:27–38

Annex 3a: Satellite images

A.J. Prata

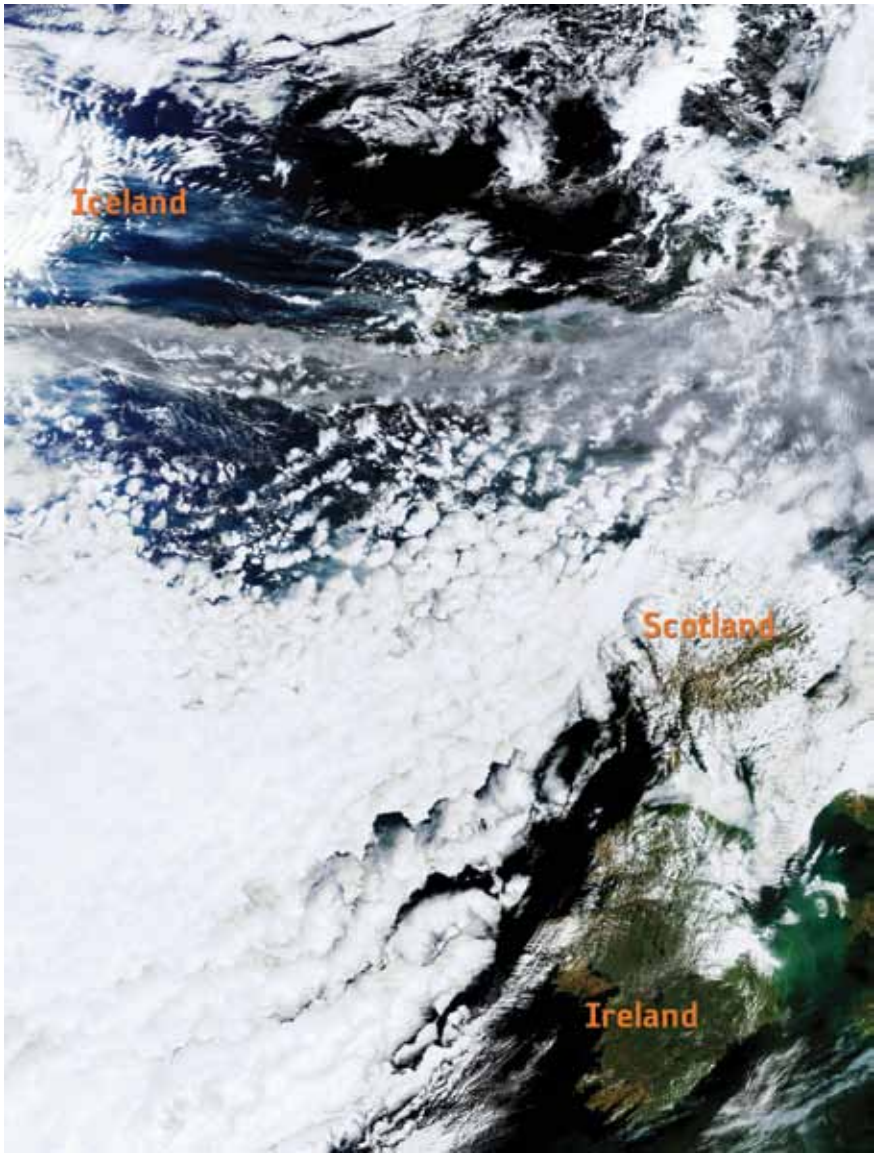

Fig. 3a1. MERIS true-colour image showing the volcanic cloud from Eyjafjöll. Images like this are excellent for identifying ash in the atmosphere when it is not obscured by clouds and only during daylight hours. Similar images were routinely used from MODIS (Terra/Aqua), AVHRR, GOSAT and SEVIRI. Apart from SEVIRI these instruments are in polar orbit and some have narrow swath widths making rapid and frequent identification of the plume difficult.

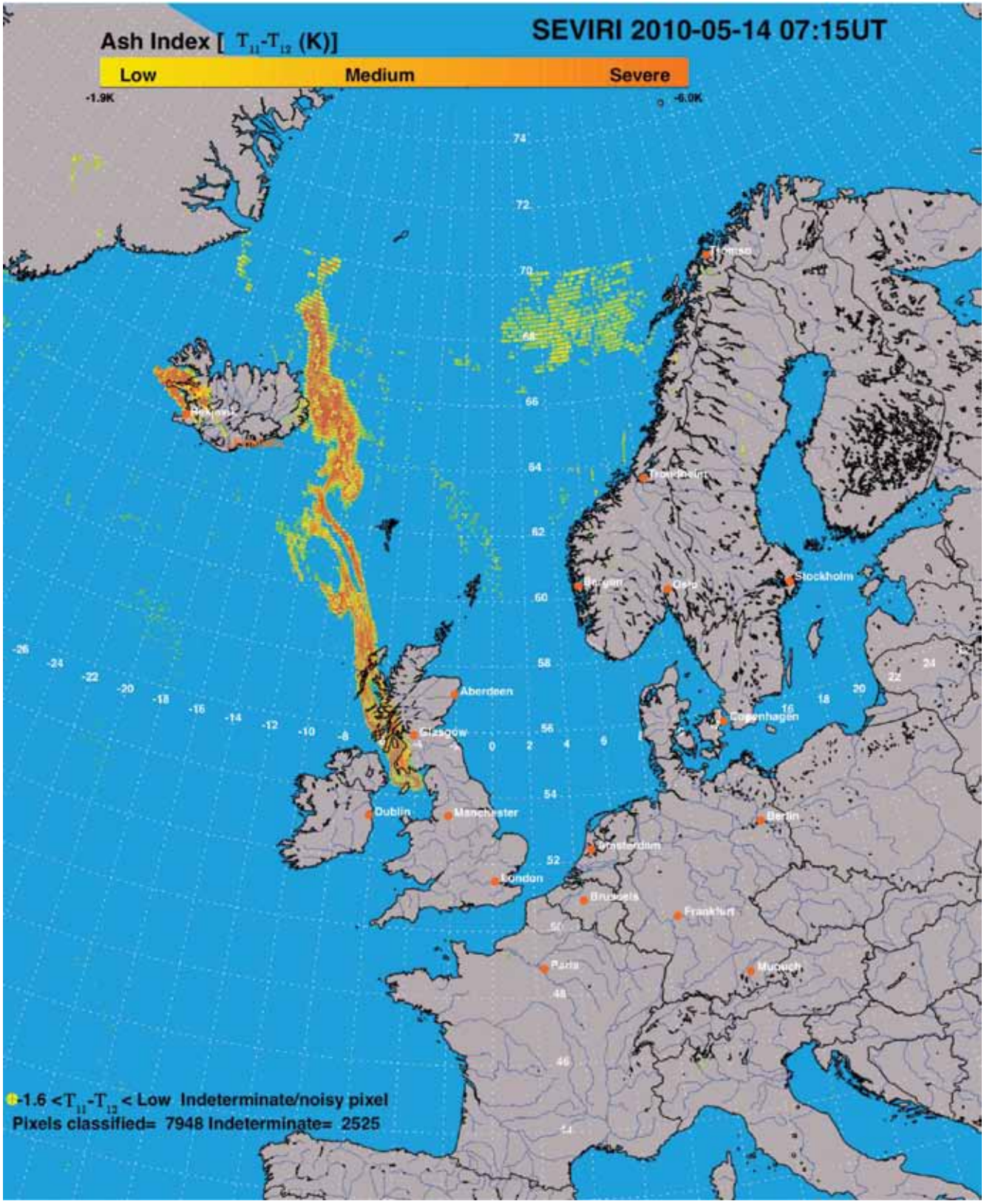

Fig. 3a2. Brightness temperature difference (BTD) image based on SEVIRI 11 and 12 μm infrared channels. Pixels coloured yellow – orange – red are identified as containing volcanic ash (not aerosol but ash). The detection limit (in this case DT=-1.9 K) can be adjusted, depending on the water vapour loading in the atmosphere.

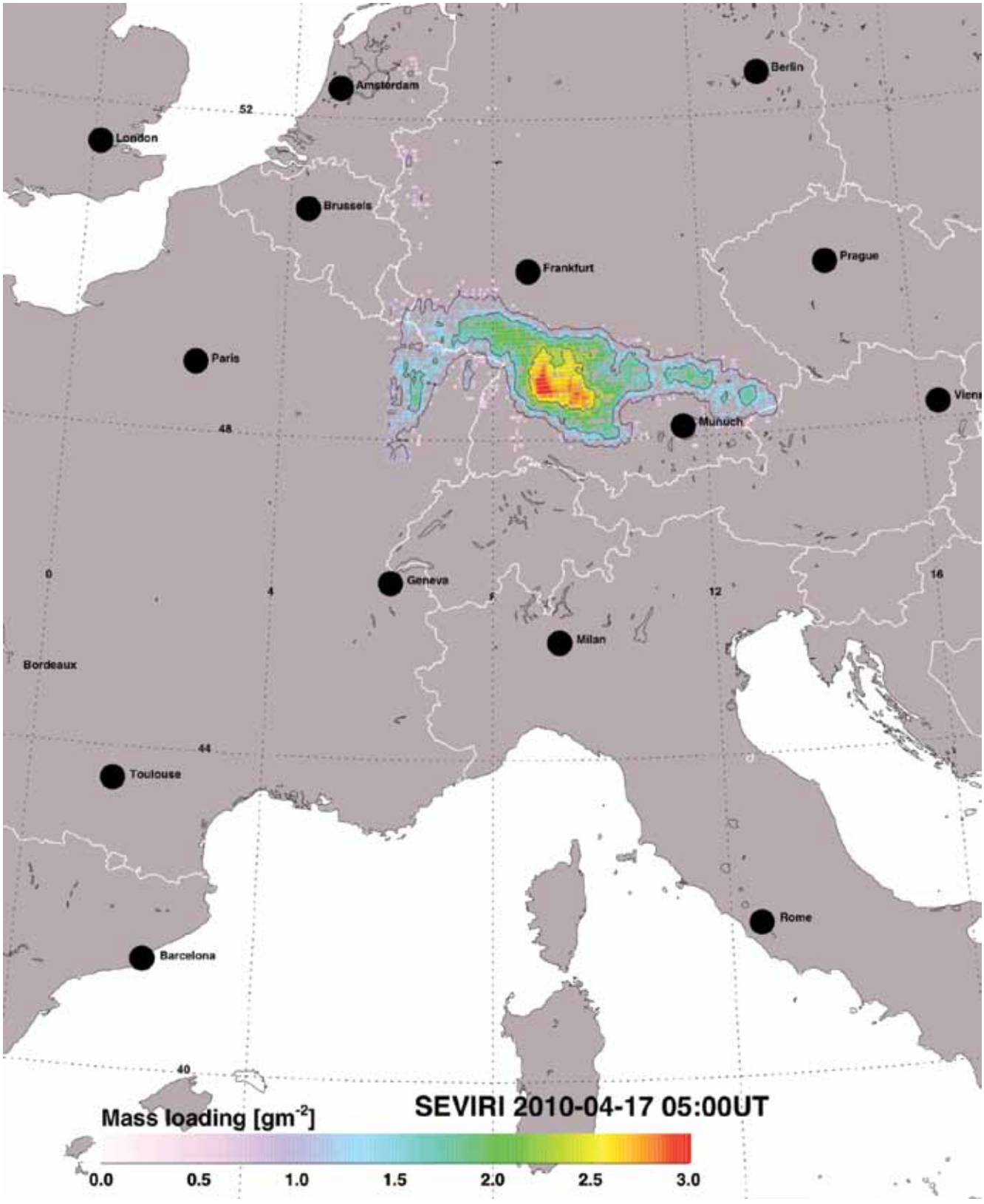

Fig. 3a3. Mass loading (g m^{-2}) of ash retrieved from SEVIRI thermal infrared data for 17.04.2010 at 05:00 UTC, when simultaneous ground-based lidar observed the periphery of the ash cloud south of Munich.

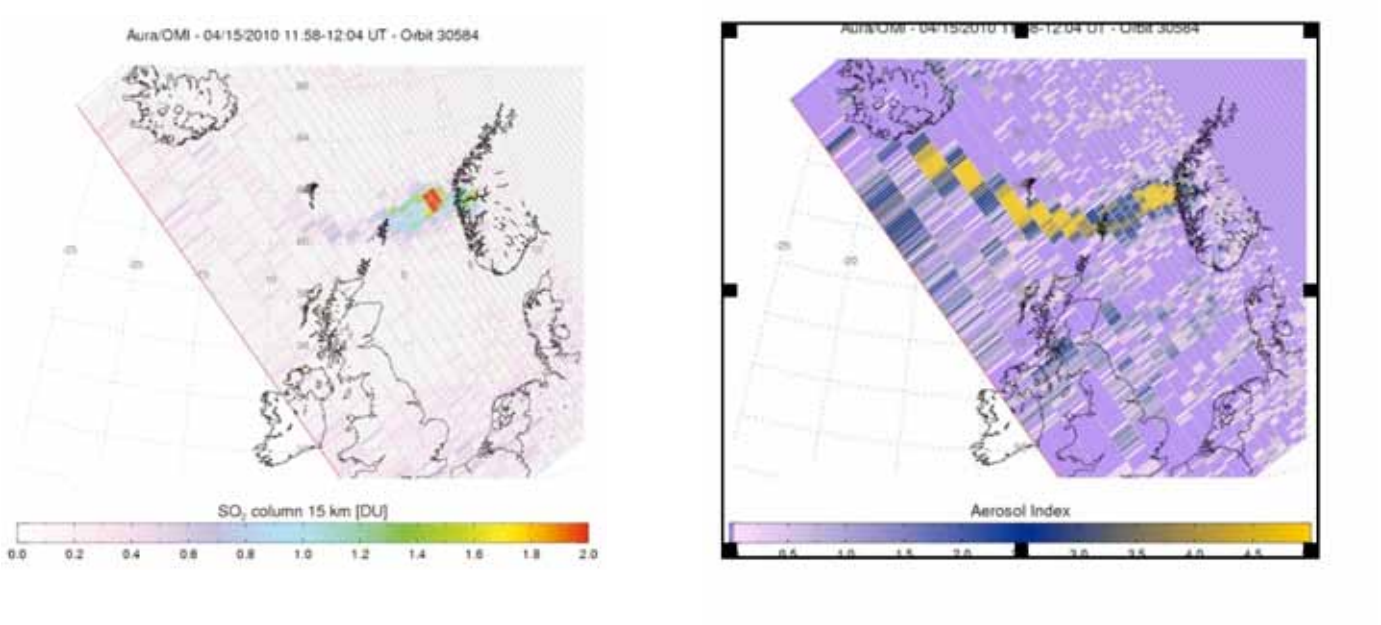

Fig. 3a4. Left: OMI SO_2 and, Right: aerosol index images on 15 April 2010.

Annex 3b: The reverse absorption algorithm

A.J. Prata

The basic principle of this algorithm for detecting ash uses the difference in absorption properties of silicate particles at two wavelengths in the thermal infrared. The two wavelengths used are 11 and 12 μm, but this is simply because these are the wavelengths generally available from several current (e.g. AVHRR, SEVIRI, MODIS) and planned (e.g. Sentinel/SLSTR) satellite instruments. The idea is to exploit the ratio of the extinction coefficients for ash at these two wavelengths as a means for discriminating ash from other atmsopheric particles. Since the extinction coefficients depend on refractive indices, particle sizes and shapes, it is also possible to perform a retrieval from the measurement space (11 and 12 μm brightness temperatures) to parameter space (infrared optical depth and effective particle size). The technique is illustrated here using highly simplified assumptions but noting that added complexity is simply a technical matter and offers marginal new insight into the principle.

Assume a gaseous-free atmospheric path with a homogenous single layer of ash cloud and monochromatic radiation. Then for radiation at wavelength l_1,

$$B_1 = \varepsilon_1 B_1(T_c) + (1-\varepsilon_1)B_1(T_s) \qquad (1)$$

Likewise for radiation at a second wavelength, l_2:

$$B_2 = \varepsilon_2 B_2(T_c) + (1-\varepsilon_2)B_2(T_s) \qquad (2)$$

where T_c is the ash cloud temperature (assumed uniform) and T_s is the temperature of the environment behind the ash cloud (this could be the surface below, if viewing from a satellite).

Linearising these equations and after some manipulation it is possible to derive the following:

$$\Delta T = \Delta T_c (X - X^{\beta}) \qquad (3)$$

where:

$$\Delta T = T_1 - T_2$$

$$X = 1 - \frac{\Delta T_1}{\Delta T_c}$$

$$\Delta T_c = T_s - T_c$$

$$\Delta T_1 = T_s - T_1$$

$$\beta = \frac{k_1}{k_2}$$

$$\varepsilon_i = 1 - \exp(-k_i L)$$

It can be seen that the form of the relationship (3) depends on a few simple parameters and in particular on the ratio of extinction coefficients at the two chosen wavelengths.

Note that when $\beta < 1$, the curve of ΔT vs. T_2 is U-shaped, whereas if $\beta > 1$ the curve is arch-shaped. Thus the shape of the distribution curve is a remarkably reliable indicator of the presence of ash in an image. The value of β depends on a number of factors, effective particle radius being of prime importance (see Figure 3b1).

Fig. 3b1 Top panel: Extinction ratio (k1/k2) vs. effective particle radius for andesite particles. Bottom panel: 12 μm brightness temperature vs 11–12 μm brightness temperature difference, showing the characteristic curve for ash particles (andesite) with effective particle radius of 5 μm and mass loading of 2 mg m^{-3}. The temperature difference signal of −4K is easily detected using IR satellite data and demonstrates the great utility of these measurements for the ash hazard problem.

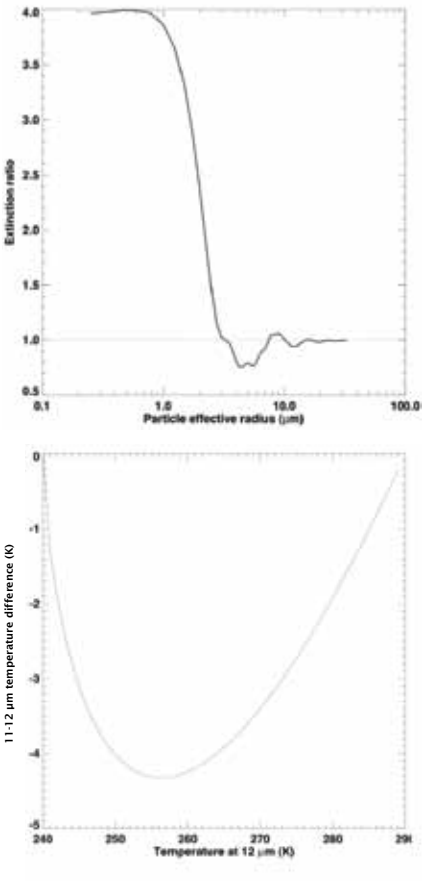

In order to understand the sensitivity of this algorithm to silicate mass we will assume that the ash cloud consists of a monomodal size distribution with zero spread and particle radius of 5 µm. The mass concentration (mg m^{-3}) in a given pixel may be written:

$$M = \frac{4}{3}\rho r \frac{\tau_i}{k_i L} \qquad (4)$$

with $\rho = 2.6 \times 10^6$ g m^{-3}; $r = 5 \times 10^{-6}$ m; $M = 2$ mg m^{-3}; L= 1 km; $k_1 = 2.859$ ($k_2 = 3.615$); $\beta = 0.79$; gives $\tau_1 = 0.30$, and $\tau_2 = 0.38$. We can also work backwards using these values in (1) and (2), and assuming values of $T_s = 290$K and $T_c = 240$K results in the U-shaped curve shown in Figure 3b1 (bottom panel).

An example of an ash mass loading retrieval (i.e. M/L) is shown in Fig. 3b2.

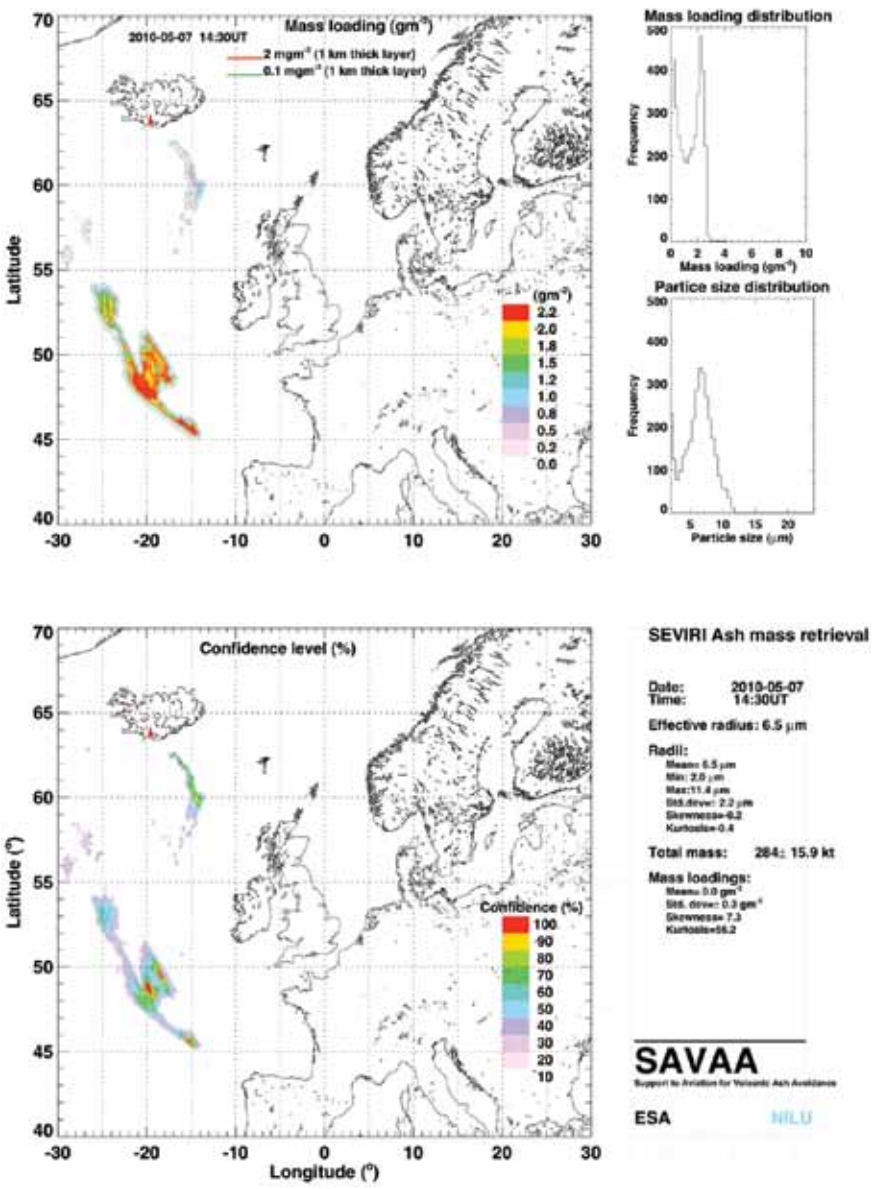

Fig. 3b2: Ash mass loadings (g m^{-2}), confidence level (in %), mass distribution and effective particle size retrieval from SEVIRI infrared data.

Annex 3c: Future ESA/EUMETSAT satellite missions

T. Fehr and R. Munro

1. Research missions

1.1 EarthCARE

1.1.1 Objectives

The Earth Clouds, Aerosols and Radiation Explorer Mission (EarthCARE) was selected as an Earth Explorer Core Mission in 2004 to cover primary research objectives set out in the ESA Living Planet Programme. Its primary objective is to contribute to the understanding of Earth's radiation budget by providing global observations of vertical cloud and aerosol profiles.

Specific targets addressed by the mission with relevance for the determination of volcanic ash include the observation of the vertical profiles of natural and anthropogenic aerosols on a global scale, their radiative properties and interaction with clouds. In addition, EarthCARE will allow the observation of the vertical distributions of atmospheric liquid water and ice on a global scale, as well as the cloud distribution, cloud-precipitation interactions and the characteristics of vertical motions within clouds.

1.1.2 Instruments

The EarthCARE mission objectives will be addressed by the synergistic use of active and passive sensors. The instrument suite will consist of an ATmospheric LIDar (ATLID), a Cloud Profiling Radar (CPR), a Multi-Spectral Imager (MSI) and a BroadBand Radiometer (BBR). For optimal exploitation of the data, the instrument footprints are carefully aligned (see Fig 3c1).

Atmospheric Lidar (ATLID)

ATLID is a UV backscatter lidar at 355 nm emitting circular polarised pulses. It is equipped with a high spectral resolution receiver allowing separation of the Rayleigh and Mie backscatter return. The receiver includes a cross-polar and a

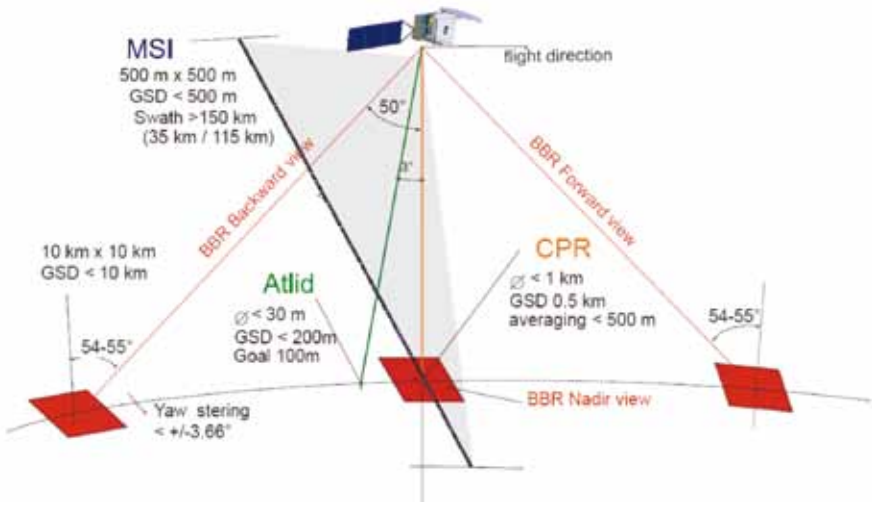

Fig. 3c1: EarthCARE observational concept

co-polar Mie channel, as well as a Rayleigh channel. The nominal horizontal sampling is 200 m with a vertical sampling of 100 m, and an altitude range covering –0.5 km to 40 km.

Cloud Profiling Radar (CPR)

The CPR is a JAXA contribution to the EarthCARE mission. It is a high power millimetre-wave Doppler radar for the measurement of vertical profiles of clouds along the sub-satellite track. It emits microwave pulses at an operating frequency of 94 GHz, with a sensitivity of at least –35 dBZ at 20 km altitude. The altitude range covers –0.5 km to 20 km. The vertical resolution is 500 m with a sampling interval of 100 m. The Doppler accuracy is expected to be 1 m s^{-1}.

Multi-Spectral Imager (MSI)

The MSI is a nadir-viewing push-broom imager with seven spectral channels at 670 nm, 865 nm, 1.65 µm, 2.21 µm ('solar channels') and at 8.80µm, 10.80 µm, 12.00µm ('TIR channels'). Its swath extends from –35 km to 115 km with respect to nadir with a sampling distance of 500 m.

Broadband Radiometer (BBR)

The BBR measures Earth's radiance in a shortwave channel between 0.2 µm and 4 µm, as well as in a longwave channel covering 4 µm to 50 µm. To cover the total radiance field, observations of the same area will be done in a forward-, nadir- and backward-looking view with a 10x10 km ground spot.

1.1.3 Orbit Parameters

EarthCARE will be operated in a Sun-synchronous orbit at a mean local solar time which will be fixed at a value between 13:45 and 14:00. The foreseen repeat cycle will be 25 days with a mean geodetic altitude of 408 km.

1.1.4 Products

EarthCARE will provide a broad range of products that can be retrieved from single sensors as well as through the exploitation of the synergy between the instruments. The list of EarthCARE Level 2 products is not consolidated; several product studies are ongoing.

Potential products with relevance to the volcanic ash observations will include the lidar backscatter, extinction and depolarisation ratio, target classification and aerosol layer descriptor, the imager aerosol optical thickness and Angstrom coefficient over oceans, the radar reflectivity, cloud mask, cloud particle type identification and vertical motion.

Foreseen synergetic products include target classifications, aerosol extinction coefficients, aerosol spectral optical thickness, aerosol particle size, aerosol type and convective velocity.

Currently only off-line processing of the EarthCARE products is foreseen. However, the requirements for near-realtime processing are under review.

1.1.5 Mission Status

The launch of the mission is currently foreseen in 2015. The design lifetime of the EarthCARE mission is 3+1 years.

1.2 ADM-Aeolus

1.2.1 Objectives

The primary, long-term objective of the Atmospheric Dynamics Mission Aeolus is to provide observations of global wind profiles along the line-of-sight direction. The data will be assimilated into numerical forecasting models leading to an improvement in objective analyses and hence in numerical weather prediction. The retrieval of aerosol properties is not a priority.

1.2.2 Instrument

The Aeolus payload is the High Spectral Resolution Lidar ALADIN with one single wavelength in the UV at 355 nm HSRL with a Rayleigh and a Mie channel. There is no depolarisation capability and there are no complementary instruments. It is optimised for wind measurements therefore the retrieval of spinoff products is limited. The vertical sampling of the atmospheric layers is adjustable from 0.25 km to 2 km thickness. The lidar operates in a burst mode allowing 50 km measurements every 200 km (see Figure 3c2).

1.2.3 Orbit Parameters

ADM-Aeolus is in a Sun-synchronous orbit with 18:00 UTC+1 at ascending node with a seven-day repeat cycle. The mean altitude is 408 km.

1.2.4 Products

Apart from the atmospheric dynamics products, a cloud/aerosol mask, optical depths, scattering ratios and backscatter-to-extinction rations are foreseen.

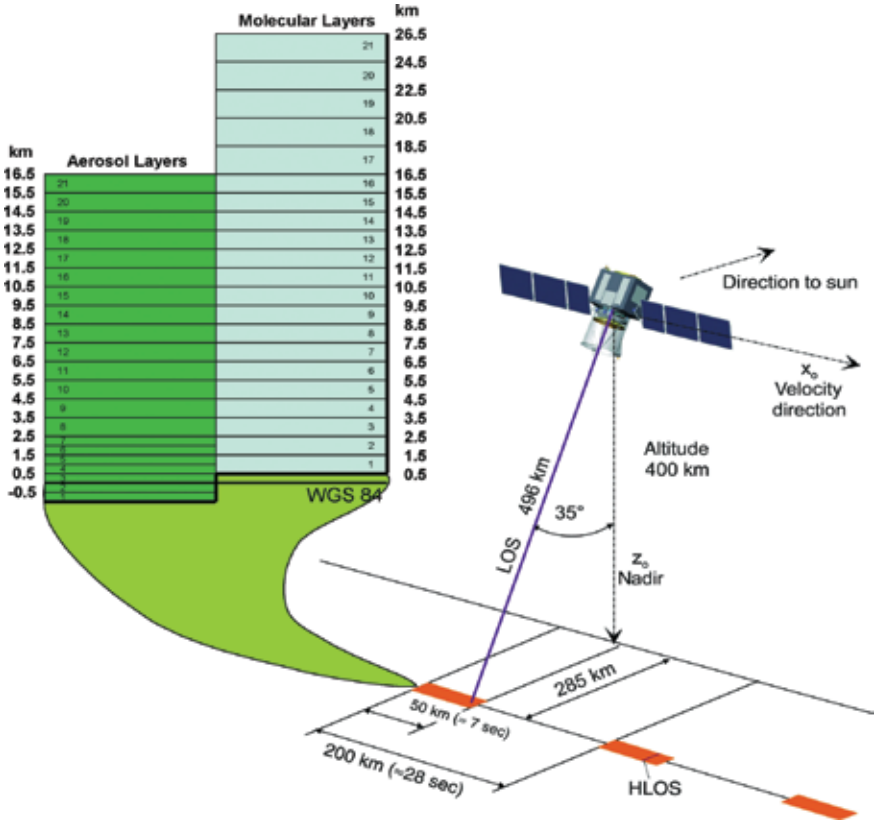

Fig. 3c2: ADM-Aeolus observation concept.

1.2.5 Mission Status

The launch of ADM-Aeolus is foreseen in 2013. The mission design lifetime is three years, plus three months commissioning phase.

2. Operational missions

The value of the current operational satellites systems, both geostationary (Meteosat Second Generation – MSG) and polar-orbiting (the European Polar System – EPS) has been clearly demonstrated, specifically with the capability to provide imagery products and estimates of ash extent, SO_2, cirrus and ice.

These capabilities will be enhanced with the launch of the next generation of European operational satellites (Meteosat Third Generation – MTG) and polar-orbiting satellites (the European Polar System Second Generation – EPS-SG).

The MTG system will comprise two satellites: an imaging platform (to be launched in ~2017), carrying the Flexible Combined Imager (FCI), the Lightning Imager (LI), the data collection system and search and rescue; and a sounding platform (to be launched in ~2019) carrying the InfraRed Sounder (IRS) and the GMES Sentinel 4 Ultraviolet Visible Near-infrared sounder (UVN).

The imagery, cloud, SO_2 and ash products anticipated from the MTG-FCI will be available with improved spatial (1–2 km) and temporal (10 mins) resolution as compared to MSG, and the aerosol detection capabilities will be enhanced with the inclusion of the 0.444 µm and 0.51 µm bands. Additionally the MTG-IRS (with heritage from the EPS/Metop IASI instrument) will provide improved ash detection capabilities with high temporal resolution (~30 minutes over Europe). However, unlike IASI, it will not provide information on SO_2. The Sentinel-4 UVN will however provide estimates of SO_2 at ~8 km spatial resolution and 1 hr temporal resolution over Europe. Information on aerosol optical depth and an absorbing aerosol index will also be provided.

In addition to the operational geostationary missions, the next generation of operational polar orbiting satellites is currently being planned. Missions under consideration include an imaging mission (VII) with similar capabilities for aerosol detection to MODIS, providing aerosol optical depth information at high spatial resolution; an infrared sounding mission (IRS), with enhanced spectral and radiometric performance as compared to EPS/Metop IASI, which will provide improved detection of ash, SO_2, cirrus and ice; and the Sentinel-5 UVNS which will continue the aerosol optical depth and absorbing aerosol index measurements provided by GOME-2/SCIAMACHY and OMI but with significantly improved spatial resolution. Also under consideration is a multi-angle, multi-polarisation, multispectral instrument (3MI) (similar in concept to POLDER) which if realised will provide targeted aerosol information (including information on aerosol optical depth, coarse/fine mode, size, refractive index, height).

Other operational missions of relevance include the GMES Sentinel-2 and -3 missions targeting ocean and global land monitoring. In addition to ocean and land products, aerosol optical depth can also be provided.

Table 3c1: Satellite missions planned for Europe and possibility of deriving relevant data for volcanic plume monitoring

Instrument/Satellite	SO_2	Ash	Spatial coverage	Status and launch date
IASI/MetOpB	Total column + altitude ±2 km Detection limit 2 DU	Estimated concentration (needs altitude assumption)	Polar (9:30; 21:30) Pixel 12 km	Phase C 2012
GOME2/MetOpB	Total column + altitude Detection limit 2 DU	AAI, AOD	Polar (9:30) Pixel 40 x 80 km	Phase C 2012
IASI/MetopB	Total column + altitude ±2 km Detection limit 2 DU	Estimated concentration (needs altitude assumption)	Polar (9:30; 21:30) Pixel 12 km	Phase C 2017
GOME2/MetopB	Total column + altitude Detection limit 2 DU	AAI, AOD	Polar (9:30) Pixel 40 x 80 km	Phase C 2017
Sentinel-Precursor Tropomi (OMI heritage)	Total column + altitude Detection limit 1 DU	AAI, AOD	Polar (13 :30) Pixel 7 x 7 km	Phase B 2014
Imagers/MTG (Severi heritage)	IR UT/LS	IR ash concentration	GEO Full disc	Phase A 2017
IRS/MTG (IASI heritage, coarser spectral res.)	Only the n_1 band – low altitude detection only	Estimated concentration (needs altitude assumption)	GEO Full disc, pixel 4 km 30/60 min	Phase A 2019
UVS/MTG (Sentinel 4) (GOME2-OMI heritage)	Total column + altitude Detection limit 1 DU	AAI, AOD	GEO 25°W–30°E/ 25°N–60°N 10/20 min Pixel 8 x 8 km	Phase A 2019
IASI-NG/Post-EPS (IASI heritage, better spectral res.)	Total column + altitude ±1 km Detection limit 1 DU	Estimated concentration (needs altitude assumption)	Polar (9:30; 21:30) Pixel 12 km	Phase 0 2010
UVS/Post-EPS (Sentinel 5) GOME2 heritage	Total column + altitude Detection limit 1 DU	AAI, AOD	Polar (9 :30) Pixel 7 x 7 km	Phase 0 2010
3MI/Post-EPS (Polder- Parasol heritage)	-	AOD, Coarse/fine mode, size, refractive index, height	Polar (9 :30) Pixel 4 km	Phase 0 2010
AAI= Absorbing Aerosol Index AOD= Aerosol Optical Depth				

References

Barton IJ, Prata AJ, Watterson IG, Young SA (1992) Identification of the Mount Hudson volcanic cloud over SE Australia. Geophys Res Lett 19:1211–1214

Bernard A, Rose WI (1984) The injection of sulfuric acid aerosols in the stratosphere by the El Chichon volcano and its related hazards to the international air traffic. Nat Hazards 3(1):59–67. doi:10.1007/ BF00144974

Bluth GJS, Schnetzler CC, Krueger AJ, Walter LS (1993) The contribution of explosive volcanism to global atmospheric sulphur dioxide concentrations. Nature 366:327–329

Carn SA, Krueger AJ, Krotkov NA, Gray MA (2004) Fire at Iraqi sulfur plant emits SO2 clouds detected by Earth Probe TOMS. Geophys Res Lett 31:L19105. doi:10.1029/2004GL020719

Carn SA, Krotkov NA, Yang K, Hoff RM, Prata AJ, Krueger AJ, Loughlin SC, Levelt PF (2007) Extended observations of volcanic SO2 and sulphate aerosol in the stratosphere. Atmos Chem Phys Discuss 7:2857–2871

Carn SA, Prata AJ, Karlsdottir S (2008) Circumpolar transport of a volcanic cloud from Hekla (Iceland). J Geophys Res 113. doi:10.1029/2008JD009878

Casadevall TJ (1994) The 1989/1990 eruption of Redoubt Volcano Alaska: impacts on aircraft operations. J Volcanol Geotherm Res 62(30):301–316

Casadevall TJ, Delos Reyes PJ, Schneider DJ (1996) The 1991 Pinatubo eruptions and their effects on aircraft operations. In: Newhall CG, Punongbayan RS (eds) Fire and mud: eruptions and lahars of Mount Pinatubo, Philippines. Philippines Institute of Volcanology and Seismology, Quezon City, University of Washington Press, Seattle, pp 625–636

Clerbaux C, Hadji-Lazaro J, Turquety S, George M, Coheur P-F, Hurtmans D, Wespes C, Herbin H, Blumstein D, Tournier B, Phulpin T (2007) The IASI/MetOp I mission: first observations and highlights of its potential contribution to GMES. COSPAR Inf Bull 2007:19–24

Constantine EK, Bluth GJS, Rose WI (2000) TOMS and AVHRR sensors applied to drifting volcanic clouds from the August 1991 eruptions of Cerro Hudson. In: Mouginis-Mark P, Crisp J, Fink J (eds) AGU Monograph 116—Remote Sensing of Active Volcanism, pp 45–64

Eckhardt S, Prata AJ, Seibert P, Steibel K, Stohl A (2008) Estimation of the vertical profile of sulfur dioxide injection into the atmosphere by a volcanic eruption using satellite column measurements and inverse transport modeling. Atmos Chem Phys Discuss 8:3761–3805

Eisinger M, Burrows JP (1998) Tropospheric sulfur dioxide observed by the ERS-2 GOME instrument. Geophys Res Lett 25(22):4177–4180

Ellrod GP, Connell BH, Hillger DW (2003) Improved detection of airborne volcanic ash using multispectral infrared satellite data. J Geophys Res 108(D12):4356. doi:10.1029/2002JD002802

Fleming EL, Chandra S, Shoeberl MR, Barnett JJ (1988) Monthly mean global climatology of temperature, wind, geopotential height and pressure for 0–120 km. NASA, Technical Memorandum 100697, Washington, DC

Guffanti M, Albersheim S (2008) The United States national volcanic ash operations plan for aviation. Nat Hazards Special Issue: Aviation hazards from volcanoes. doi:10.1007/ s11069-008-9247-1

Hanstrum BN, Watson AS (1983) A case study of two eruptions of Mount Galunggung and an investigation of volcanic eruption cloud characteristics using remote sensing techniques. Aust Meteorol Mag 31:131–177

Hillger DW, Clark JD (2002a) Principal component image analysis of MODIS for volcanic ash. Part I: most important bands and implications for future GOES imagers. J Appl Meteorol 41:985–1001

Hillger DW, Clark JD (2002b) Principal component image analysis of MODIS for volcanic ash. Part II: simulation of current GOES and GOES-M imagers. J Appl Meteorol 41:1003–1010

Holasek RE, Rose WI (1991) Anatomy of 1986 Augustine volcano eruptions as recorded by multispectral images processing of digital AVHRR weather satellite data. Bull Volcanol 53:42–435.

Holasek RE, Woods AW, Self S (1996) Experiments on gas-ash separation processes in volcanic umbrella clouds. J Volcanol Geotherm Res 70:169–181.

Krotkov NA, Carn SA, Krueger AJ, Bhartia PK, Yang K (2006) Band residual difference algorithm for retrieval of SO2 from the Aura Ozone Monitoring Instrument (OMI). IEEE Trans Geosci Remote Sens 44(5):1259–1266.

Krueger AJ (1983) Sighting of El Chichon sulfur dioxide clouds with the nimbus 7 total ozone mapping spectrometer. Science 220:1377–1379.

Krueger AJ, Walter LS, Bhartia PK, Schnetzler CC, Krotkov NA, Sprod I, Bluth GJS (1995) Volcanic sulfur dioxide measurements from the total ozone mapping spectrometer instruments. J Geophys Res 100(D7):14057–14076.

Krueger AJ, Schaefer SJ, Krotkov N, Bluth GJS, Baker S (2000) Ultraviolet remote sensing of volcanic emissions. In: Mouginis-Marks PJ, Crisp JA, Fink JH (eds) Remote sensing of active volcanism. Geophys Monogr Ser 116:2543, AGU, Washington, DC.

Malingreau J, Kaswanda P (1986) Monitoring volcanic eruptions in Indonesia using weather satellite data: the Colo eruption of July 28, 1983. J Volcanol Geotherm Res 27(1–2):179–194.

Matson M (1984) The 1982 El Chichon volcano eruptions—a satellite perspective. J Volcanol Geotherm Res 23:1–10.

Miller TP, Casadevall TJ (1999) Volcanic ash hazards to aviation. In: Sigurdsson H, Houghton B, McNutt SR, Ryman H, Stix J (eds) Encyclopedia of volcanoes. Academic Press, San Diego, pp 915–930.

Mosher FR (2000) Four channel volcanic ash detection algorithm, Preprint Volume. 10th Conference on Satellite Meteorology and Oceanography, Long Beach, California, 9–14 January, 2000, pp 457–460.

Pavolonis MJ, Feltz WF, Heidinger AK, Gallina GM (2006) A daytime complement to the reverse absorption technique for improved automated detection of volcanic ash. J Atmos Oceanic Technol 23:1422–1444.

Pergola N, Tramutoli V, Marchese F, Scaffidi I, Lacav T (2004) Improving volcanic ash cloud detection by a robust satellite technique. Remote Sens Environ 90:1–22.

Pieri D, Ma C, Simpson JJ, Hufford G, Grindle T, Grove C (2002) Analyses of in-situ airborne ash from the February 2000 eruption of Hekla volcano, Iceland. Geophys Res Lett 29:16. doi:10.1029/2001GL013688.

Prata AJ (1989a) Observations of volcanic ash clouds using AVHRR-2 radiances. Int J Remote Sens 10(4–5):751–761.

Prata AJ (1989b) Radiative transfer calculations for volcanic ash clouds. Geophys Res Lett 16(11): 1293–1296.

Prata AJ, Grant IF (2001) Retrieval of microphysical and morphological properties of volcanic ash plumes from satellite data: application to Mt. Ruapehu, New Zealand. Q J R Meteorol Soc 127(576B): 2153–2179.

Prata AJ, Kerkmann J (2007) Simultaneous retrieval of volcanic ash and SO2 using MSG-SEVIRI measurements. Geophys Res Lett 34:L05813. doi:10.1029/2006GL028691.

Prata AJ, Bluth GJS, Rose WI, Schneider DJ, Tupper AC (2001) Comments on failures in detecting volcanic ash from a satellite-based technique. Remote Sens Environ 78:341–346.

Prata, A. J., and Tupper, A. T., (2009) Aviation hazards from volcanoes: the state of the science, Nat Hazards doi: 10.1007/s11069-009-9415-y.

Prata AJ, Rose WI, Self S, O'Brien DM (2003) Global, long-term sulphur dioxide measurements from TOVS data: a new tool for studying explosive volcanism and climate. Volcanism and the Earth's atmosphere, Geophysics Monograph 139 AGU, pp 75–92.

Prata AJ, Carn SA, Stohl A, Kerkmann J (2007) Long range transport and fate of a stratospheric volcanic cloud from Soufriere Hills volcano, Montserrat. Atmos Chem Phys 7:5093–5103.

Richardson AJ (1984) El Chichon volcanic ash effects on atmospheric haze measured by NOAA-7 AVHRR data. Remote Sens Environ 16:157–164.

Richter A, Wittrock F, Burrows JP (2006) SO2 measurements with SCIAMACHY. In: Proceedings of the first conference on atmospheric science, Frascati, Italy, 8–12 May 2006. ESA SP-628.

Rose WI, Delene DJ, Schneider DJ, Bluth GJS, Kruger AJ, Sprod I, McKee C, Davies HL, Ernst GJ (1995) Ice in the 1994 Rabaul eruption: implications for volcanic hazard and atmospheric effects. Nature 375:477–479.

Sawada Y (1987) Study on analysis of volcanic eruptions based on eruption cloud image data obtained by the Geostationary Meteorological Satellite (GMS). Technical reports of the Meteorological Research Institute, vol 22, 335 pp.

Sawada Y (1996) Detection of explosive eruptions and regional tracking of volcanic ash clouds with geostationary meteorological satellites (GMS). In: Scarpa R, Tilling RI (eds) Monitoring and mitigation of volcano hazards. Springer-Verlag, Berlin, Heidelberg, pp 299–314.

Schneider DJ, Rose WI, Kelley L (1995) Tracking of 1992 eruption clouds from Crater Peak of Mount Spurr volcano, Alaska, using AVHRR. US Geol Surv Bull 2139:27–36.

Schneider DJ, Rose WI, Coke LR, Bluth GJS (1999) Early evolution of a stratospheric volcanic eruption cloud as observed with TOMS and AVHRR. J Geophys Res 104(D4):4037–4050.

Simkin T, Seibert L (1994) Volcanoes of the world, 2nd edn. Geoscience Press, Tucson

Simpson JJ, Hufford G, Pieri D, Berg J (2000) Failures in detecting volcanic ash from a satellite-based technique. Remote Sens Environ 72:191–217.

Simpson JJ, Hufford G, Pieri D, Servranckx R, Berg J (2002) The February 2001 eruption of Mount Cleveland, Alaska: case study of an aviation hazard. Weather Forecast 17:691–704.

Thomas W, Erbertseder T, Ruppert T, Van Roozendael M, Verdebout J, Balis D, Meleti C, Zerefos C (2004) On the retrieval of volcanic sulfur dioxide emissions from GOME backscatter measurements. J Atmos Chem 50:295–320. doi:10.1007/s10874-005-5079-5.

Torres O, Bhartia PK, Herman JR, Ahmad Z, Gleason J (1998) Derivation of aerosol properties from satellite measurements of backscattered ultraviolet radiation: theoretical basis. J Geophys Res, 103(D14):17099–17110.

Tupper A, Carn SA, Davey J, Kamada Y, Potts RJ, Prata AJ, Tokuno M (2004) An evaluation of volcanic cloud detection techniques during recent significant eruptions in the western ring of fire. Remote Sens Environ., 91:27–46.

Urai M (2004) Sulfur dioxide flux estimation from volcanoes using advanced spaceborne thermal emission and reflection radiometer—a case study of Miyakejima volcano, Japan. J Volcanol Geotherm Res., 134(1–2):1–13.

Van Geffen J, Van Roozendael M, Di Nicolantonio W, Tampellini L, Valks P, Erbetseder T, Van der A, R. (2007) Monitoring of volcanic activity from satellite as part of GSE PROMOTE. Proceedings of the first conference on atmospheric science, Frascati, Italy, 8–12 May 2006. ESA SP-628.

Watkin SC (2003) The application of AVHRR data for the detection of volcanic ash in a volcanic ash advisory centre. Meteorol Appl 10:301–311.

Wen S, Rose WI (1994) Retrieval of sizes and total masses of particles in volcanic clouds using AVHRR bands 4 and 5. J Geophys Res 99(D3):5421–5431.

Witham CS, Hort MC, Potts R, Servranckx R, Husson P, Bonnardot F (2007) Comparison of VAAC atmospheric dispersion models using the 1 November 2004 Grimsvötn eruption. Meteorol Appl 14: 27–38.

Yu T, Rose WI, Prata AJ (2002) Atmospheric correction for satellite-based volcanic ash mapping and retrievals using split window IR data from GOES and AVHRR. J Geophys Res 107(D16):4311. doi:10.1029/2001JD000706.

Acronyms

AAI	Absorbing Aerosol Index
ACE	Atmospheric Chemistry Experiment
ACTRIS	Aerosols, Clouds and Trace Gases Research Infrastructure Network
ADM-Aeolus	Atmospheric Dynamics Mission - Aeolus
AERONET	AErosol RObotic NETwork
AI	Absorption Index
AIRS	Atmospheric Infrared Sounder
AOD	Aerosol Optical Depth
AOT	Aerosol Optical Thickness
ARPEGE	Action de Recherche Petite Echelle Grande Echelle
ASTER	Advanced Spaceborne Thermal Emission and Reflection Radiometer
ATHAM	Active Tracer High Resolution Atmospheric Model
ATLID	Atmospheric LIDar
ATSR	Along Track Scanning Radiometer
AVHRR	Advanced Very High Resolution Radiometer
BBR	Broad Band Radiometer
BTD	Brightness Temperature Difference
CAA	Civil Aviation Authority
CALIOP	Cloud-Aerosol LIdar with Orthogonal Polarisation
CALIPSO	Cloud-Aerosol Lidar and Infrared Pathfinder Satellite Observation
CETEMPS	Centre of Excellence for the forecast of Severe Weather
CIMSS/SSEC	Cooperative Institute for Meteorological Satellite Studies/ Space Science and Engineering Center
CNRS	Centre National de la Recherche Scientifique
COSMO	Consortium for Small-Scale Modelling
CPR	Cloud Profiling Radar
CrIS	Cross-track Infrared Sounder
CSA	Canadian Space Agency
CTBTO	Comprehensive Nuclear-Test-Ban Treaty Office
CTH	Cloud Top Height
CTM	Chemistry Transport Model
CTT	Cloud Top Temperature
DLR	Deutsches Zentrum fur Luft –und Raumfahrt (German space agency)
DU	Dobson Unit
EARLINET	European Aerosol Research Lidar Network
EarthCARE	Earth Clouds, Aerosols and Radiation Explorer
EC	European Commission
ECMWF	European Centre for Medium-Range Weather Forecasts
EMEP	European Monitoring and Evaluation Programme
EMPA	Eidgenössische Materialprüfungs- und Forschungsanstalt
EPS	EUMETSAT Polar System
EPZ	Enhanced Procedures Zone
ESA	European Space Agency
ESRIN	European Space Research Institute
ETEX	European Tracer Experiment
EUFAR	European Facility For Airborne Research
EUMETNET	European National Meteorological Services Network
EUMETSAT	European Organisation for the Exploitation of Meteorological Satellites
EURAD	EURopean Air Pollution Dispersion
FCI	Flexible Combined Imager
FL	Flight Layer
FT	Free troposphere
FY	Fengyún (Chinese weather satellite)
GAW	Global Atmospheric Watch
GEO	Geostationary Earth Orbit
GFS	Global Forecasting System
GIS	Geographic Information System
GMES	Global Monitoring for Environment and Security
GOES	Geostationary Operational Environmental Satellite
GOME	Global Ozone Monitoring Experiment
GPS	Global Positioning System
HAZMAP	Hazardous environment Mapping system
HIRS	High Resolution Infrared Radiation Sounder
HRV	High Resolution Visible
HSRL	High spectral resolution lidar
HYSPLIT	Hybrid Single Particle Lagrangian Integrated Trajectory Model
IAGOS	Integration of routine Aircraft measurements into a Global Observing System
IASI	Infrared Atmospheric Sounding Interferometer
IATA	International Air Transport Association
IAVCEI	International Association of Volcanology and Chemistry of the Earth's Interior
IAVW	International Airways Volcano Watch
ICAO	International Civil Aviation Office
IES	Institute of Earth Sciences (Univ. Iceland)
IGC	Institute of Chemistry and Dynamics of the Geosphere (Germany)
IM	Inverse Model
IMAA-CNR	Institute of Methodologies for Environmental Analysis – National Research Council
IMO	Icelandic Meteorological Office
IMPROVE	Interagency Monitoring of Protected Visual Environments
IPSL	Institut Pierre-Simon Laplace

IR	Infrared
IRS	Infrared Sounder
ISAC-CNR	Institute of Atmospheric Sciences and Climate – National Research Council
IUGG	International Union of Geodesy and Geophysics
JMA	Japan Meteorological Agency
JRC	Joint Research Centre
KIT	Karlsruhe Institute of Technology
LATMOS	Laboratoire Atmosphères, Milieux, Observations Spatiales
LCBR	Laser Cloud Base Recorder (also known as a ceilometer)
LEO	Low Earth Orbit
LIDAR	LIght Detection And Ranging
LPDM	Lagrangian Particle Dispersion Model
MACC	Monitoring Atmospheric Composition and Climate
MALE	Medium Altitude, Long Endurance
MDA	MacDonald Dettwiler and Associates
MDZ	Minimum Detectable Z-reflectivity
MetOp	Polar Orbiting Meteorological Satellite
METUM	Met Office Unified Model
MIPAS	Michelson Interferometer for Passive Atmospheric Sounding
MIR	Middle Infra Red
MISR	Multi-angle Imaging SpectroRadiometer
MLDP	Lagrangian Particle Dispersion Model
MLS	Microwave Limb Sounder
MM5	Mesoscale Model version 5
MOCAGE	*Modèle de Chimie Atmosphérique à Grande Echelle*
MODIS	Moderate-resolution Imaging Spectroradiometer
MOHP	Meteorological Observatory Hohenpeissenberg
MOR	Mandatory Occurrence Report
MPLNet	Micropulse Lidar Network
MSG	Meteosat Second Generation
MSI	Multi-Spectral Imager
MTG	Meteosat Third Generation
MTP	Meteosat Transition Programme
MTSAT	Multifunctional Transport Satellite
MWO	Meteorological Watch Office
NAME	Numerical Atmospheric-dispersion Modelling Environment
NASA	National Aeronautics and Space Administration
NATS	National Air Traffic Services
NCEP	National Center for Environmental Prediction
NESDIS	National Environmental Satellite, Data, and Information Service
NFZ	No Fly Zone
NILU	Norwegian Institute for Air Research
NIR	Near Infrared
NOAA	National Oceanic and Atmospheric Administration
NPOESS	National Polar-orbiting Operational Environmental Satellite System
NPP	NPOESS Preparatory Project
NRT	Near Real Time
NUI	National University of Ireland
NWP	Numerical Weather Prediction
OLCI	Ocean Land Color Instrument
OMI	Ozone Monitoring Instrument
OMPS	Ozone Mapping and Profiler Suite
PMS	Particle Measurement System
POLDER	POLarisation and Directionality of the Earth's Reflectances
PRF	Pulse repetition frequency
R&D	Research and Development
RADAR	Radio Detection And Ranging
RADM2	Regional Acid Deposition Model version 2
REMOTE	Regional Model with Tracer Extension
SAR	Synthetic Aperture Radar
SBUV	Solar Backscatter Ultraviolet Radiometer
SCIAMACHY	Scanning Imaging Absorption Spectrometer for Atmospheric CHartographY
SEVIRI	Spinning Enhanced Visible and Infrared Imager
SILAM	Emergency dispersion modelling system
SLST	Sea Land Surface Temperature Radiometer
SNR	Signal to Noise Ratio
STP	Standard temperature and pressure
SWIR	Short Wavelength Infra Red
TES	Technology Experiment Satellite
TIR	Thermal Infra Red
TLZ	Time Limited Zone
TM	Transport Model
TOVS	TIROS Operational Vertical Sounder
UAS	Unmanned Aircraft System
UAV	Unmanned Aerial Vehicle
ULB	Université Libre de Bruxelles
USGS	United States Geological Survey
UTC	Universal Time Coordinate
UT/LS	Upper Troposphere / Lower Stratosphere
UV	Ultraviolet
UVN	Ultraviolet Visible Near-infrared sounder
VAAC	Volcanic Ash Advisory Centre
VARR	Volcanic Ash Radar Retrieval
VIIRS	Visible Infrared Imager Radiometer Suite
VIS	Visible
WMO	World Meteorological Organisation
WRF	Forecast Modelling System

An ESA Communications Production